Regulation of MH Class II Associated Invariant Chain in *Oncorhynchus mykiss*

by

Darah Christie

A thesis
presented to the University of Waterloo
in fulfillment of the
thesis requirement for the degree of
Master of Science
in
Biology

Waterloo, Ontario, Canada, 2007

AUTHOR'S DECLARATION

I hereby declare that I am the sole author of this thesis. This is a true copy of the thesis, including any required final revisions, as accepted by my examiners.

I understand that my thesis may be made electronically available to the public.

Abstract

Major histocompatibility complex (MHC) class II associated invariant chain is a chaperone of the mammalian MHC class II antigen presentation pathway. It is responsible for targeting the MHC class II dimer to the endocytic pathway, which allows for the loading of exogenous antigens onto the MHC class II receptor. Two genes showing significant sequence similarity to the mammalian invariant chain gene have been identified in rainbow trout. S25-7 and INVX are thought to play a role within the teleost MH class II antigen presentation pathway similar to that performed by the mammalian invariant chain. *In vivo* and *in vitro* methods have been used to investigate the regulation of these genes upon immune system activation. To induce an immune response both rainbow trout and the macrophage-like cell line RTS-11 were treated with phorbol myristate acetate (PMA). PMA is a stimulator of protein kinase C, which is involved in the activation of both B and T cells. After PMA treatment, individuals were sacrificed at several time points and tissues were collected for analysis. Up-regulation of IL-1β transcript, as detected by RT-PCR analysis, demonstrated the successful induction of an immune response *in vivo*. S25-7 transcript levels remained unchanged in gill, spleen, peripheral blood leukocytes and liver. However, the transcript was found to be significantly decreased in head kidney beginning 24 hours post-stimulation. INVX transcript levels remained unchanged in all tissues analyzed. In addition, the level of S25-7 transcript is higher in all tissues than INVX transcript.

Western blot analysis detected both S25-7 and INVX proteins within gill and spleen, indicating the presence of cell populations capable of presenting extracellular antigen within the MH class II dimer. Similar to transcript analysis, the level of invariant chain in these tissues remained unchanged during immune system activation. Neither INVX nor S25-7 was detected in head kidney, indicating this tissue may not function as a secondary immune tissue, as previously thought. Finally, western blot analysis failed to detect either INVX or S25-7 protein within liver, as expected in a non-immune tissue.

RTS11 analysis demonstrated a similar pattern of invariant chain expression *in vitro*. S25-7 transcript levels remained stable throughout the PMA stimulation time course, while INVX transcript was down-regulated at 48 and 96 hours post-stimulation, with a subsequent increase at 168 hours. However, both S25-7 and INVX protein levels remained unchanged during immune stimulation.

These results demonstrate a pattern of invariant chain tissue expression, providing information about the type of immune functions carried out at these sites. In addition, the results indicate that

neither INVX nor S25-7 is up-regulated, at either the transcript or protein level upon immune system activation. This is in contrast to the mammalian invariant chain, which is up-regulated at both the transcript and protein level during an immune response, indicating that teleosts have evolved a unique system of immune regulation.

Acknowledgements

I would like to begin by thanking my supervisor, Dr Brian Dixon, whose knowledge and support has helped me immensely as I worked to complete my master's project. I would also like to thank Dr Kazuhiro Fujiki, who first identified invariant chain in rainbow trout, and who taught me approximately 95% of everything I know in regards to molecular biology research. I would also like to thank all of the Dixon lab members who have helped me with this project, including Dr Stephen Kales, Pablo Conejeros, Marsela Braunstein, Stacey Clarence, Shathi Eshaque, Leo Becker, Anna Phan and our very entertaining co-op student Paul Binns. I would also like to thank Dr Stephanie DeWitte-Orr for supplying me the elusive RTS11. I would also like to thank our esteemed DNA sequencer and flow cytometry specialist Mishi Savulescu. Finally, I would like to thank my family and friends for their love and support during my extended stay at the University of Waterloo.

Table of Contents

List of Figures

List of Tables

Chapter 1
Introduction

1.1 General Overview of the Vertebrate Immune System

Leukocytes are the effector cells of the immune system and are responsible for the elimination of foreign pathogens. In mammals these cells are produced within bone marrow from a multipotent stem cell precursor (Kaushansky, 2006). These stem cells undergo a number of differentiation processes to give rise to a variety of cell populations, including monocytes, neutrophils, eosinophils, basophils, T cells, B cells and natural killer (NK) cells, which are all involved in the immune response. The bone marrow is known as a primary immune organ because immune cells mature within this tissue. In teleosts, the head kidney functions as a primary immune organ as it is the site of hematopoiesis (Fange, 1986). In addition, the thymus also serves as a primary immune organ in both mammals and teleosts as the site of T cell maturation (Janeway *et al*, 2001, Press and Hansen, 1999).

Mature immune cells exit the primary immune organs and enter circulation. These cells migrate throughout the body to provide constant surveillance for potential pathogens. Upon infection, the circulating B and T cells must be activated to respond to the pathogen. In mammals, this activation occurs within the lymph nodes and the spleen, which are known as secondary immune organs. Within teleosts, the spleen and head kidney are thought to function as secondary immune organs (Press and Evensen, 1999, Kaattari and Irwin, 1985)

Upon exposure to a pathogen, the first line of defense is the effector cells of the innate immune system. A number of these cells are phagocytic and capable of ingesting and degrading pathogens. In addition, many innate effectors cells express Toll-like receptors (TLR) that recognize conserved structures on pathogen surfaces (Tosi, 2005). When a TLR binds to a pathogen, a signaling cascade pathway is initiated, resulting in the expression of a number of genes involved in the immune response. Many activated cells express cytokines and chemokines, small secreted proteins, which can recruit and activate other immune cells (Janeway *et al*, 2001).

In cases where the innate immune system is unable to eliminate a pathogen, the adaptive immune system is recruited and activated. The effector cells of the adaptive immune system are the B lymphocytes and T lymphocytes. These cells express surface receptors which bind to foreign protein fragments. During cellular maturation, genes encoding the B cell and T cell receptors undergo a

series of recombination events, which leads to the generation of a large number of cells capable of recognizing very diverse ligands (Janeway *et al*¸2001). Thus, these cells are able to bind and activate a response against a very large number of foreign peptides. The B lymphocytes are responsible for humoral immunity. These cells synthesize and secrete antibodies upon stimulation by a specific pathogen. The secreted antibodies coat pathogen surfaces to inhibit entry into a target cell and also facilitate phagocytosis and destruction of pathogen by macrophage, a type of innate effector cell.

Once a pathogen has entered a cell, antibodies are no longer able to control the infection. In this case, T lymphocytes, the effectors of cellular immunity, are required. These cells are able to mediate the specific killing of infected cells, to prevent the proliferation and spread of the pathogen. There are two types of T cells, identified as $CD4^+$ or $CD8^+$, depending on which of these cell surface molecules are expressed. The $CD8^+$ T cells are cytolytic cells and are responsible for the killing of infected cells, while the $CD4^+$ T cells are helper cells which synthesize and secrete a number of factors that maintain an immune response.

T lymphocytes express surface receptors, the T cell receptors, which are activated upon the specific binding of a small foreign peptide fragment present on the surface of target cells. These peptides are presented by the MHC proteins, which are surface-bound heterodimers that interact with both the T cell receptor and the co-receptor molecules CD4 and CD8. The interaction of CD4 and CD8 with the MHC proteins differentiates between the target cells recognized by each T cell subtype. The $CD8^+$ T cells bind to MHC class I proteins, which are present on all nucleated cells, allowing any cell with the potential for a pathogen infection to activate a cytolytic response. On the other hand, the $CD4^+$ T cells are helper cells and are activated by a small population of cells known as antigen presenting cells (APCs), which express MHC class II. These cells are able to endocytose pathogens, cleave pathogenic proteins into small peptides and present these peptides to activate $CD4^+$ T cells. Macrophage, dendritic cells and B cells are the major antigen presenting cells (Janeway *et al*, 2001).

The $CD4^+$ T cells are further divided into the T_H1 and T_H2 subpopulations, which are defined by the repertoire of cytokines produced. T_H1 cells produce IL-2 and IFNγ, which are required for the proliferation of $CD8^+$ T cells as well as for the activation of macrophage (Wang, 2001; Pardoll and Topalian, 1998). T_H2 cells express IL-4, IL-5 and IL-10, which are involved in the activation of B cells (Janeway *et al*, 2001). In addition, the cytokines produced by T_H1 cells inhibit T_H2 cell responses and vise versa. Once a specific response is induced, the activated T_H cells stimulate this response while simultaneously suppressing the other response.

1.2 The Major Histocompatibility Complex

The MHC, or major histocompatibility complex, is a region of DNA which encodes a number of genes involved in the presentation of foreign peptides to T lymphocytes (Williams, 2001). In humans, the MHC is located on chromosome 6 and in mice it is located on chromosome 17 (Janeway *et al*, 2001). This region encodes the MHC class I and MHC class II genes, along with various accessory molecules for these antigen presentation pathways as well as a number of non-related genes (Williams, 2001). Since these genes are located together on the same chromosome, they are linked and will be inherited as a set by offspring.

The MHC class I and MHC class II genes are highly polymorphic, with the majority of the polymorphism occurring within sequences encoding the peptide binding groove (Williams, 2001). Both MHC receptors are heterodimers, with MHC class I being composed of an α-chain bound to β_2-microglobulin while the MHC class II is composed an α-chain and β-chain. The peptide binding groove is formed by the α1 and α2 domains in MHC class I and the α1 and β1 domains in MHC class II, thus the majority of the polymorphism is found within these regions (Williams, 2001). This peptide binding groove polymorphism allows binding of a wide variety of peptides by MHC alleles. In humans, the inheritance of three MHC class I heavy chain genes and three MHC class II loci from each parent results in a total of 6 alleles for each MHC class, and the gene polymorphism increases the chance that each allele will bind a different peptide repertoire. Thus, the MHC is capable of presenting a diverse selection of peptides to T lymphocytes.

The segregation of the MHC class I and MHC class II antigen presentation pathways results in a distinct set of peptides presented for $CD8^+$ and $CD4^+$ T cells activation, as shown in figure 1.1. MHC class I presents a variety of intracellular peptides, which allows $CD8^+$ T cells to detect infected cells (Janeway *et al*, 2001). In contrast, MHC class II presents extracellular peptides, as antigen presenting cells endocytose and process extracellular pathogens to activate a $CD4^+$ T cell response without being directly infected by the pathogen. The distinction between class I and class II is essential for the activation of the proper effector function.

1.2.1 MHC Class I Antigen Presentation Pathway

As stated above, MHC class I is present on the surface of all nucleated cells and is responsible for the presentation of intracellular peptides. Peptide loading of MHC class I occurs within the endoplasmic reticulum, as shown in figure 1.1. The newly synthesized MHC class I heavy chain and β_2-

Figure 1.1: Schematic representation of MHC antigen presentation pathways. (A) An overview of the MHC class II pathway is shown on the left side of this figure (Li *et al*, 2005). After associating with the invariant chain in the ER, the MHC class II complex travels through the Golgi apparatus and enters the endosomal pathway. The class II dimer traffics through multiples intracellular pathways to maximize the variety of antigens loaded into the peptide binding groove. Pathway 1 represents the direct transport from the Golgi apparatus into lysosomal compartments, while pathway 2 represents the transport of the complex to the cell surface, followed by endocytosis of this complex into early endosomal compartments. Pathway 3 represents the transport of the complex from the Golgi apparatus through the early endosomes. Finally, pathway 4 represents the endocytosis of mature loaded MHC class II dimers from the cell surface for reloading with new antigen. Upon exposure to antigens, the CLIP peptide is exchanged for antigenic peptide by the chaperone DM. The loaded class II complex then travels to the cell surface to activate $CD4^+$ T cells. (B) The MHC class I antigen presentation pathway is summarized on the right side of this diagram. Proteins present in the cytoplasm are degraded by the proteasome and transported into the ER by the transporter associated with antigen presentation (TAP). The peptide antigens are then loaded into the peptide binding groove of the MHC class I dimer, and this complex travels to the cell surface for $CD8^+$ T cell activation.

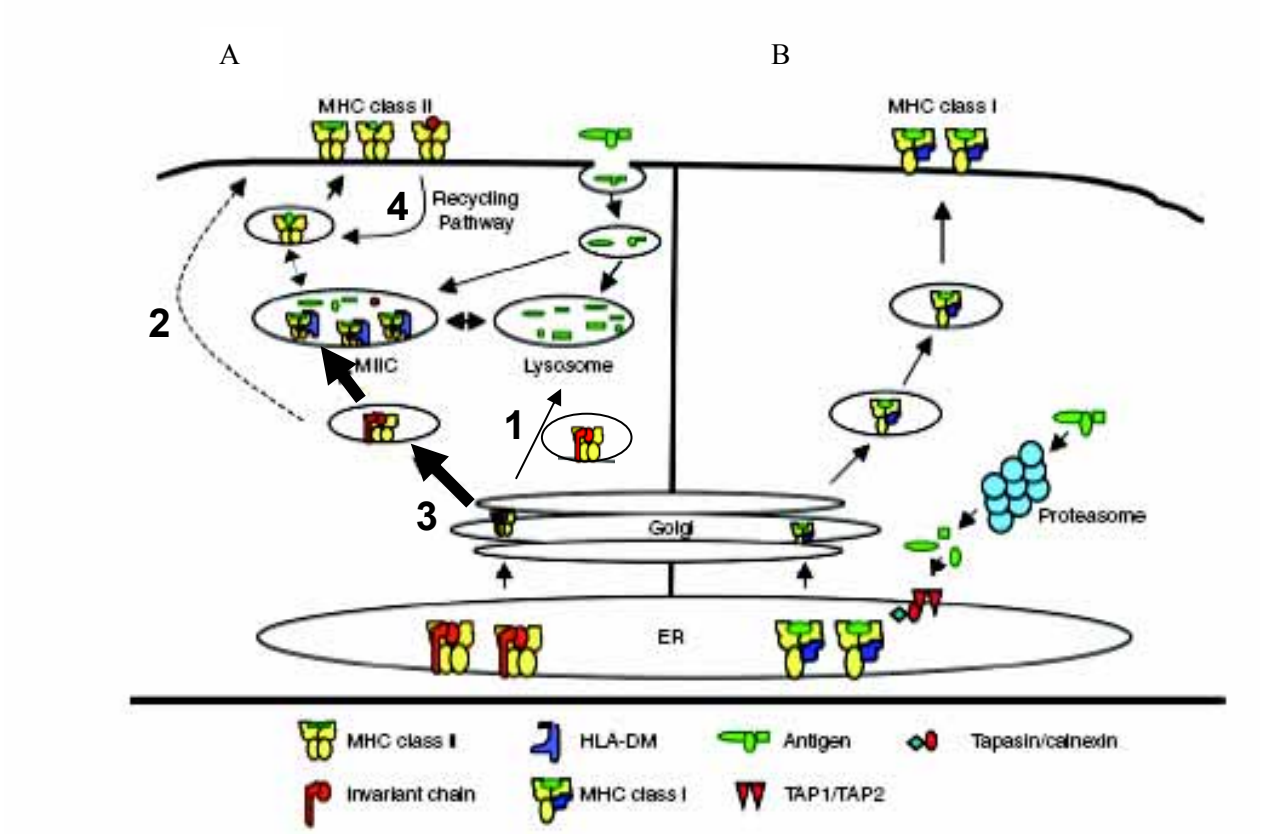
A
B
MHC class II
MHC class I
4
Recycling
Pathway
2
MIIC
Lysosome
1
3
Golgi
Proteasome
ER
MHC class II
HLA-DM
Antigen
Tapasin/calnexin
Invariant chain
MHC class I
TAP1/TAP2

microglobulin initially interact with the ER chaperone calnexin, which facilitates the assembly of the class I complex (Ahluwalia *et al*, 1992). Once this complex has formed, calnexin dissociates and is replaced by the ER chaperones calreticulin and Erp57, as well as the protein tapasin (Pamer and Cresswell, 1998). Tapasin is responsible for the association of the empty MHC class I complex with the TAP transporter, which transports short peptides from the cytosol into the ER. These peptides are produced by proteasome-mediated degradation of cytosolic proteins (Pamer and Cresswell, 1998). Once an empty class I dimer has bound an antigenic peptide, the loaded complex dissociates from the ER chaperones and travels through the Golgi apparatus to the cell surface. Expression of MHC class I genes, as well as TAP and some proteasome subunits are upregulated by IFNγ, which is expressed by virally infected cells (Janeway *et al*, 2001). Thus, the cellular response to viral infection is the induction of the MHC class I antigen presentation pathway, leading to an increased expression of foreign peptide at the cell surface to activate cytolytic $CD8^+$ T cells.

1.2.2 MHC Class II Antigen Presentation Pathway

The MHC class II is present on the surface of antigen presenting cells and is responsible for the presentation of extracellular peptides. The loading of these peptides occurs within endosomal vesicles. To begin, the α- and β- chains are translated and transported into the endoplasmic reticulum, where they rapidly associate with the ER chaperone calnexin (Anderson and Cresswell, 1994). The MHC class II dimer then binds to another chaperone, the MHC class II associated invariant chain (Anderson and Miller, 1992). Calnexin remains associated with both the MHC class II dimer and the invariant chain until a nonomeric complex is formed consisting of an invariant chain trimer bound to three class II dimers (Anderson and Cresswell, 1994). Once the nonamer has formed, calnexin dissociates and the complex traffics out of the endoplasmic reticulum, through the Golgi apparatus and enters the endocytic pathway, where antigen loading can occur.

There are four possible pathways for the intracellular transport, which are shown in figure 1.1. Cellular fractionation experiments of B lymphoblasts show that MHC class II is located within the early and late endosomes as well as lysosomes, indicating that MHC class II traffics through the endosomal pathway (Castellino and Germain, 1995). The complex may travel from the Golgi apparatus to the cell surface, where it is rapidly endocytosed, or it may travel directly to the endosomal pathway, entering either an early endosome or a lysosomal compartment (Roche *et al,* 1993; Brachet *et al,* 1999; Pond and Watts, 1999; Peters *et* al, 1991). The major pathway for MHC class II trafficking likely involves direct entry into the endosomal pathway, while a minor pathway

consists of uptake from the cell surface or direct entry into a lysosomal compartment, since the removal of early endosomes greatly decreases the production of stable class II dimers (Brachet *et al,*1999). Finally, another minor trafficking pathway involves the recycling of mature MHC class II dimers from the cell surface. Evidence for this minor pathway is demonstrated in studies of truncated MHC class II dimers lacking the internalization signals in the cytoplasmic domain (Pinet *et al*, 1995). Some antigenic peptides are not presented by the truncated dimer but are presented by the full length dimer. These results indicate that some mature MHC class II complexes may be internalized from the cell surface independent of invariant chain and loaded with new peptides. This ability to enter several endosomal and lyosomal compartments likely increases the variety of antigens presented by the MHC class II dimer.

As the MHC class II - invariant chain complex travels through the endosomal pathway, the invariant chain is degraded in a stepwise manor by a number of proteases found within various endosomal compartments (Villadangoes *et al*, 1999). The initial cleavage removes the trimerization domain, resulting in the Iip22 peptide (Villadangoes *et al*, 1999). Next, another large portion of the extracellular domain is cleaved off, giving the Iip10 peptide, which consists of only the CLIP domain and the N-terminal region. The final cleavage leaves only the CLIP associated with the MHC class II peptide binding groove. This stepwise degradation is essential for the removal of invariant chain from the class II dimer and the subsequent loading of antigen into the peptide binding groove.

The cleavage of invariant chain is carried out by a variety of cellular proteases, including the asparagine-specific endopeptidase (AEP) as well as a number of cysteine proteases, specifically cathepsin S and cathepsin L (Lautwein *et al*, 2004; Villadangoes *et al,* 1999). While the proteases involved in the initial steps of invariant chain degradation have not yet been identified, knockout studies have illustrated the essential roles played by cathepsin L (Cat L) and Cat S in the cleavage of Iip10 to CLIP. These two proteases are differentially expressed, with Cat S being expressed in B cells, dendritic cells and macrophages while Cat L is expressed by macrophage and cortical thymic epithelial cells (cTECs) (Lennon-Dumenil *et al*, 2002). MHC class II dimers remain bound to Iip10 in cTECs of Cat L deficient mice resulting in an impaired in $CD4^+$ T cell selection, while the MHC class II – Iip10 complex is found in dendritic cells and B cells in Cat S deficient mice (Nakagawa *et al*, 1999). Studies have shown that active AEP, Cat S and Cat L are all located in late endosomal structures, which matches well with results showing that the invariant chain is mostly intact in within the early endosomal compartments, while it is present at a much lower level in late endosomal

structures (Romagnoli *et al*, 1993; Lautwein *et al*, 2004). Thus, as the invariant travels into the late endosomal structures, it undergoes proteolytic cleavage until only the CLIP domain remains bound the MHC class II dimer.

In addition to the processing of the invariant chain, antigenic proteins from the extracellular space must also be degraded into short peptide of approximately 13-17 amino acids for loading into the peptide binding groove of the MHC class II dimer (Janeway *et al*, 2001). Antigen presenting cells can take up antigen by nonspecific endocytosis or by receptor mediated endocytosis (Wolf Bryant *et al*, 2002). The antigens enter the endocytic pathway where they encounter the same variety of proteases that are responsible for invariant chain degradation (Lennon-Dumenil *et al*, 2002). The reductase GILT (γ-IFN induced lysosomal thiol reductase) is thought to be involved in the initial steps of disulfide bond reduction to unfold proteins (Hsing and Rudensky, 2005). The subsequent steps involve both endopeptidases, which release internal epitopes, as well as exopeptidases, which trim the ends of the peptides (Lennon-Dumenil, 2002). The degradation of proteins into antigenic peptides is carried out by a number of proteases, as evidenced by the variety of terminal residues found in class II bound peptides (Wolf-Bryant *et al*, 2002). Studies have shown that AEP, as well as Cat B and Cat S are the basic requirements for complete antigen processing (Wolf-Bryant *et al*, 2002). Since invariant chain and antigenic proteins are degraded by the same types of proteases, this indicates that antigens are targeted to the same intracellular compartments as the MHC class II dimers.

The final step in the MHC class II antigen loading pathway involves the removal of the CLIP peptide, which occurs within the MHC class II compartment (MIIC) (Sanderson *et al*, 1994). There has been some debate as to the identity of the MIIC, as some believe it is a unique late endosomal-like compartment that is not part of the endosomal pathway (Peters *et al*, 1991), while others argue that it is a classical late endosomal compartment (Castellino and Germain, 1995). Subsequently, there have been some guidelines put forth to define the identity if the MIIC. A MIIC is an acidic intracellular structure containing the chaperone DM and MHC class II which is accessible by bulk phase endocytosed or receptor mediated antigen uptake. This compartment must have both unloaded and loaded MHC class II, and it must have the ability to transport MHC class II molecules to the cell surface (Neefjes, 1999). It is likely that there is not one single MIIC that can be defined for all cell types, and both late endosomal and early lysosomal structures can be thought of as the MIIC. Once the MHC class II reaches the MIIC, the CLIP must be removed from the peptide binding groove to

allow for the binding of an antigenic peptide. The release of CLIP is mediated by the chaperone DM (Denzin and Cresswell, 1995). This molecule is a dimer of α- chain and β- chain proteins which form a complex very similar in structure to MHC class II, but lacking the peptide binding groove (Mosyak *et al*, 1998). In the absence of DM, the majority of MHC class II dimers remain associated with the CLIP (Denzin and Cresswell, 1995). It is thought that DM binds to an unstable MHC class II dimer and stabilizes an open conformation of the peptide binding groove, facilitating the release of unstably bound peptides (Busch *et al*, 2000). The empty MHC class II can either bind antigenic peptide or may aggregate with other empty class II molecules and be degraded. In addition to the removal of CLIP, DM can also facilitate the removal of other peptides (Sloan *et al*, 1995). In this way DM acts to edit the peptides presented by MHC class II to ensure the most stable binding, resulting in MHC class II antigen complexes with a longer half life at the cell surface. However, there are some alleles of MHC class II that have a very low affinity for CLIP, and the CLIP peptide can dissociate naturally in the absence of HLA-DM (Busch *et al*, 2005). This allows DM independent antigen loading to occur in endosomal structures other than the MIIC, which leads to the presentation of antigenic peptides that may be degraded in more acidic compartments. Thus, it is likely that the picture of MHC class II intracellular transport and antigen loading is very complicated in which some DM independent loading can occur for certain MHC class II alleles within the early endosomal compartments while the majority of antigen loading occurs by a DM dependent mechanism within the MIIC. After peptide loading, a vesicular intermediate forms from the MIIC and fuses with the cell membrane to carry the antigen loaded MHC class II complex to the cell surface (Pond *et al*, 1997).

1.3 Functions of Invariant Chain

The invariant chain is a type II transmembrane protein originally identified by co-precipitation with MHC class II dimers (Jones *et al*, 1978). The human invariant chain is encoded by a gene located on chromosome 5, which is not linked to the MHC region (Claesson-Welsh *et al*, 1984). The single invariant chain gene undergoes alternative splicing and alternative translational initiation to produce four different protein isoforms (Strubin *et al*, 1986). As shown in figure 1.2, p35 and p43 have an additional 16 amino acid N-terminal sequence while p41 and p43 have an additional domain within the C-terminal extracellular region. The following sections will describe the function of invariant chain and will illustrate how each isoform carries out slightly different functions within antigen presenting cells.

Figure 1.2: Schematic representation of the various isoforms of invariant chain. Mammalian invariant chain isoforms p35/33 and p43/41 are shown at the top of this figure. In addition, the three invariant chain proteins from rainbow trout, INVX, S25-7 and 14-1 are also shown, along with the zebrafish invariant chain-like proteins, Iclp-1 and Iclp-2. Abbreviations: TMD – transmembrane domain, CLIP – class II associated invariant chain peptide, TD – trimerization domain, tTD – truncated trimerization domain, Tg – thyroglobulin domain, RR – ER retention signal, ML, LL and IL – endosomal targeting signals. Arrows represent translational start sites.

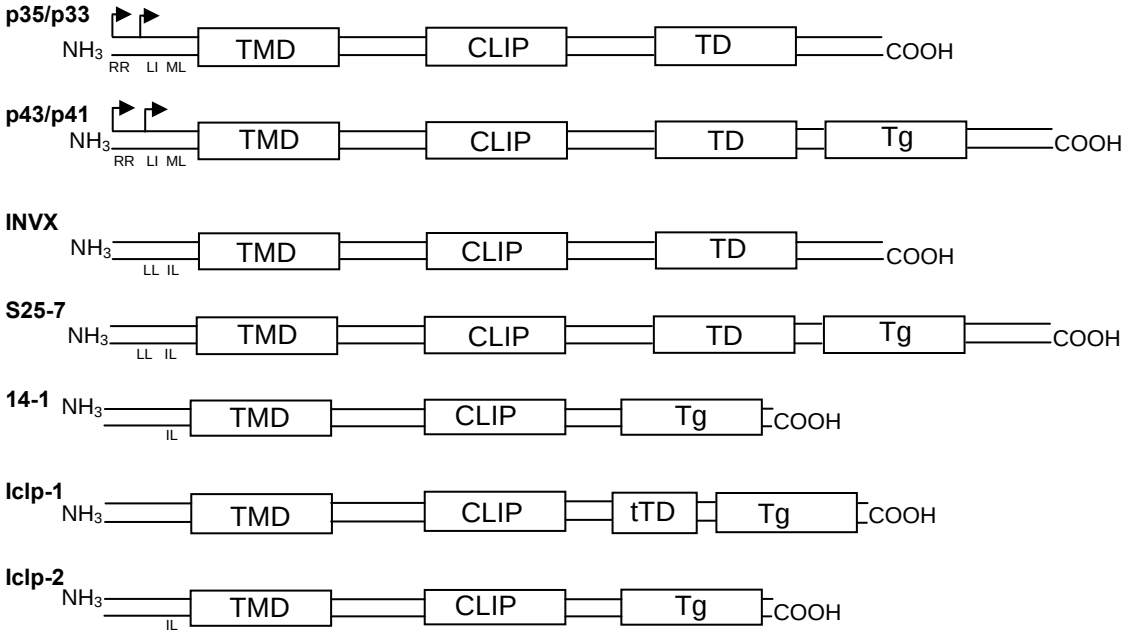
p35/p33
NH3
RR LI ML
TMD
CLIP
TD
COOH
p43/p41
NH3
RR LI ML
TMD
CLIP
TD
Tg
COOH
INVX
NH3
LL IL
TMD
CLIP
TD
COOH
S25-7
NH3
LL IL
TMD
CLIP
TD
Tg
COOH
14-1
NH3
IL
TMD
CLIP
Tg
COOH
Iclp-1
NH3
TMD
CLIP
tTD
Tg
COOH
Iclp-2
NH3
IL
TMD
CLIP
Tg
COOH

1.3.1 Chaperone that Differentiates MHC Class II from MHC Class I

The invariant chain plays an essential role in the MHC class II antigen presentation pathway, which is required not only for the activation of $CD4^+$ T cells, but also for the development of these cells (Janeway *et al,* 2001). Mice lacking the invariant chain gene have only 30% of the normal $CD4^+$ T cell population (Viville *et al*, 1993). Although the animals from this study remained healthy, this is because they were raised in a pathogen free environment. The greatly decreased $CD4^+$ T cell population would interfere with the ability of these animals to maintain a $CD8^+$ T cell response as there would be a deficient level of IL-2 production, which is needed for T cell survival.

The major role of all isoforms of invariant chain is to act as a chaperone for the MHC class II dimer (Anderson and Miller, 1991). When αβ dimers are expressed in cells in the absence of invariant chain, there is very slow transport of the dimers to the Golgi apparatus as the majority of dimers are retained in the ER. In addition, those dimers that are eventually transported to the cell surface have an altered conformation compared to dimers from invariant chain expressing cells. Furthermore, in invariant chain knockout mice, MHC class II also has an altered conformation and the majority of the MHC class II is retained in the ER (Viville *et* al, 1993). Thus, invariant chain is required for the proper folding of the MHC class II dimers and the subsequent delivery of these dimers out of the ER.

It has been shown that invariant chain binds directly to the peptide binding groove and this interaction is required for proper folding of the dimer (Ghosh *et al*, 1995). In addition to chaperone function, the blocking of the peptide binding groove also plays an essential role in the functional separation of MHC class II from MHC class I. As described above, MHC class I is loaded with intracellular antigens within the ER (Pamer and Cresswell, 1998). If the peptide binding groove of MHC class II remained unoccupied in the ER, it could also bind to intracellular antigens, resulting in an overlap in the peptide repertoire of MHC class I and MHC class II. However, invariant chain is able to block the binding of peptide to MHC class II in the ER. When empty MHC class II dimers are exposed to an antigen, 94% of the dimers are able to bind the peptide, however, in the presence of invariant chain less than 0.3% of the dimers bind to the peptide (Roche and Cresswell, 1990). Treatment of the MHC class II- invariant chain complex with SDS increases the ability of the dimer to bind to antigenic peptide and indicates that the invariant chain must be removed for the loading of the peptide binding groove. Thus, binding of invariant chain to the MHC class II dimer within the ER

is able to block the binding of any intracellular peptides to maintain the segregation of antigens presented by MHC class I and MHC class II.

1.3.2 MHC Class II Intracellular Trafficking

Once the MHC class II dimer has bound to the invariant chain, it leaves the ER and enters the endosomal pathway. The intracellular transport of MHC class II is controlled by the invariant chain (Lotteau *et al*, 1990). When MHC class II dimers are expressed in the absence of invariant chain, the dimers are only found in the ER, the Golgi apparatus and at the cell surface (Lotteau *et al*, 1990). However, when the invariant chain is co-expressed, the dimer is localized to endosomal compartments. In order for proper intracellular targeting, proteins must contain the proper sorting signal, in the absence of a sorting signal the protein will remain in the cytosol (Alberts *et al*, 2002). To identify the sorting signal in invariant chain responsible for endosomal targeting, a series of invariant chain proteins containing deletions of the cytoplasmic domain were constructed and intracellular localization was examined (Pieters *et al*, 1993). The invariant chain was found to have two localization signals, as the deletion of residues 1-20 eliminated any endosomal localization while deletion of residues 1-11 or 12-20 retained endosomal localization. To identify the specific residues involved in the intracellular sorting, researchers looked for similarities to other known sorting signals. A tyrosine based sorting signal has been identified for a number of endosomal and lysosomal resident proteins (Peters *et al*, 1990; Williams and Fukuda, 1990). In addition, a di-leucine targeting signal has also been identified in studies of the T cell receptor components CD3-γ and CD3-δ (Letourneur and Klausner, 1992). While there is no tyrosine based sorting signal present in the first 20 residues of the invariant chain, there does appear to be two leucine based signals, L^7I^8 and $M^{16}L^{17}$ (Bremnes *et al*, 1994). Point mutation of any of one of these residues decreased, but did not eliminate, the endosomal targeting of a chimeric protein (Odorizzi *et al*, 1994). This indicates that L^7I^8 and $M^{16}L^{17}$ are responsible for the targeting of invariant chain and the MHC class II dimer to the endosomal pathway. All four isoforms of invariant chain contain these residues and are able to mediate the trafficking of MHC class II.

The intracellular targeting of the MHC class II invariant chain complex is dependent on the multimerization of the invariant chain. After synthesis of the invariant chain, it forms a homotrimer, which subsequently binds three MHC class II dimers to give a nonomeric complex (Lamb *et al,* 1992; Roche *et al*, 1991). Studies of invariant chain targeting show that the invariant chain must be present at least as a dimer for proper intracellular transport (Arneson and Miller, 1995). This study used a

non-immune cell line expressing MHC class II, along with either wild type invariant chain or an invariant chain lacking residues 2-17. The results show that a complex containing a single wild type invariant chain, and thus only one targeting sequence, targets the complex to the cell surface. Complexes containing more than one wild type invariant chain traffic to the endosomal pathway. This demonstrates that the formation of the invariant chain trimer is essential for proper intracellular trafficking.

In addition to the endosomal targeting signals, the alternatively spliced p35 and p43 also have an ER retention sequence (Schutze *et al*, 1994). When p35 is expressed alone in the absence of MHC class II dimers it remains in the ER, while p33 travels to the endosomal pathway (Lotteau *et al*, 1990). To identify the exact residues within the amino-terminal extension required for this retention, a series of deletion constructs were tested for intracellular location (Schutze *et al*, 1994). Deletion of the first four residues eliminated the ER retention and point mutation analysis indicated that any two of the three arginine residues $R^3R^4R^5$ are involved in retention as mutation of any one but not two of these residues retain ER localization. In addition, the expression of p35 together with p33 also results in retention within the ER (Arunachalam *et al*, 1994). Thus, as long as a single ER retention signal is present within an invariant chain trimer, the entire complex will remain in the ER. This is essential to the role of invariant chain as a chaperone, as this ensures a pool of invariant chain will always be available in the ER to associate with new class II dimers. Since p43 has the same amino-terminal extension, it will also mediate the ER retention of unbound invariant chain trimers.

Once the MHC class II has been bound, the complex must overcome this ER retention signal for entry into the endosomal pathway. This appears to be reliant on both the phosporylation of the invariant chain and also the association with MHC class II dimers. Analysis shows that the p35 invariant chain is phosporylated at both S^6 and S^8, which are not present in p33 (Anderson and Roche, 1998). Inhibition of phosphorylation decreases the trafficking rate of MHC class II complexes out of the ER. The trafficking was not entirely blocked because p33 is also expressed and any complexes containing trimers of p33 are able to enter the endosomal pathway due to the absence of the ER retention signal. In addition to phosphorylation, the association with the MHC class II is also required for the exit of the p35 invariant chain from the ER (Khalil *et al*, 2003). When a truncated class II β chain, lacking the cytoplasmic domain is expressed along with p35, the complex is retained in the ER. However, a complex of p35 with full length MHC class II proteins can exit the ER. Thus,

the phosphorylation of p35 as well as the association with MHC class II dimers is required for transport out of the ER.

It has been shown that phosphorylated p35 can also associate with the protein 14-3-3, which is known to bind to phosphoserine motifs (Kuwana *et al*, 1998; Aitken, 1996). This interaction may influence the intracellular transport of the MHC class II complex as 14-3-3 has been shown to rescue a clathrin mutation in *S. cerevisiae* (Gelperin *et al*, 1995). Since p33 and p41 do not have this S^6S^8 motif, p35 and p43 may be able to interact with different cellular components to alter the path the MHC class II complex travels through the endosomal pathway. This may be beneficial to increase the variety of antigens the complex is exposed to, thus increasing the peptide repertoire expressed on the cell surface.

1.3.3 Mediator of Self Release

As stated above, in studies of cells lacking DM, the vast majority of MHC class II dimers remain bound to CLIP, indicating the importance of DM in the loading of peptides (Busch *et al*, 2005). However, a small number of dimers are bound to antigenic peptide, indicating that MHC class II has the ability to release CLIP without DM, albeit at a greatly reduced rate. The release of CLIP has been shown to be mediated by the invariant chain, by a sequence located within the CLIP region (Vogt *et al*, 1995). The CLIP peptide is composed of 81-104 in human p33 and 81-109 in mouse p31 (Bijlmakers *et al*, 1994; Freisewinkel et al, 1993). Subsequent analysis has indicated that this region can be thought to contain three separate regions, the N-terminal CLIP region, the CLIP and the C-terminal CLIP region (Kropshofer et al, 1995; Ghosh et al, 1995). The CLIP region is composed of residues 91 to 99 and this segment lies within the peptide binding groove to directly inhibit the binding of endogenous peptides (Ghosh et al, 1995). The N-terminal and C-terminal regions also interact with the MHC class II dimer, but they do so at a separate site, located outside of the peptide binding groove (Vogt et al, 1995; Siebenkotten et al, 1998). The separate site of interaction indicates that these regions are not directly involved in blocking antigen binding; however, the additional interaction with the MHC class II dimer likely has a function.

The N-terminal region, consisting of residues 77-92, appears to play a role in peptide loading of the class II dimers through the interaction with an allosteric binding site on the MHC class II dimers (Adams and Humphreys, 1995; Vogt *et al*, 1995). The MHC class II dimer exists in two different conformations, an immature conformation with a rapid on/off rate for peptide binding, and a mature

conformation with a slow on/off rate (Sadegh-Nasseri *et al*, 1994). The loading of antigens within the endosomal pathway benefits from a rapid on/off rate, as this allows for the release of peptides that do not bind strongly to the peptide binding groove. However, once a high affinity antigen has been bound, a slow on/off rate increases the half life of the surface antigen- class II complex, allowing more time for T cell activation. It appears that the N-terminal region may increase the amount of time the MHC class II dimer spends in the immature rapid on/off conformation. When Ii(71-88) was incubated with empty MHC class II dimers and an antigenic epitope, initially there was an inhibition of antigenic peptide binding, although the antigenic peptide eventually bound and resulted in the inhibition of Ii(71-88) binding (Vogt *et al*, 1995). This is not due to direct binding of Ii(71-88) to the peptide binding groove as the CLIP region is not included in this peptide. These results indicate that MHC class II exists in two different conformational states, one which is capable of binding Ii(71-88) and one which is not. The ability of invariant chain to increase the half life of the rapid on/off MHC class II conformation may allow for easier release of invariant chain from the peptide binding groove, as well as increase the time for peptide exchange within the endosomal pathway, which will lead to formation of more stable antigen- class II complexes. This mechanism likely interacts with the DM-mediated peptide release to increase the repertoire of peptides presented by MHC class II at the cell surface.

1.3.4 Protease Inhibition Activity

The alternative splicing of the invariant chain gene leads to the inclusion of a 65 residue domain with sequence similarity to the thyroglobulin type 1 domain in both p41 and p43 isoforms (O'Sullivan *et al*, 1987). This domain is found in a variety of proteins with multiple functions (Turk *et al*, 1999). To determine the function of the thyroglobulin domain in the invariant chain, *in vitro* studies were performed in which either p41 or p33 were expressed along with the MHC class II genes (Fineschi *et al*, 1995). The cells expressing p41 have a longer invariant chain half life compared to the p33 expressing cells, indicating a difference in protease degradation. Furthermore, when p41 and p33 were expressed together, it was shown that p41 also increases the half life of p33. Thus, the thyroglobulin domain appears to play a role in modulating the proteases involved in the invariant chain degradation.

The thyroglobulin domain of p41/p43 has been found to associate with cathepsin L *in vivo* (Ogrinc *et al*, 1993). Subsequent studies have shown that the p41/p43 thyroglobulin domain inhibits Cat L as the incubation of free Cat L with this fragment leads to the rapid inhibition of enzyme

activity (Bevec *et al*, 1996). This p41/p43 thyroglobulin domain represents a new class of protease inhibitor, as it does not show sequence similarity to any other cysteine protease inhibitors (Guncar *et al*, 1999). The inhibition mediated by the p41/p43 thyroglobulin domain is also very specific, as it does not inhibit Cat B, Cat C or Cat S, in contrast to many cysteine protease inhibitors which have a broad specificity (Bevec *et al*, 1996; Guncar *et al*, 1999). In addition to invariant chain, other proteins containing the thyroglobulin domain have also been shown to modulate proteolytic activity (Lenarcic and Bevec, 1998). It appears that the conserved thyroglobulin type I domain may be able to interact with a variety of proteases, and it is the individual variations of this conserved domain that give protease specificity to each protein (Turk *et al*, 1999). Structural comparisons of the interaction between Cat L and either p41/43 thyroglobulin domain or stefin B, a broad specificity inhibitor, demonstrates the specificity of p41/p43 (Guncar *et al*, 1999). While both p41/43 and stefin B bind to the bottom of the Cat L active site, the p41/43 thyroglobulin domain also binds to two regions higher up in the active site. It is these interactions that give specificity to p41, as these interactions with Cat S are unfavorable due to steric hindrance as well as electrostatic clashes between Cat L and p41 residues (Turk *et al*, 1999). Thus, multiple contact points with the cathepsin L active site results in the specific inhibition of Cat L.

In addition to a role in modulating the degradation of invariant chain, the binding of p41 to Cat L also appears to be required for the maturation of Cat L (Lennon-Dumenil *et al*, 2001). In a study of transgenic mice expressing no invariant chain or either p41 or p33 alone, it was found that there was a decrease in mature Cat L in both $Ii^{-/-}$ mice as well as p31 expressing mice, while the p41 expressing mice had normal levels of mature Cat L. It appears that p41 protects Cat L from degradation, in the absence of p41, pro-cathepsin L is processed to the active form, but it is then further degraded, either by other cysteine proteases or by active Cat L proteins.

Finally, Cathepsin L may play a role in the degradation of the extracellular matrix during an immune response (Fiebiger *et al*, 2002). In cells expressing only p41 or wild type cells, Cat L is found to be secreted from the cell. The Cat L-p41 complex is stable at neutral pH, the Cat L is active and has been shown to degrade an elastin substrate. Furthermore, there is an increase in Cat L–p41 complexes when cells are treated with IFNγ. Thus, immune system activation has the effect of increasing the secretion of active Cat L from any antigen presenting cells at the site of infection, which results in the local destruction of the extracellular matrix, allowing effector cells access to the infected site.

1.3.5 Cell Surface Expression of Invariant Chain

The invariant chain also carries out a number of functions in antigen presenting cells independent of MHC class II chaperone function. The invariant chain has been shown to be expressed at the cell surface in the absence of MHC class II (Henne *et al*, 1995). The surface expressed invariant chain appears to be the cellular receptor for the macrophage inhibitory factor (MIF), a cytokine responsible for macrophage activation (Leng *et al*, 2003). Macrophage that do not express invariant chain are unable to respond to MIF. Although the invariant chain is likely involved in the cell signaling cascade initiated by MIF binding, the cytoplasmic domain of the invariant chain is very short and unlikely to initiate the signal cascade on its own. To identify a co-receptor, groups used the results from previous studies demonstrating an interaction between invariant chain and CD44, an adhesion molecule present on the surface of all leukocytes (Naujokas *et al*, 1993; Ponta *et al*, 2003). Subsequent studies have shown that the activation of macrophage by MIF requires both invariant chain and CD44 (Shi *et al*, 2006). CD44 acts as a co-receptor for the MIF-invariant chain signal cascade by interacting with the tyrosine kinase family Src (Bourguignon *et al*, 2001). In addition, the invariant chain is phosphorylated by protein kinase A (PKA) at residues S^6 and S^8 in response to MIF binding (Shi *et al*, 2006). Thus, the binding of MIF to the invariant chain results in the activation of the intracellular protein kinases PKA and the Src family, which in turn phosphorylate the cytoplasmic domains of both invariant chain as well as CD44. This leads to the recruitment and activation of other kinases by the associated activated kinases, thus initiating the MIF signal transduction cascade, which results in the expression of genes required for activated macrophage functions.

1.3.6 Role in B Cell Maturation

The invariant chain also plays an important role in B cell maturation as invariant chain knockout mice show lower B cell proliferation in response to immunization compared to wild type mice (Shachar and Flavell, 1996). Analysis of B cells isolated from these mice shows that the cells all have an immature phenotype, as indicated by the pattern of surface markers. This inhibition of B cell maturation is caused by the absence of invariant chain as the removal of MHC class II does not result in a halt in the B all maturation process. Further analysis shows that the amino terminal region of invariant chain, from residues 1 to 82 is capable of inducing B cell maturation, as mice expressing only this fragment show a normal B cell population (Matza *et al*, 2002a). This region is able to interact with and activate the transcription factor NF-κB and its co-activator $TAF_{II}105$ and this interaction is likely required for B cell maturation (Matza *et al*, 2001).

Mutation studies have subsequently shown that the cleavage of the transmembrane segment of the invariant chain is required for the activation of NF-κB (Matza *et al*, 2002b). Recently a new strategy for the regulated release of proteins has been described (Hoppe *et al*, 2001). In this mechanism, a transcription factor is part of a larger transmembrane protein. The regulated cleavage of the larger protein results in the release of the transcription factor and this cleavage event relies on a signal to activate intramembrane cleavage proteases. The regulated intramembrane proteolysis event occurs in two steps, beginning with the removal of the large extracellular domain followed by the cleavage of the transmembrane segment (Matza *et al*, 2003). After the stepwise degradation of the invariant chain within the endosomal pathway, an unidentified protease cleaves the remaining membrane bound peptide to release the N-terminal fragment, which interacts with NF-κB to activate gene expression necessary for B cell maturation. While the signal for the activation of the regulated intramembrane proteolysis of the invariant chain has not been identified, it may come from B cell receptor activation, as the activation of the BCR causes a reorganization of MHC class II vesicles (Siemasko *et al*, 1998). This may change the pattern of invariant chain degradation and activate an intramembrane cleavage protease.

To prevent a prolonged activation of NF-κB, the invariant chain amino terminal fragment must be rapidly degraded. The invariant chain contains the destruction box sequence $R^{29}X^{30}X^{31}L^{32}$ sequence, and the mutation of this sequence increases the life span of the invariant chain fragment (Matza *et al*, 2002 b). This sequence targets the protein for ubiquitin-dependent degradation by the proteasome, which ensures a short half life for active NF-κB. This limits the length of time various genes are expressed for B cell maturation.

1.4 Coordinated Regulation of MHC Class II and Invariant Chain Expression

MHC class II dimers are constitutively expressed in macrophage, monocytes, dentritic cells and B cells. Upon exposure to IFN-γ, expression of class II genes is up-regulated in these professional antigen presenting cells and can also be induced in other cell types. This tissue specific constitutive and inducible expression of MHC class II genes is controlled by the MHC class II promoter and a number of transcription factors. A schematic representation of MHC class II promoter region is shown in figure 1.3. This region is highly conserved across the MHC class II genes and consists of three main elements, the W, X and Y boxes (Ting and Zhu, 1999). The Y box binds NF-Y while the X box binds CREB and RFX (Boss and Jensen, 2003). These transcription factors are constitutively

Figure 1.3: Transcriptional regulation of MHC class II antigen presentation pathway. (A) A schematic representation of the promoter region of the human MHC class II gene HLA-DRA, invariant chain and HLA-DM is shown. The W, X, Y and TATA box elements are common to all three genes, giving rise to coordinated constitutive and inducible tissue expression. However, each promoter also has unique elements which allows for individual control of the expression of each gene. (B) Schematic representation of the transcription factors involved in the control of expression from the class II promoter. With the exception of the Oct region, these transcription factors are also involved in the control of the invariant chain and DM expression (Ting and Zhu, 1999).

A

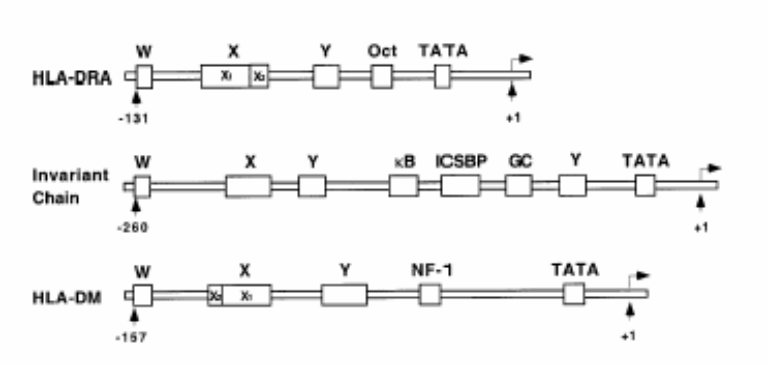
HLA-DRA
W
X
Y
Oct
TATA
X1
X2
-131
+1
Invariant Chain
W
X
Y
κB
ICSBP
GC
Y
TATA
-260
+1
HLA-DM
W
X
Y
NF-1
TATA
X2
X1
-157
+1

B

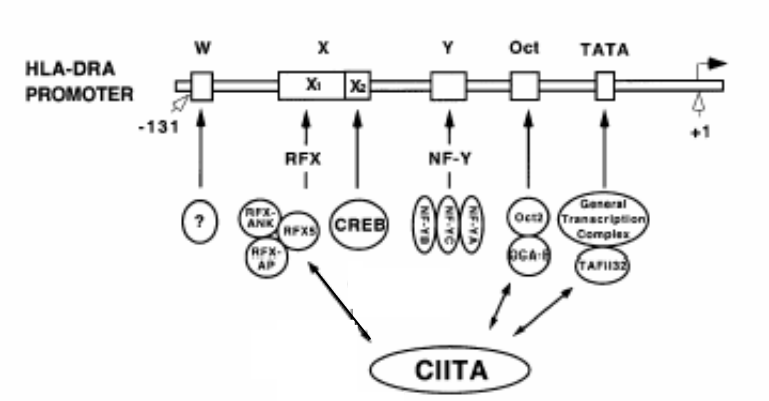
HLA-DRA PROMOTER
W
X
Y
Oct
TATA
X1
X2
-131
+1
RFX
NF-Y
?
RFX-ANK
RFX5
RFX-AP
CREB
NF-YB
NF-YC
NF-YA
Oct2
OCA-B
General Transcription Complex
TAFII32
CIITA

expressed and the complex acts as a scaffold to recruit additional transcription factors. The master control of MHC class II expression is carried out by the class II transactivator (CIITA). The expression pattern of this protein matches that of the MHC class II dimers, and genetic defects in the CIITA gene result in complete loss of MHC class II expression (Ting and Trowsdale, 2002). Regulation of CIITA expression is very complex as this gene contains four different promoter regions, with differential use of these promoters resulting in tissue-specific MHC class II expression. One of these promoters contains interferon-responsive elements, which is responsible for the up-regulation of MHC class II expression upon IFN-γ stimulation. Other promoters are constitutively expressed in the antigen presenting cells. Once the CIITA has bound to the transcription complex at the MHC class II promoter, it stabilizes the complex and recruits the general transcription factor $TAF_{II}32$, a component of the TFIID complex (Ting and Trowsdale, 2002). This facilitates the binding of RNA polymerase to the MHC class II promoter region and the subsequent transcription of the gene.

In order for proper functioning of the MHC class II antigen presentation pathway, invariant chain and DM must be coordinately expressed with the MHC class II genes. Analysis of the promoter region of both of these genes demonstrates the presence of the W, X and Y boxes, similar to those of the MHC class II promoter (Ting and Zhu, 1999). This results in a coordinated expression pattern of invariant chain and DM with MHC class II by CIITA. However, invariant chain must be present in excess of the MHC class II dimers to function properly as a chaperone. It has been shown that invariant chain is expressed in mutant antigen presenting cells which have normal MHC class II genes, but are unable to express class II due to a mutated trans-acting factor, likely the CIITA (Long *et al*,1984). As shown in figure 1.3, the invariant chain promoter contains addition elements, including the ICSBP, an element capable of responding directly to interferon stimulation (Barr and Saunders, 1991). The conserved X, Y and W boxes allow for coordinated constitutive and induced expression of the invariant chain and MHC class II, while additional elements ensure that invariant chain is expressed at a higher level than MHC class II genes, to provide a large pool of invariant chain to mediate class II folding and transport.

1.5 Immune System of Teleost Fish

The preceding discussion of the immune system is based upon the known structure and function of the mammalian immune system. While MHC receptors have been identified in all jawed vertebrates,

the immune system of humans and mice remain the most thoroughly studied. However, various groups are working to elucidate the structure and function of the immune system in a number of different species. A more thorough knowledge of various immune systems will provide insight into the evolution of the immune system and may also identify novel functions of known immune system effectors. The following discussion will focus on the current understanding of the teleost immune system, in the context of the teleost MHC genes.

1.5.1 MH Structure

A major difference between mammalian and teleost immune systems occurs within the chromosomal organization of the MHC genes. As described above, mammalian MHC genes, along with a number of genes involved in the MHC antigen loading pathways, are all encoded within the same region of a single chromosome, resulting in the linked inheritance of multiple MHC alleles by offspring. In the case of teleost fish, the MHC genes are not linked in this fashion (Shand and Dixon, 2001, Sato *et al,* 2000). A single class I loci is not linked to class II loci and in addition, class II genes also are found within two or more unlinked loci. This allows for offspring to inherit a combination of the various MHC alleles from each parent. It has yet to be determined if there is any evolutionary advantage to this organization of the immune system. Since the MHC genes are not found in a complex in teleost fish, they are instead referred to as the major histocompability (MH) genes.

There are also many similarities between the mammalian and teleost immune systems, which have been shown mainly at the level of sequence comparison between species. Multiple alleles of the MH class I and MH class II have been identified within single fish for a number of different teleost species (Shand and Dixon, 2001). This is similar to the inheritance of multiple MHC class I heavy chain genes and MHC class II loci in humans. In addition, teleosts also have a high sequence polymorphism for MH class I and class II genes (Shand and Dixon, 2001, Hasen *et al,* 1999). Thus, the inheritance of multiple polymorphic alleles from each parent occurs in teleost fish as well as mammals.

Finally, recent analysis has identified MH class II promoter elements and transcription factors with sequence similarity to mammalian genes. In zebrafish, sequences with high similarity to the human X, Y and TATA box have been identified upstream of the MH class II α genes while sequences with high similarity to the X and Y box have been identified upstream of the MH class II β (Sultmann *et al*, 1993, Sultmann *et al*, 1994). Furthermore, sequences with similarity to the transcription factor

RFX-B and its paralogue ANKRA2 have been identified in carp, zebrafish, Atlantic salmon and Japanese medaka (Long and Boss, 2005). This indicates that while the MH genes are unlinked in teleost fish, they may be regulated in a similar fashion to mammalian MHC genes.

1.5.2 Invariant Chain

In addition to the identification of MH genes, invariant chain sequences have also been identified in a number of species, including zebrafish, Atlantic salmon, fugu, catfish, carp and rainbow trout (Yoder *et al*, 1999, Sakai *et al*, 2004, Fujiki *et al*, 2003). The presence of the invariant chain gene indicates that antigen loading in the MH class II antigen presentation pathway may occur in a similar manner to the mammalian MHC class II pathway.

Two genes, the invariant like proteins Iclp-1 and Iclp-2, have been identified in zebrafish (Yoder *et al*, 1999). A schematic diagram of the proteins encoded by these genes is shown in figure 1.2. Both encode a type II transmembrane protein containing a thyroglobulin domain as well as a transmembrane domain (Yoder *et al*, 1999). In addition, Iclp-1 also has a truncated trimerization domain, which is absent in Iclp-2. The highest sequence similarity between the two zebrafish genes and the mammalian invariant chain gene occurs within the transmembrane and thyroglobulin domains. In addition, both contain putative endosomal targeting sequences in the amino-terminal cytoplasmic domain. These features indicate that the role carried out by these domains may be conserved in the zebrafish immune system. Since Iclp-2 is unable to trimerize, it is unlikely to facilitate MH class II trafficking, but may play a role in modulating protease activity, as described above for p41/p43. Iclp-1 likely performs the chaperone functions for the MH class II antigen presentation pathway in zebrafish, although no functional analysis has been performed on these genes.

Three invariant chain genes have also been identified in rainbow trout (Fujiki *et al*, 2003). Two of these genes, S25-7 and INVX are homologues of mammalian p33 and p41, while the third gene, 14-1 appears to be more closely related to zebrafish Iclp-2. A schematic diagram of the proteins encoded by these genes is shown in figure 1.2. The 14-1 sequence encodes a 21.3 kDa protein containing a thyroglobulin domain and transmembrane domain. These regions exhibit high sequence similarity to invariant chain genes in other species, including human, mouse and chicken. However, the absence of a trimerization domain indicates that this protein is not likely to act as a chaperone to facilitate MH class II trafficking, and similar to the case of Iclp-2, may be involved in modulating protease activity.

In addition, 14-1 encodes an endosomal targeting sequence in the cytoplasmic domain, which may allow co-localization with MH class II dimers in the endosomal pathway to control protease activity.

INVX, the p33 homologue, encodes a 24.6 kDa protein containing a transmembrane domain and a trimerization domain while S25-7, the p41 homologue, encodes a 31.8 kDa protein containing a transmembrane domain, a trimerization domain and a thyroglobulin domain. The transmembrane, trimerization and thyroglobulin domains of S25-7 and INVX show strong sequence similarity to tetrapod invariant chain sequences. Both S25-7 and INVX contain two endosomal targeting signals in the cytoplasmic domain, which, along with the presence of a trimerization domain indicates that both of these proteins may be capable of trafficking to the endosomal pathway. In addition, both S25-7 and INVX sequences have very hydrophobic and proline rich CLIP domains. Thus, the S25-7 and INVX may have the ability to bind to MH class II dimers to form a nonomeric structure, which can then be targeted to the endosomal pathway. Furthermore, the thyroglobulin domain in S25-7 may also play a role in the modulation of protease activity, as described for p41.

Each invariant chain is encoded by a single copy gene in rainbow trout and INVX is not alternatively spliced to give rise to S25-7, which is in contrast to the alternative splicing and alternative translational initiation associated with the mammalian invariant chain isoforms. In addition, while all three trout invariant chain genes are constitutively expressed at the transcript level in peripheral blood leukocytes, gill and head kidney, S25-7 is found at the highest levels. Within the mammalian system, in only p31 is constitutively expressed while p41 is upregulated upon IFN-γ stimulation (Albanesi *et al*, 1998). The significance of this difference in expression pattern of invariant chain isoforms between the mammalian and teleost immune system is unknown.

1.6 Purpose of Study

The purpose of this research is to study the regulation of rainbow trout S25-7 and INVX genes in response to immune system stimulation. Initial studies have indicated that there is a difference in the regulation of these genes compared to mammalian invariant chain regulation as both S25-7 and INVX are expressed in non-stimulated fish. Both *in vivo* and *in vitro* methods will be used to measure changes in S25-7 and INVX transcript and protein levels in response to PMA stimulation of the immune system. The results of this study will provide a more complete picture of the regulation of the teleost immune system and will allow further analysis of the results of the divergent evolution of teleost and mammalian immune systems.

A long term goal of this project is the production of more effective vaccination strategies for use in the aquaculture industry. In general, vaccinations consist of the injection of either live attenuated pathogens or killed pathogens. However, a new DNA vaccination strategy has recently been developed in which genes of antigenic proteins or peptides are cloned into an expression vector and this vector is injected into an individual. The plasmid is taken up by cells at the injection site and the encoded peptide is expressed and presented in MHC for T cell activation. In general, it is fairly easy to target antigenic peptides to the MHC class I antigen presentation pathway because all proteins expressed in the cytosol can be degraded and transported into the ER. However, for a prolonged $CD8^+$ T cell response, $CD4^+$ T cells must also be activated because these cells synthesize and secrete IL-2, a cytokine required for T cell proliferation (Wang, 2001). The challenge associated with activating a $CD4^+$ T cell response lies in the targeting of antigenic peptide into the endosomal pathway. This has been accomplished by manipulating an invariant chain sequence (van Bergen *et al,* 1997, Barton *et al,* 1998, Fujii *et al*, 1998). In this strategy, a full length invariant chain sequence is cloned into an expression plasmid and the CLIP region is replaced with a short antigenic sequence. The modified invariant chain protein can bind to MHC class II dimers in the ER and the complex is targeted to the endosomal pathway in the same way a wild type invariant chain protein would be. The modified invariant chain is then processed but instead of CLIP remaining in the class II groove, the antigenic peptide is bound. This complex then travels to the cell surface for presentation to $CD4^+$ T cells. By understanding the function of the teleost invariant chain proteins, it is possible to create a new invariant chain vaccination strategy to help eliminate infections in fish stocks.

Chapter 2
Materials and Methods

2.1 Cloning a Truncated INVX Fragment

2.1.1 Primer Design and PCR Conditions

The open reading frame of INVX has previously been cloned into the pGEM T easy vector and this was used as a template to clone a truncated fragment of the INVX gene, lacking both the amino-terminal intracellular domain as well as the transmembrane domain. A truncated sequence was used to increase the protein expression level as previous work has shown low expression of transmembrane proteins. The truncated fragment was amplified with a sense primer that binds 3' to the transmembrane domain, as shown in figure 2.1 (5' CGCCGGATCCCTGGTCTTGAACCAGAGG 3') and an antisense primer spanning the stop codon (5' CGCCCTCGAGGCTGTGGTTACTCATTC 3'). These primers include a GC-clamp and a restriction enzyme site at the 5' end, with a *BamHI* site in the sense primer and a *XhoI* site in the antisense primer. The fragment was amplified under the following conditions: 5 minutes at 95°C followed by 30 cycles of 95°C for 30 seconds, 51°C for 30 seconds, 72°C for 1 minute followed by a 5 minute extension at 72°C. The PCR reaction was performed in the PTC-200 thermal cycler (MJ Research). Amplification of an expected 467 base pair band was confirmed by electrophoresis on a 1% agarose gel stained with ethidium bromide and imaged on the Fluorchem 8000 chemiluminescent and visible imaging system (Alpha Innotech).

2.1.2 Ligation into pRSETA

The truncated INVX PCR fragment was digested for directional ligation into the pRSET A vector. The fragment was extracted by the addition of an equal volume of PCI (1:1 mixture of saturated phenol pH6.6 and CIAA, a 24:1 mixture of chloroform and isoamyl alcohol) followed by centrifugation at 13,000 rpm for 3 minutes in an IEC Mixromax centrifuge (Thermo Scientific). An equal volume of CIAA was added to the upper layer and the solution was centrifuged at 13,000 rpm for 1 minute. The DNA was precipitated by the addition of 1:10 volume of 3M sodium acetate and a 2:5 volume of 100% ethanol followed by incubation at -80°C for 30 minutes and centrifugation at 15,000 rpm for 15 minutes. The pellet was washed once with 70% ethanol and re-suspended in 20 μL

Figure 2.1: The position of the primers used to amplify truncated INVX DNA fragment. A 467 base pair truncated INVX fragment was amplified with a forward primer 3' to the transmembrane domain. Arrows represent primers. Abbreviations: TMD – transmembrane domain, CLIP – class II associated invariant chain peptide, TD – trimerization domain.

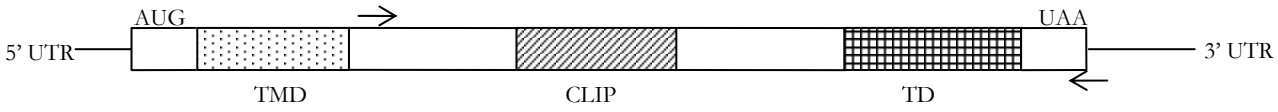
AUG
UAA
5' UTR
3' UTR
TMD
CLIP
TD

of de-ionized water. The purified fragment was then digested with 1 unit each of *BamHI* and *XhoI* overnight at 37°C, followed by a PCI/CIAA extraction and sodium acetate/ethanol precipitation as described above. The re-suspended product was separated on a 1.5% agarose gel run in 0.5 x TBE (45mM Tris-HCl, 90mM boric acid and 1mM EDTA pH8) and the 476 base pair fragment was cut out of the gel and purified with a GenElute agarose spin column (Sigma).

The pRSET A vector, shown in figure 2.2, was also digested with 2 units each of *BamHI* and *XhoI* for 2 hours at 37°C. The cut plasmid was then PCI/CIAA extracted, sodium acetate/ethanol precipitated, re-suspended in de-ionized water and gel purified as described above. The concentration of the purified plasmid was measured with a Cary 50 Bio UV visible spectrophotometer (Varian) and was adjusted to 50ng/µL with de-ionized water.

Ligation of the INVX fragment into pRSET A was performed overnight at 4°C. Briefly, 3.5µL of the INVX PCR product was mixed with 1µL of digested pRSET A, along with 4.5µL of ligation buffer and 1µL of T4 DNA ligase from the pGEM T easy kit (Promega). The reaction mixture was incubated overnight at 4°C on ice followed by one hour incubation at 14°C before transformation.

2.1.3 Transformation of Rosetta cells

The Rosetta (DE3) pLysS strain (Novagen) was chosen as a host to maximize recombinant protein expression. The DE3 strains contain a chromosomal T7 RNA polymerase gene under the control of the *lacUV5* promoter (Baneyx, 1999). In these strains the *lacUV5* promoter is repressed until the addition of isopropyl-β-D-1-thiogalactopyranoside (IPTG), which allows for strict control of recombinant protein expression. The limited T7 RNA polymerase expression allows for faster bacterial growth as transcription from the pRSET A plasmid is prevented. However, in the DE3 strains, there is some leaky expression from the *lacUV5* promoter which can result in slower cell growth. In order to prevent the expression of low levels of T7 RNA polymerase, this strain contains the pLysS plasmid which encodes the T7 RNA polymerase inhibitor T7 lysozyme. Upon IPTG induction of the *lacUV5* promoter T7 RNA polymerase is expressed and its levels exceed that of T7 lysozyme allowing for transcription from pRSET A. Finally, the pLysS plasmid in the Rosetta strain also encodes several tRNAs for codons that are rarely used in *E. coli*, allowing for higher levels of expression of mammalian proteins.

After incubation at 14°C for one hour, a 50µL aliquot of competent cells was added to the ligation reaction and this mixture was incubated on ice for 30 minutes. To transform the cells, the mixture

Figure 2.2: pRSET A plasmid map. The pRSET A plasmid has many features that make it useful as a protein expression vector. It contains a T7 promoter which allows for tight control of recombinant protein expression in DE3 IPTG inducible host cells. The vector encodes a ribosome binding sequence and an initiation ATG which allows for efficient translation initiation. In addition, the vector encodes an N-terminal tag, consisting of a 6xHis tag, the T7 gene 10 sequence and the Xpress epitope tag. This sequence is translated along with the gene of interest to result in a fusion protein that can easily be purified with metal-chelating resins. In addition, the T7 gene 10 sequence increases the stability of the recombinant protein and the Xpress epitope can be used to detect the fusion protein by western blot analysis with an anti-Xpress antibody. After the N-terminal tag sequence, there is an enterokinase cleavage site which allows cleavage of this tag from the fusion protein. A multiple cloning site allows the insertion of the gene of interest and the T7 terminator sequence ensures efficient transcriptional termination.

To allow for selection of transformed host cells, the plasmid also encodes the β-lactamase gene under the control of the *bla* promoter, resulting in host cell ampicillin resistance. Finally, the plasmid contains the pUC origin for high copy number and growth in *E. coli*. The pRSET A plasmid was chosen to give the proper reading frame of the insert

(Invitrogen, http://www.invitrogen.com/content.cfm?pageid=3436).

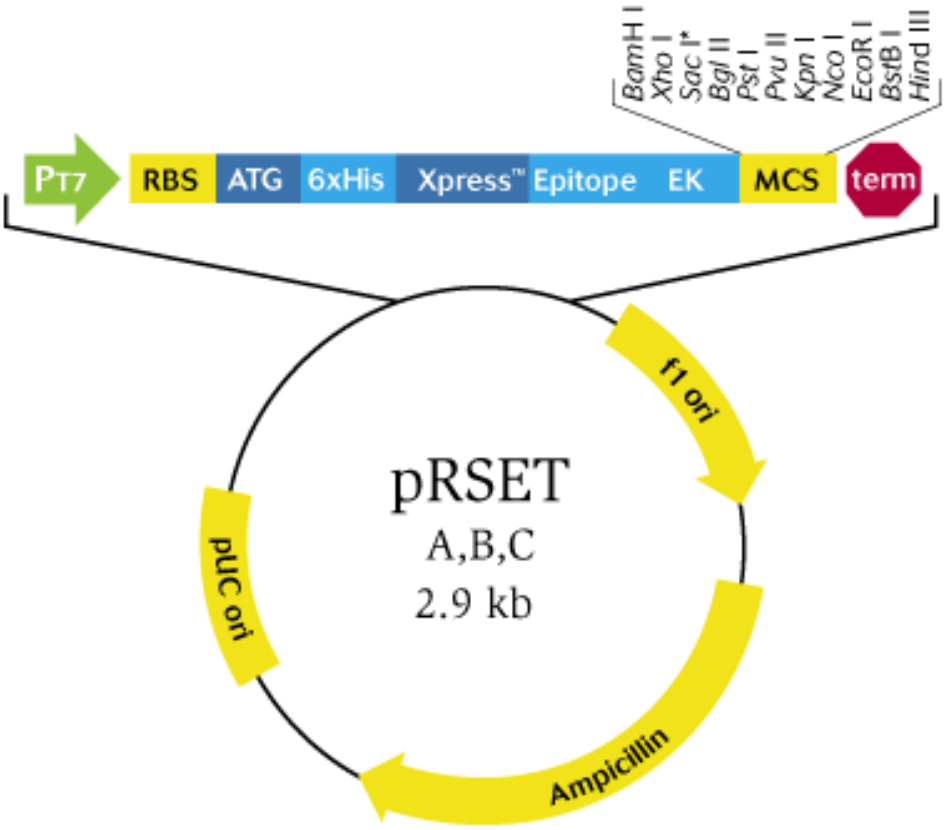
BamH I
Xho I
Sac I*
Bgl II
Pst I
Pvu II
Kpn I
Nco I
EcoR I
BstB I
Hind III
PT7
RBS
ATG
6xHis
Xpress™ Epitope
EK
MCS
term
f1 ori
pRSET
A,B,C
2.9 kb
pUC ori
Ampicillin

was heat shocked at 42°C for 45s followed by the addition of SOC media (2% tryptone, 0.5% yeast extract, 8.55mM sodium chloride, 2.5mM potassium chloride, 10mM magnesium chloride and 10mM glucose). The cells recovered for 30 minutes at 37°C before being plated on LB media (1% tryptone, 0.5% yeast extract and 172mM sodium chloride) supplemented with 100µg/mL ampicillin and 40µg/mL chloramphenicol (LB/amp/cam). The transformed cells were incubated overnight at 37°C.

2.1.4 Plasmid Isolation and Sequencing

The tINVX : pRSET A plasmid was isolated from transformed cells and subjected to sequencing to confirm the cloning of a non-mutated truncated INVX (tINVX) sequence. A single colony from the transformation plate was used to inoculate LB/amp/cam media and the bacteria were cultured overnight. The next day the cells were centrifuged at 10,000 rpm for 3 minutes and the cell pellet was re-suspended in 100 µL of solution I (50mM glucose, 25mM Tris-HCl pH8 and 10Mm EDTA pH8) followed by the addition of 200 µL of solution II (0.2N sodium hydroxide and 1% sodium dodecyl sulfate) to lyse the cells. After five minute incubation on ice, the solution was neutralized by the addition of 150µL of solution III (3M potassium acetate and 11.5% acetic acid). The mixture was then centrifuged at 15,000 rpm for 5 minutes to clear the protein-SDS complexes. Intracellular RNA was degraded by the addition of 20 µg of ribonuclease A (RNase A) followed by incubation at 37°C for 30 minutes and contaminating proteins, RNA and chromosomal DNA were removed by PCI/CIAA extraction, as described. Finally, the plasmid was precipitated with 2-propanol and the pellet was re-suspended in 20µL of de-ionized water. The concentration of the plasmid was measured with the Cary 50 Bio UV spectrophotometer and the plasmid was diluted to 0.2µg/µL and submitted to the University of Waterloo molecular core facility for sequencing. The sequencing was performed for both the forward and reverse direction and these were compared to the known INVX sequence (Fujiki *et al*¸ 2003) using Gene Runner v3.05. The amino acid sequence was identical to the published sequence.

2.2 Recombinant Truncated INVX Protein Expression

2.2.1 Pilot Expression

A small scale pilot induction experiment was performed to select high expressing, fast growing colonies and to determine the time required after induction for maximal levels of rtINVX. Single colonies were inoculated into LB/amp/cam media and were grown overnight at 37°C. The following

day, 500μL of the overnight culture was centrifuged at 4,000 rpm for 2 minutes and used to inoculate fresh LB/amp/cam media to an optical density, measured at 600nm (OD_{600}), greater than 0.1, as measured on the VERSAmax tunable microplate reader (Molecular Devices). These cultures were incubated at 37°C in the Gyrotary G10 shaker incubator (New Brunswick Scientific Company) and the OD_{600} was closely monitored. When the OD_{600} was between 0.4 and 0.6, expression of rtINVX was induced by the addition of 1mM IPTG to the culture. Before the addition of IPTG, 1mL of the culture was collected, centrifuged at 4,000rpm for 2 minutes and the pellet was stored at -20°C. Every hour after the IPTG induction, 1mL of culture was collected, centrifuged and stored at -20°C. Samples were collected for a total of 6 hours post-induction.

After collecting rtINVX-expressing cells during the pilot induction, western blot analysis was performed on these samples to examine the levels of protein expression. To lyse the cells, pellets were incubated in 8M urea buffer pH8 (8M urea, 100mM sodium phosphate and 10mM Tris-HCl) for 1 hour at room temperature on the BD Clay Adams Nutator mixer (BD Diagnostics). To denature the proteins for size separation on a polyacrylamide gel, 20μL of 5x Laemmli buffer (25% glycerol, 125mM Tris-HCl pH 6.8, 10% SDS, 0.05% bromophenol blue and 2.5% β-mercaptoethanol) was added to each sample and samples were boiled for 5 minutes. After allowing the samples to cool, 6μL of each was loaded into a 12% SDS polyacrylamide gel. The 12% resolving gel was made with 30% acrylamide/biacrylamide 37.5:1 (Biorad) and 0.375M Tris-HCl pH 8.8, along with 0.1% SDS, 0.05% ammonium persulfate and 0.05% TEMED (Sigma). The 4% stacking gel was made with the same components with the substitution of 0.125M Tris-HCl pH 6.8 for 0.375M Tris-HCl pH8.8. The electrophoresis was performed using the Mini Protein II gel apparatus (Bio-Rad) in a Tris glycine running buffer (0.2M glycine, 0.025M Tris, 0.1% SDS) at 130V until the dye front reached the bottom of the glass plates, which took approximately 2 hours.

After electrophoresis was complete, the gel was removed from the glass plates and the protein was transferred onto a nitrocellulose membrane (Pall Corporation). Briefly, the gel and membrane were sandwiched between two filter papers (Fisher) and two sponges and this was placed in the Transblot Cell (Bio-Rad) and transferred overnight at 22V. Following the transfer, the membrane was removed and stained with Ponceau S stain (0.2% Ponceau S in 5% acetic acid) to examine transfer and analyze equal protein loading between samples. After scanning with the AIO Printer A920 (Dell Computers), the membrane was de-stained in T-TBS pH8 (140mM sodium chloride, 2.5mM potassium chloride, 2.5mM Tris and 0.05% Tween20).

To block unbound regions, the membrane was incubated in blocking buffer (5% skim milk in T-TBS) for 2 hours at room temperature. The express epitope encoded within the amino-terminal tag of rtINVX was detected by probing with the anti-express antibody (Invitrogen) at a 1:5,000 dilution in blocking buffer. Binding of the primary antibody was detected by probing with the goat anti-mouse IgG alkaline phosphatase linked secondary antibody (Sigma) at a 1:30,000 dilution in blocking buffer. Both the primary and secondary antibodies were incubated with the membrane for 1 hour at room temperature. To eliminate non-specific binding of either primary or secondary antibodies, a series of three 5 minute washes in T-TBS was repeated after both primary and secondary incubations. After the final wash, the membrane was equilibrated in alkaline phosphatase buffer pH9.5 (100mM Tris, 100mM sodium chloride and 5mM magnesium chloride) for 5 minutes and rtINVX was detected with bromochloroindolylphosphate (BCIP) / nitro blue tetrazolium (NBT) substrate (0.0165% BCIP and 0.033% NBT in alkaline phosphatase buffer). The membrane was incubated in the substrate in the dark until a purple band developed, at which time de-ionized water was added to stop the reaction.

2.2.2 Full Scale Protein Induction

A single colony was inoculated into 50mL of LB/amp/cam and incubated overnight at 37°C. The culture was centrifuged at 4,000 rpm for 2 minutes in the IEC desktop centrifugre (Fisher Scientific) and used to inoculate 2L of fresh LB/amp/cam to an OD_{600} greater than 0.1. This was incubated at 37°C in the Gyrotary G10 shaker incubator until the OD_{600} was between 0.4 and 0.6 at which time protein expression was induced by the addition of 1mM IPTG. Two hours after induction, the culture was centrifuged at 10,000 rpm for 10 minutes in the Sorval RC5B (DuPont) centrifuge. The cell pellet was then lysed for protein purification, as described in the next section.

2.2.3 Protein Purification

The positive charge of the poly-histidine tag was exploited to isolate rtINVX protein by affinity purification using nickel resin. The cell pellet was re-suspended in 5mL of lysis solution (25% sucrose, 50mM Tris-HCl pH8, 1mM EDTA, 1mM PMSF, 1mM DTT, 1% Triton X-100 and 0.1% lysozyme) and incubated on ice for 30 minutes. Genomic DNA was degraded by the addition of 30mM magnesium chloride and 150µg of deoxyribonuclease I (Sigma) with 30 minute incubation at room temperature on the Nutator mixer. The volume of the lysate was then topped to 100 mL with 8M urea buffer pH8 and incubated on the Nutator mixer for 2 hours at room temperature. Cellular debris was cleared by centrifugation at 10,000 rpm for 20 minutes, followed by the addition of 2mL

Figure 2.3: Nickel Column Purification of rtINVX protein. The rtINVX expressing cells were lysed under denaturing conditions with 8M urea buffer. The recombinant fusion proteins have a positively charged 6xHis tag at the amino-terminus, which binds to negatively charged nickel resin to allow for protein purification. After an overnight incubation with Ni-NTA resin, the unbound proteins were removed from the column. Stepwise decreases in the pH of the 8M urea buffer allowed for the elimination of non-specifically bound host proteins followed by the elution of the fusion rtINVX protein.

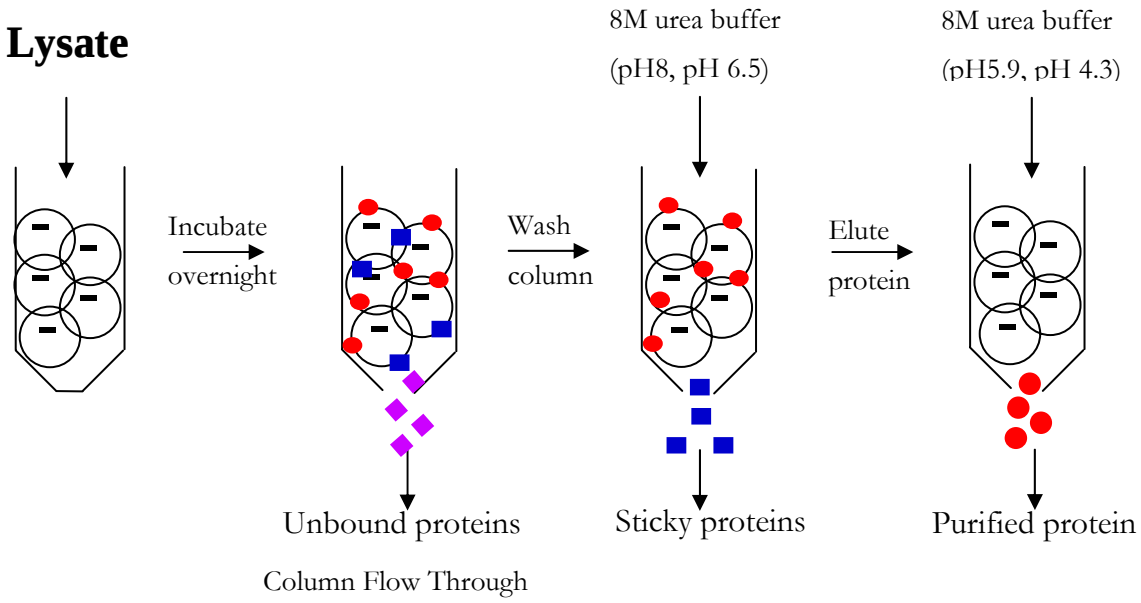
Lysate
Incubate
overnight
Unbound proteins
Column Flow Through
Wash
column
8M urea buffer
(pH8, pH 6.5)
Sticky proteins
Elute
protein
8M urea buffer
(pH5.9, pH 4.3)
Purified protein

of 50% Nickel –nitrilotriacetic acid resin (Qiagen) in 8M urea buffer pH8. The lysate was incubated with the nickel resin overnight on the Nutator Mixer at room temperature to allow for rtINVX binding.

To clear unbound proteins, the mixture was centrifuged at 4,000 rpm for 5 minutes and the supernatant, containing the unbound protein fraction, was removed. The resin was washed once with 10mL of 8M urea buffer pH8 and was re-suspended in 10mL of 8M urea buffer pH6.5. The slurry was then poured into a column and the flow through was collected. To elute non-specifically bound proteins, the resin continued to be washed with 8M urea buffer pH6.5 until no protein was detected in the column flow through, as determined by Bradford assay. The Bradford assay was performed by combining 20µL of the column flow through with 180µL of Bradford reagent (10% coomassie brilliant blue in 8.5% phosphoric acid). The colour of this reaction was compared by eye to the colour of a blank reaction in which 20µL of 8M urea buffer pH 6.5 was added to 180µL Bradford reagent. The pH of the 8M urea buffer was decreased when the reactions appeared to be the same colour as this indicated the complete elution of non-specific protein. Elution of rtINVX was achieved by the addition of 8M urea buffer pH5.9 to the column. The resin was washed with 1mL volumes of this buffer until the Bradford assay showed no protein in the column elution. Finally, the resin was washed with 8M urea buffer pH4.3 to elute any remaining protein bound to the nickel resin. Protein elutions were stored at 4°C.

Elutions from the nickel resin were separated on a 12% polyacrylamide gel and subjected to both western blotting and coomassie staining to examine the quality of the isolated protein. Samples from the unbound protein fraction, pH8 and pH6.5 washes, along with pH5.9 elutions were analyzed by western blotting, as described above. For coomassie staining, 16µL of each sample was mixed with 4µL of 5x Laemmli buffer, boiled and separated at 130V as described for the western blot. However, instead of transferring the proteins to a nitrocellulose membrane, the gel was stained in Coomassie blue G-250 (J. T. Chemical Co.) for one hour, de-stained in 45% methanol, 10% acetic acid and imaged with the Fluorchem 8000.

The concentration of the rtINVX elutions were measured by the Bradford assay. Briefly, 20µL of the sample was mixed with 180µL of Bradford reagent and the absorbance was read at 595nm on the VERSAmax tunable plate reader. A standard curve was also generated by mixing 20µL of BSA standards at 1mg/mL, 0.6 mg/mL, 0.5 mg/mL, 0.4 mg/mL, 0.3 mg/mL, 0.2 mg/mL, 0.1 mg/mL and

0.05 mg/mL in 8M urea buffer pH8 with 180µL of Bradford reagent. The standard curve was used to calculate the concentration of the elutions based on the absorbance from the Bradford assay.

2.3 Development of a Polyclonal Rabbit Anti-rtINVX Antibody

2.3.1 Preparation of Antigen for Immunization and Serum Collection

In order to produce polyclonal antibodies, two female New Zealand White rabbits (Charles River Canada) were immunized with rtINVX. The rtINVX-containing nickel column elutions were pooled together in dialysis tubing (Fisher) and concentrated using polyethylene glycol. The sample was then dialyzed into 4M urea buffer pH8 for 3 hours at 4°C and the concentration was measured by Bradford assay, as described above. A BSA standard curve was constructed as described above with the exception that the BSA was diluted in 4M urea buffer pH8. Once the sample reached 1mg/mL, it was further dialyzed into 2M urea buffer for 3 hours at 4°C, into 1M urea buffer overnight at 4°C and finally into 1xPBS (140mM sodium chloride, 2.7mM potassium chloride, 4.3mM sodium phosphate and 1.5mM potassium phosphate) overnight at 4°C.

To prepare the sample for immunization, 500µL of rtINVX was combined with 500µL of Freund's complete adjuvant (Sigma) and 20µg of Keyhole Limpet Hemocyanin (Calbiochem). This mixture was vortexed on high for 45 minutes and was taken up into a 1mL syringe. This was performed in duplicate for the immunization of two animals. The vaccine was injected intramuscularly at 4 sites by the animal care technician.

In order to maximize the antibody production, these animals were boosted three times over 9 a week period at 3 week intervals. The vaccine was prepared in the same manner as described above except that Freund's incomplete adjuvant was substituted for the complete adjuvant and the amount of KLH was decreased by half for each subsequent boost. Twelve weeks after the initial immunization the animals were exsangunated and the rtINVX antiserum was collected.

2.3.2 ELISA: Determination of Antibody Titre

Enzyme-linked immunosorbent assays were performed to monitor anti-rtINVX antibody titre during the rabbit immunizations. Before the initial immunization and before each boost, approximately 10mL of blood was collected from the ear canula of each rabbit. The blood was left to clot for 2 hours at room temperature followed by an overnight incubation at 4°C. The blood was then

centrifuged at 3,000 g for 10 minutes at 4°C and the serum was transferred into a fresh tube and stored at -20°C until ELISA analysis was performed.

A 96 well plate (Evergreen Scientific) was incubated overnight with 1µg of either rtINVX or KLH diluted in coating buffer pH9.6 (15mM sodium carbonate, 35mM sodium bicarbonate and 0.02% sodium azide) at room temperature to allow antigen binding. The next morning the antigen suspensions were removed and 300µL of blocking solution (1%BSA in 1xT-TBS) was added, followed by incubation at 37°C for 1 hour. After the blocking step, 100µL of the following serum dilution, made in blocking buffer, were added to the plate: $^{1}/_{100}$, $^{1}/_{500}$, $^{1}/_{1,000}$, $^{1}/_{5,000}$, $^{1}/_{10,000}$, $^{1}/_{50,000}$, $^{1}/_{100,000}$ and $^{1}/_{500,000}$. Analysis of each dilution was performed in triplicate. To detect the serum antibodies 100µL of anti-rabbit IgG alkaline phosphatase conjugated antibody (Sigma), diluted to 1:5,000 in blocking buffer was added to the plate. Both primary and secondary antibody incubations were performed for 1 hour at room temperature. After both the primary and secondary antibody incubations the plate was washed three times with T-TBS. Bound secondary antibody was detected with the p-NPP alkaline phosphatase substrate from the Sigma FAST™ p-Nitrophenyl Phosphate tablet system. Briefly, one of each tablet from the kit was dissolved in 20mL of Milli-Q water, and 50µL of this substrate was added to each well. After 30 minute incubation in the dark at room temperature, 50µL of 0.03M sodium hydroxide was added to stop the reaction and the absorbance was read at 405nm.

2.3.3 Antibody Purification

To reduce background noise when performing western blot analysis, the anti-rtINVX antibody was affinity purified from the antiserum. The first step of the purification involved the binding of rtINVX to sulfolink resin (Pierce). This resin has an iodoacetyl group which can bind to reduced cysteine residues on any protein. To begin, 6mg of rtINVX, at a concentration of 0.5mg/mL, was dialyzed into coupling buffer pH8.5 (50mM Tris and 5mM EDTA). Sulfolink resin was then washed with 8mL of coupling buffering to remove the storage buffer (10mM EDTA, 0.05% sodium azide and 50% glycerol) and 3mL of rtINVX was added to column. The protein was incubated with the resin at room temperature with rocking for 15 minutes and then overnight at 4°C. The unbound protein was collected from the column and another 3mL of rtINVX was added and allowed to bind. This was repeated for all 6mg of rtINVX.

Figure 2.4: Affinity purification of anti-rtINVX antibody. The rtINVX protein was linked to sulfolink resin by the reaction of a reduced rtINVX cysteine side chain with an iodoacetyl group on the resin. After blocking any unbound iodoacetyl groups, crude antiserum was added to the column. After an overnight incubation unbound antibodies were removed from the column and non-specially bound antibodies were eliminated with sample buffer washes. Finally, the anti-rtINVX antibody was eluted in 100mM glycine pH2.5.

Binding of rtINVX to Sulfolink Resin

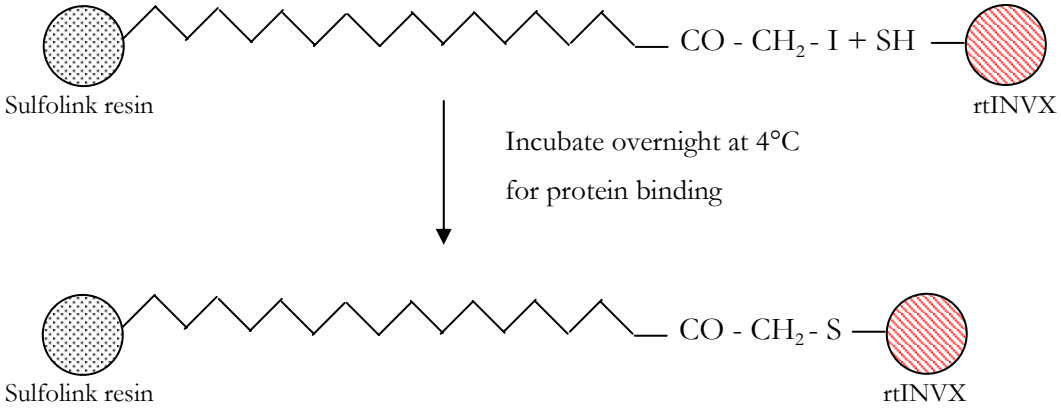

Affinity Purification of anti- rtINVX antibody

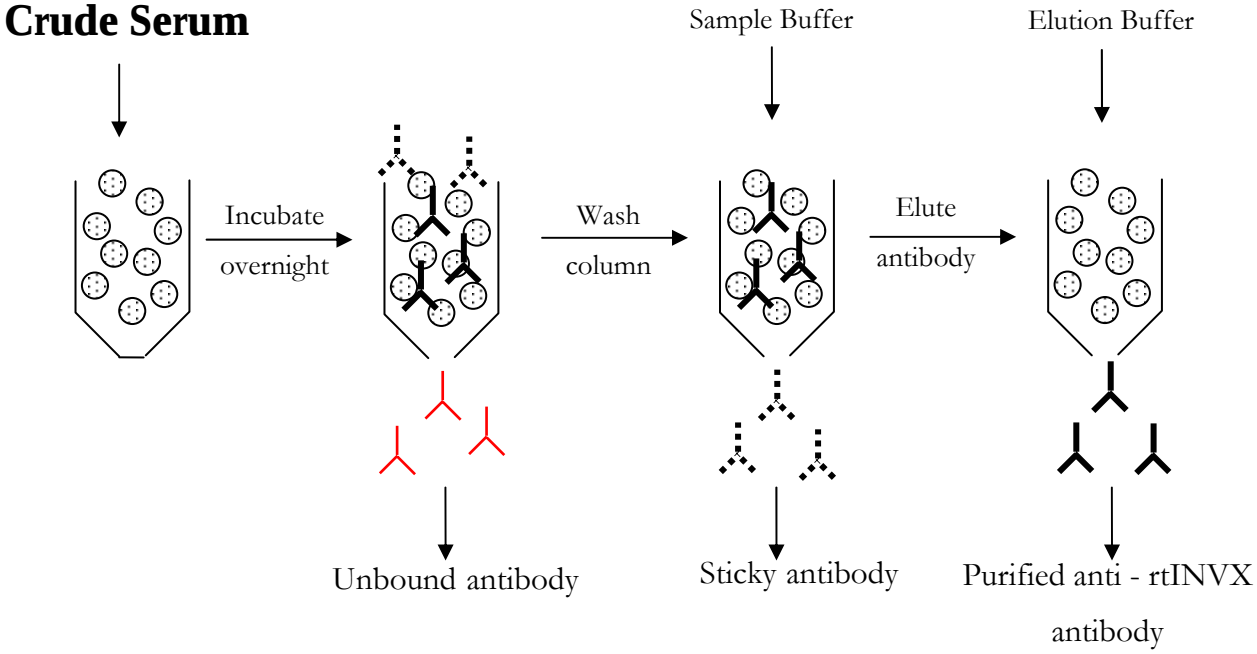

Coomassie staining was performed to examine the protein bound sulfolink resin. Briefly, 100µL of resin was collected from the column, mixed with 20µL of 5x Laemmli buffer, boiled for 5 minutes and centrifuged. The supernatant was loaded onto a 12% polyacrylamide gel along with samples from the column flow through and sample of 0.5mg/mL rtINVX. Electrophoresis and staining were performed as described above. Since the resin showed a high level of rtINVX binding, excess iodoacetyl residues were blocked by the addition of 16mg of cysteine to the column. The column was incubated for 15 minutes at room temperature with rocking followed by 30 minutes without rocking to allow the resin to settle. The cysteine was removed from the column and the resin was washed with 12mL of wash buffer (1M sodium chloride and 0.05% sodium azide). Finally, the resin was washed with 1xPBS + 0.05% sodium azide and the column was stored at 4°C until needed for antibody purification.

To purify anti-rtINVX antibodies, 1.5mL of crude serum was added to the column. This was incubated with rocking for 15 minutes at room temperature followed by 30 minutes without rocking and overnight at 4°C. The column flow through was collected and the resin was washed with 12mL of sample buffer pH8 (0.1M sodium phosphate and 5mM EDTA). The antibody was eluted in 1mL volumes of 100mM glycine pH2.5. A Bradford assay was performed to monitor antibody elution, as described above for protein purification, with the exception of 100mM glycine pH2.5 as the blank. The eluted antibody was neutralized with 100µL of 1M Tris-HCl pH7.5 + 0.05% azide and stored at -20°C until needed. The column was neutralized with 1xPBS + 0.05% sodium azide and stored at 4°C.

2.4 *In vivo* Time Course

2.4.1 PMA Immunostimulation and Tissue Collection

Eighty rainbow trout ranging in size from 150g to 300g were obtained from Mimosa Springs trout farm in Guelph, Ontario. These animals were maintained in 13°C water in the aquatic facility at the University of Waterloo for two months before starting the immunostimulation time course.

Phorbol 12-myristate 13-acetate (PMA, Sigma) is a stimulator of protein kinase C (Nishizuka, 1984). This was used to stimulate an immune response because PKC is involved in a number of signal transduction cascades, including B and T cell receptor signaling cascades (Janeway *et al*,

2001). Fish were anesthetized in ethyl 3-aminobenzoate methanesulfonate salt (MS-222, Sigma), weighed and injected intraparetioneally with 0.5µg PMA per gram body weight. This concentration of PMA was chosen based on preliminary studies comparing the ability of a variety of PMA concentrations to induce an immune response. Sixty fish were treated with PMA, placed in two tanks and sacrificed at regular time points. At 8 hours, 48 hours and 120 hours after treatment, 9 fish were collected from tank 1 and at 24 and 96 hours after treatment 9 fish were collected from tank 2. At the 168 hour time point only 7 fish were collected as some fish died after the injection. Since mineral oil was used as a carrier for the PMA, 9 fish were treated with mineral oil as a control and tissues were collected from these fish 168 hours after treatment.

For tissue sampling, the fish were again anesthetized in MS-222. Blood was collected from the caudal vein and 200 units of heparin (in 0.85% sodium chloride) was added to prevent clotting. In addition, gill, spleen, head kidney and liver samples were collected from all fish. These tissues were placed in sterile eppindorf tubes and flash frozen in liquid nitrogen and stored at -80°C until needed for analysis.

The peripheral blood leukocytes were isolated from blood based on the differing density of leukocytes compared to erythrocytes. Blood was centrifuged at 200g for 10 minutes at room temperature and the buffy coat was transferred into a new tube. The volume was topped up to 25mL with L-15 media (Sigma) and 10mL of histopaque-1077 (Sigma) was layered at the bottom of the sample. This was centrifuged for 1 hour at 400g and the leukocyte layer at the histopaque-L15 interface was transferred into a new tube. An equal volume of L-15 was added and the sample was centrifuged at 400 g for five minutes. The pellet was re-suspended in 1mL of 1xPBS, transferred into an eppindorf tube and centrifuged at 400g for 1 minute. The pellet was flash frozen in liquid nitrogen and stored at -80°C until needed for analysis.

2.4.2 Total RNA Isolation

Total RNA was isolated from 50mg tissue pieces. Tissue was homogenized in 500µL of Trizol (Invitrogen) with a motorized pellet pestle and genomic DNA was sheared with a 23 gauge needle. An additional 500µL of Trizol was added and the mixture was incubated at room temperature for 5 minutes, after which 200µL of chloroform (Fisher Scientific) was added. This mixture was vortexed for 20 seconds, allowed to settle and centrifuged for 15 minutes at 12,000 g. RNA was precipitated by the addition of 500µL of 2-propanol to the upper layer, followed by 10 minute incubation at room

temperature and centrifugation for 10 minutes at 12,000 g. The RNA pellet was washed with 1mL of 70% ethanol in DEPC-water and centrifuged for 5 minutes at 7,500 g. The pellet was re-suspended in 20µL - 80µL of DEPC-water (Fermentas first strand cDNA synthesis kit), depending on the pellet size, and heated at 70°C to aid dissolving. The concentration of the RNA was measured at 260nm on the Cary UV 50 visible spectrophometer and was stored at -80°C until needed for analysis.

2.4.3 Northern Blotting

Three micrograms of total RNA was separated on an agarose gel and transferred to a nylon membrane for detection of S25-7 and INVX transcripts. The RNA was denatured with 1 hour incubation at 50°C in 6.75% glyoxal, 50% dimethyl sulfoxide and 20mM sodium phosphate pH7. Following this incubation the mixture was quenched on ice for 3 minutes and 2µL of loading dye (50% glycerol, 10mM sodium phosphate pH7, 0.25% bromophenol blue, 0.25% xylene cyanol) was added. The entire sample was then loaded into a 1% agarose gel and separated in 10mM sodium phosphate pH7. To prevent RNA degradation the Mupid electrophoresis unit (Helix technologies) was treated with 5% hydrogen peroxide and the running buffer was treated with diethyl pyrocarbonate (DEPC, Sigma). The samples were elctrophoresed at 50V until the bromophenol blue dye front reached approximately ¼ from the bottom of the gel, which took approximately 90 minutes. During the elctrophoresis 100mL of running buffer was circulated from the cathode to the anode every 15 minutes to ensure constant pH. After electrophoresis the gel was stained with 1µg/mL of ethidum bromide in 50mM sodium hydroxide, followed by neutralization in 0.2M Tris-HCl pH7.4. The gel was visualized on the Fluorchem 8000 followed by incubated in 10xSSC (1.5M sodium chloride and 0.15M trisodium citrate dehydrate).

After the electrophoresis, RNA was transferred onto a nylon membrane (Osmonics Inc). A long piece of filter paper was soaked in 10xSSC and the ends were placed in a pool of 10xSSC. This was used as the wick to draw up 10xSSC for RNA transfer. The gel was placed onto a soaked filter paper and both were placed on top of the wick. A nylon membrane cut to the exact size of the gel was soaked in de-ionized water, equilibrated in 10xSSC and placed on top of the gel. To prevent buffer bypass plastic wrap was placed around the gel and another soaked filter paper, also cut to the size of the gel, was placed on top of the membrane. A pipette was rolled across the filter paper to remove any air bubbles trapped between the gel and the membrane. Finally, two more filter papers and a stack of paper towels, all cut to the size of the gel, were placed on top of the filter paper. A weight was placed on top of the transfer apparatus and this was left overnight to allow for RNA transfer.

The next morning the transfer was disassembled and the gel was imaged on the Fluorochem 8000 to ensure RNA transfer. The membrane was soaked in 2xSSC and air dried for 30 minutes, followed by UV crosslinking on Fluorchem 8000. The membrane was then stored at room temperature between two filter papers until probed.

2.4.4 Preparation of a DIG-Labeled Probe

Digoxigenin labeled DNA probes were used to detect S25-7 and INVX transcripts in the northern blots. As a control, the 40S ribosomal protein S11 transcript was also detected and used to correct for any unequal RNA loading. Plasmids encoding fragments of these genes were used as a template to amplify the DIG-labeled probes. A cDNA fragment of S25-7 previously cloned into pcDNA3.1 was used as a template for S25-7 DIG probe synthesis. A template for the INVX probe was constructed by amplifying a fragment of the INVX 3' UTR from gill cDNA and cloning it into pGEM T-easy (Promega) with the following primers: INVX sense (5' TCAACCACAGCACCTGATGG 3') and INVX antisense (5'GGGATGGGAAAGTTTGGGTG '3). A fragment of the S11 cDNA sequence was also amplified and cloned into pGEM T easy with the following primers: S11 sense (5' AGCAGCCAACCATCTTCCAG 3') and S11 antisense (5' ACTCTCCGACGGTAACAATG 3'). Both INVX and S11 fragments were amplified under the following conditions: 95°C for 5 minutes, 35 cycles of 95°C for 30 seconds, 55°C for 30 seconds, 72°C for 1 minute, followed by a 5 minute extension at 72°C. The INVX and S11 fragments were separated on a 1% agarose gel, purified and ligated as described for pRSET A ligation, with the substitution of 50ng pGEM T-easy plasmid for pRSET A. The ligation reaction was transformed into XL1-blue *E. coli* competent cells and plasmids were purified from white colonies and sequenced to verify the INVX and S11 inserts.

The DIG labeled probes were synthesized with the DIG probe synthesis kit (Roche) which contains dUTP nucleotides bound to digoxigen molecules. The DIG label is inserted into the PCR product and can be recognized by an antibody during northern blot detection. Plasmids encoding gene fragments were used as a template for the probe reaction and the primers for S25-7 are as follows: S25-7 sense (5' GGAGAAGCCCCCCT 3') and S25-7 antisense (5'ATCATCCTGGGGAAAGCTGC 3'). The primers used to clone INVX and S11 into pGEM T easy were also used for synthesis of the DIG-labeled probes. The probes were amplified under the following conditions: 95°C for 2 minutes, 35 cycles of 95°C for 30 seconds, 55°C for 30 seconds, 72°C for 2 minutes followed by a 7 minutes extension time. A control reaction, without DIG-dUTP, was run in parallel. Both the labeled and

unlabeled fragments were separated on a 1.5% agarose gel and visualized with the Fluorchem 8000 to verify DIG labeling, indicated by a size difference between the labeled and unlabeled fragments.

2.4.5 Detection of Northern Blot

To detect INVX or S25-7 transcripts, the membrane was first soaked in 2xSCC and placed in hybridization buffer (4.65xSSC, 46.5% formamide, 46.5 mM sodium phosphate pH7, 1.9% blocking reagent, 0.1% sarkosyl and 6.5% SDS). Pre-hybridization of the membrane was carried out at 50°C for 2 hours. During this time the probe solution was prepared by the addition of 19μL of either the S25-7 and S11 probes or the INVX and S11 probes to 6mL of hybridization buffer. This solution was boiled for 10 minutes, quenched on ice and added to the membrane. The hybridization of the probe to the blot was performed overnight at 50°C with gentle rotation. After hybridization, the membrane was washed for 5 minutes at 20°C with 2 x wash buffer (2xSSC with 0.1% SDS) followed by two washes at 65°C with 0.1 x wash buffer (0.1xSSC with 0.1% SDS). The membrane was then incubated for 5 minutes in DIG buffer 1 (0.1M maleic acid and 0.15M sodium chloride). The membrane was blocked with DIG buffer 2 (1% blocking reagent in DIG buffer 1) for 30 minutes and then probed with an anti-digoxigenin alkaline phosphatase conjugated antibody (Roche) at a 1:10,000 dilution for 30 minutes. The membrane was washed 5 times in DIG buffer 1 containing 0.03% Tween 20, followed by a 5 minute wash with DIG buffer 3 (0.1M Tris-HCl pH9.5, 0.1M sodium chloride and 50mM magnesium chloride). The substrate CDPstar (Roche) was added to the membrane and the membrane was placed in a sealing bag and incubated for 15 minutes at 37°C.

Due to differences in signal strength between S25-7 and INVX blots, different detection methods were utilized. The S25-7 northern blots were detected on the Fluorchem 8000 using the chemiluminescence filter with an open iris and no light for 20 minutes under medium sensitivity. The INVX northern blots were detected with x-ray film (Pierce). The film was placed on the blot in an x-ray cassette and this was left to expose for 10 minutes, 15 minutes and overnight at -80°C. The film was developed with the CP1000 automatic film processor (AGFA) and the blots were scanned with the A920 printer (Dell Computers).

2.4.6 Densitometry Analysis of the Northern Blot

Densitometry analysis was performed to measure changes in S25-7 and INVX transcript levels. The intensitys of the INVX, S25-7 and S11 signals were measured with the Total Lab 100 (Fotodyne Inc.)

analysis software and the ratio of S25-7 and INVX to S11 was calculated to correct for unequal sample loading. An area of interest was created around all bands and automatic detection was used to create lanes, measure background and detect bands. The bands were detected with a minimum slope of 100, as a measure of how pronounced the band was from the background, a noise reduction value of 5 to eliminate small local peaks and a percentage maximum peak of 3 to discard peaks that were less than this percentage of the largest detected peak. The rolling ball background subtraction method was used with a radius of 200. The program did not always automatically recognize all lanes and bands, in which case manual lane addition and band detection was performed. Finally, in some cases the background of the membrane was very high and a smaller radius was used for the background. By calculating the ratio of the S25-7 and INVX band volumes to the S11 band volumes, changes in S25-7 and INVX transcript levels can be measured. The average of the INVX/S11 and S25-7/S11 ratios was calculated for each time point and the results were plotted along with error bars representing the standard deviation of these means.

2.4.7 RT-PCR

The amount of RNA isolated from peripheral blood leukocytes (PBLs) was to low to perform northern blot analysis, instead reverse transcriptase PCR was used to examine INVX and S25-7 transcript levels. The first strand cDNA synthesis kit (Fermentas) was used to synthesize cDNA from 0.5µg of total RNA. The RNA was incubated for at 70°C with a poly$(dT)_{18}$ primer for 2 minutes to allow primer binding. The reaction was quenched on ice for 3 minutes and the reverse transcriptase reaction mixture was added (5 x reaction buffer, 10mM dNTPs, RNase inhibitor and MMLV reverse transcriptase). This was incubated at 37°C for 1 hour to allow cDNA synthesis followed by 5 minutes at 95°C. The cDNA was stored at -20°C until needed.

As a control for RT-PCR, the elongation factor EF-1α transcript was used to correct for unequal loading. Amplification of PBL transcripts was performed with the following primers: INVX sense (5' CAAACCCTGAGCCTCTGACC 3'), INVX antisense (5' GTCTGGTTCACATCTCTTGG 3'), Ef1α sense (5' GAGTGAGCGCACAGTAACAC 3') and Ef1α antisense (5' AAAGAGCCCTTGCCCATCTC 3'). The primers used for S25-7 amplification are the same as described above for S25-7 DIG probe synthesis. For amplification, 1µL of undiluted cDNA was amplified under the following conditions: 95°C for 5 minutes followed by 28 cycles or 29 cycles of 95°C for 30 seconds, Tm for 30 seconds and 72°C for 1 minute followed by a 5 minute extension at 72°C. The Ef1α transcripts were amplified with 28 cycles at 57°C, S25-7 for 29 cycles at 57°C and

INVX for 29 cycles at 55°C. PCR reactions were separated on a 1% agarose gel, stained with ethidium bromide and imaged with the Fluorchem 8000.

RNA samples from all tissues collected from the first three sets were also analyzed for interleukin-1β expression by RT-PCR. The cDNA was synthesized as described above and 1μL of cDNA was amplified for either IL-1β or Ef-1α as a loading control. The following primers were used: IL-1β sense primer (5' CCTGATGAATGAGGCTATGG 3') and IL-1β reverse primer (5' TTCCTGAAACTGGCAGACTC 3'). The PCR conditions for IL-1β amplification were as follows, 95°C for 5 minutes followed by 35 cycles at 95°C for 30 seconds, 53°C for 30 seconds, 72°C for 1 minute, followed by a 5 minute extension at 72°C. These reactions were run out on a 1% agarose gel, stained with ethidium bromide and imaged with the Fluorchem 8000. The control Ef1α was also amplified, with a Tm of 57°C and 27 cycles.

Finally, to compare with northern blot results, all tissues from the first three sets were examined for INVX transcript level by RT-PCR. Again, cDNA was synthesized as described above and a duplex PCR reaction was set up with amplification of 1μL of cDNA with both the INVX primers and Ef1α primers with the following conditions: 95°C for 5 minutes followed by 27 cycles of 95°C for 30 seconds, 55°C for 30 seconds, 72°C for 1 minute followed by a 5 minute extension at 72°C. These reactions were separated on a 1% agarose gel, stained with ethidium bromide and imaged on the Fluorchem 8000.

To measure the change in INVX, S25-7 and IL-1β transcript levels, densitometry analysis was performed with the Total Lab 100 software, as described above. The ratio of the volume of the INVX, S25-7 and IL-1β bands to the volume of the Ef-1α band was used to correct for unequal sample loading.

2.4.8 Total Protein Isolation

Total cellular protein was extracted from 100 – 200mg pieces of tissue for western blot analysis. Lysis buffer (1% non-idet P40, 50mM Tris-HCl pH7.4 and 0.15M sodium chloride) was added to tissue samples at a ratio of 2.5 μL/mg tissue and samples were kept on ice at all times. To prevent protein degradation, the lysis buffer was supplemented with a number of protease inhibitors, including 2mM PMSF and a protease inhibitor cocktail (Sigma), consisting of AEBSF, EDTA, Bestatin, E-64, leupeptin and aprotinin. This resulted in wide spread inhibition of serine, cysteine and metalloprotein protease inhibitors in tissues.

The tissues were lysed on ice with brief pulses of sonication after which cellular debris was cleared by centrifugation at 15,000 rpm for 10 minutes at 4°C. The lysate was transfer to a new tube and the protein concentration was measured by a modified Bradford assay. The lysate was diluted 1:5 in lysis buffer, and 2µL of this was diluted in 80µL of de-ionized water. This dilution was used to prevent interference from the NP-40 detergent. The Bradford was performed as described above and a BSA standard curve made in a 1:40 diluted NP-40 buffer was used to calculate protein concentration.

2.4.9 Western Blot Analysis

One hundred milligrams of total protein was separated in a 12% polyacrylamide gel and transferred overnight, as described above. After ponceau staining, the membrane was blocked for 2 hours at room temperature and probed with either anti-rtINVX antibody at a 1:80 dilution or anti-rTg antibody at a 1:150 dilution in blocking buffer for 1 hour. Following three 5 minute washes in T-TBS, the membrane was probed with anti-rabbit IgG horse radish peroxidase conjugated (Promega) at a 1:2,000 dilution in blocking buffer for 1 hour. After another three 5 minute T-TBS washes, 1mL of ECL plus substrate (Amersham) was added to the membrane and incubated for 5 minutes in the dark. The blot was detected on the Fluorchem 8000 using the chemiluminescence filter for 10 minutes on medium sensitivity.

2.4.10 Densitometry Analysis for Western blotting

The densitometry analysis of western blots was performed with the Total Lab 100 software, as described above. Both S25-7 and INVX are detected as a doublet, in order to quantify the total amount of protein, the intensity of both bands in the doublet were added together. As a control for equal sample loading, the intensity of a 50kDa band from the ponceau was measured. The ratio of the S25-7 and INVX bands to this control band was calculated to measure changes in protein levels. The 50kDa band is common to all blots and was used for analysis because there is no antibody against a control protein with unchanging levels.

2.5 *In vitro* Time Course

The macrophage-like cell line RTS-11 was also stimulated with PMA to examine changes in S25-7 and INVX levels. This cell line was developed and is maintained by the Bols lab at the University of Waterloo and the cells were generously provided by Stephanie DeWitte-Orr. The cells were plated at a concentration of $2x10^7$ cells / well in 6 well tissue culture plates in L-15 media without fetal bovine

serum. The cells were treated with 2μg/mL PMA or an equivalent volume of DMSO and incubated at 18°C. The cells were collected at the following time points: 8, 24, 48, 96, 120 and 168 hours post-stimulation. The control cells were also collected at 168 hours after treatment. The cells were centrifuged at 4000 rpm and split into two equal fractions, one for western blotting and the other for RT-PCR and the cell pellets were stored at -80°C until analysis.

RT-PCR was performed on the RTS-11 sample because it is difficult to extract enough RNA for a northern blot. Total RNA isolation, cDNA synthesis and RT-PCR were performed on the RTS-11 samples in the same manner as described above for the PMA *in vivo* study.

To extract protein, the cell pellet was re-suspended in 100μL of the NP-40 lysis buffer supplemented with protease inhibitors and incubated on ice for 30 minutes. The cellular debris was cleared by centrifugation at 15,000 rpm for 10 minutes at 4°C and a modified Bradford assay was performed, as described above. Western blot analysis was performed in the same manner as described for the PMA *in vivo* study. Densitometry analysis for RT-PCR and western blotting was performed with the Total Lab 100 software, as described above.

Chapter 3
Results

3.1 Production of Polyclonal Anti-rtINVX Antibody

3.1.1 Purification of Recombinant Truncated INVX Protein

Previous attempts at expressing a full length recombinant INVX protein, as well as other transmembrane proteins, have been hindered by low expression levels. To increase recombinant protein expression, a truncated INVX gene, lacking both the cytoplasmic and transmembrane domains, was cloned into pRSET A. The tINVX : pRSET A plasmid was isolated from transformed cells and the insert sequence was compared to the published INVX sequence to ensure proper reading frame and to check for sequence mutations. This comparison verified that the INVX insert encoded a truncated protein identical to the full length INVX, lacking only the amino-terminal cytoplasmic and transmembrane domains. Subsequently, large scale expression of the recombinant truncated INVX (rtINVX) protein was performed and the 6xHis sequence in the amino-terminal tag of the fusion protein was used to purify rtINVX. Nickel resin is negatively charged, allowing the positively charged 6xHis tag to bind at alkaline pH. As the pH decreases, weakly bound proteins are eluted followed by the elution of rtINVX. To verify size and purity of the rtINVX elutions, western blot and SDS-PAGE analysis was performed, as shown in figure 3.1. Samples from the lysate, column flow through, pH8, pH6.5, pH5.9 and pH4.3 elutions were separated on a 12% SDS-PAGE gel and either stained with Coomassie blue or transferred onto a nitrocellulose membrane and probed with an anti-Xpress antibody. While rtINVX has an expected size of approximately 22.3 kDa, it migrates at an apparent size of approximately 30kDa. This discrepancy is minor and likely caused by variation in the migration of the pre-stained SeeBlue (Invitrogen) standard bands, as the expected sizes of these bands are only an estimate. The majority of the rtINVX protein is eluted in the pH5.9 wash, although some is lost in the pH6.5 wash. The rtINVX protein appears as a doublet on both the SDS-PAGE and western blot, which may be caused by a partial degradation of the rtINVX protein by the host cell. The induction of protein expression was performed for 2 hours and it is possible that during this time a portion of the carboxy-terminus was cleaved by an *E. coli* protease.

Figure 3.1: Nickel affinity purification of rtINVX. Lysates from host cells expressing rtINVX were incubated overnight with nickel resin to facilitate the binding of the 6xHis tag at the amino-terminus of rtINVX to the negatively charged resin. The column flow through, containing unbound protein was removed, sticky proteins were washed away and the rtINVX was eluted. Samples from the purification were run on a 12% polyacrylamide gel and either stained with Coomassie blue or transferred onto a nitrocellulose membrane for western blot analysis with anti-Xpress antibody. (A) Western blot analysis of the nickel column washes and elutions, including ponceau stain, to verify the identity of the isolated protein. (B) Coomassie staining analysis of nickel column to ensure purity of isolated rtINVX. Abbreviations: L – lysate, FT – flow through, numbers indicate the pH of the 8M urea buffer used for washes and elutions.

A

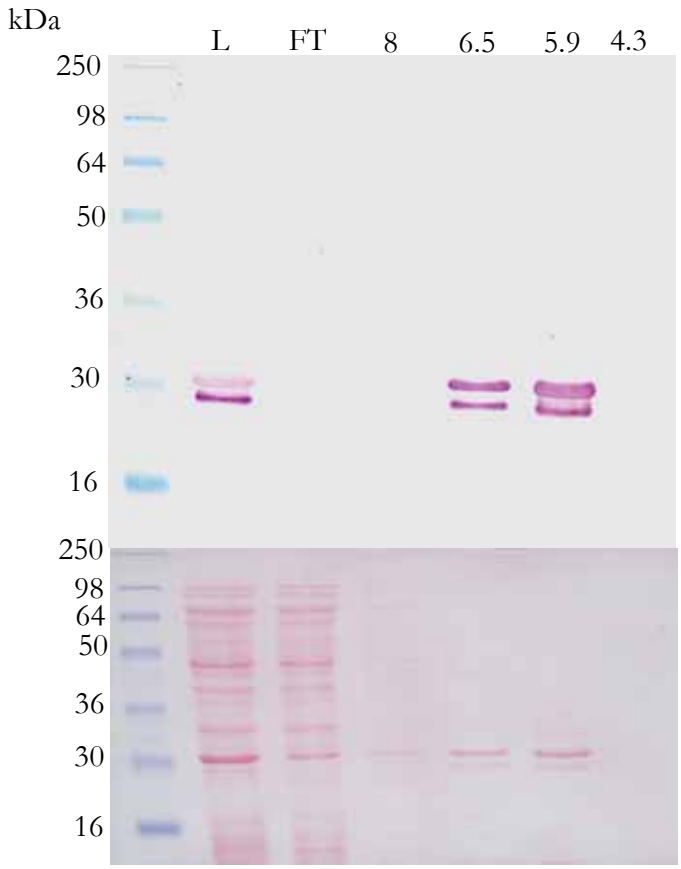
kDa
L
FT
8
6.5
5.9
4.3
250
98
64
50
36
30
16
250
98
64
50
36
30
16

B

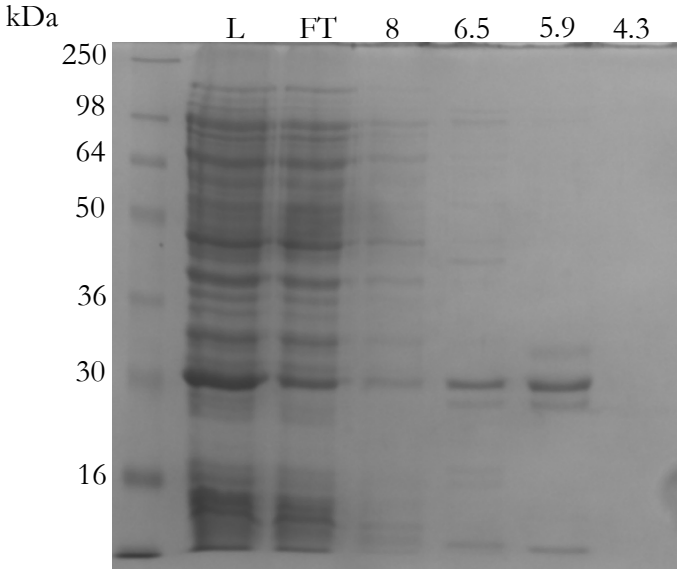
kDa
L
FT
8
6.5
5.9
4.3
250
98
64
50
36
30
16

3.1.2 Rabbit Antibody Titre

The pH5.9 elutions of rtINVX were combined, concentrated to 1mg/mL, dialyzed into 1xPBS, mixed with Freund's complete adjuvant and used to vaccinate two rabbits. The adjuvant forms an emulsion with rtINVX which delays the antigen release and aids phagocytosis by antigen presenting cells in the rabbits. In addition, Freund's complete adjuvant also contains heat-killed mycobacteria, which enhances the immune response, possibly by activating antigen presenting cells. After the initial vaccination the rabbits were boosted three times at three week intervals with an emulsion of rtINVX and Freund's incomplete adjuvant, which lacks the mycobacteria. The repeated boosts maximize the anti-rtINVX antibody production. The titre of anti-rtINVX antibody was monitored by enzyme-linked immunosorbent assays (ELISA) during the vaccination procedure, as shown in figure 3.2. The pre-immune serum, collected prior to the first immunization, shows very low levels of rtINVX reactive antibodies. However, the levels of reactive antibody increase upon each subsequent boost, with the highest level found in the exsanguination serum. The anti-rtINVX antibody in the exsanguination serum maintains reactivity up to a serum dilution of 1:500,000 and the highest level of reactivity is found in the 1:500 serum dilution. While the 1:100 would be expected to have the highest reactivity, there is an inhibition of antigen binding in this dilution because of the high antibody concentration. Although serums from both rabbits show high affinity for rtINVX, only one serum was used for all subsequent western blot analysis. The ELISA analysis of anti-rtINVX antibody titre for this rabbit is shown in figure 3.2.

3.2 Detection of an Immune Response in the *in vivo* PMA Time Course

In order to examine the success of the PMA-induced immune system stimulation, transcript levels of the cytokine interleukin-1β (IL-1β) were measured. This cytokine is produced and released by activated macrophage (Janeway *et al*, 2001) and is involved in the innate immune response. It plays a role in the recruitment of the adaptive immune system by activating T cells. IL-1β was chosen as an indicator of immune system activation because it is upregulated during an immune response. Reverse transcriptase PCR was used to measure the level of IL-1β transcript to determine if the levels increase after PMA stimulation, indicating successful immune activation.

Figure 3.2: Anti-rtINVX antibody titre as measure by ELISA. A small volume of serum was collected from each rabbit before immunization and before each subsequent boost. Levels of rtINVX reactive antibodies in these sera, as well as in the exsanguination serum were measured by ELISA analysis. Serum was diluted to 1:100, 1:500, 1:1000, 1:5000, 1:10000, 1:50000, 1:100000 and 1:500000 and incubated with rtINVX. Binding of rtINVX specific antibodies was detected with an anti-rabbit IgG alkaline phosphatase conjugated secondary antibody and p-NPP substrate. The alkaline phosphatase enzyme cleaves the p-NPP substrate to give a coloured product that can be measured at 405nm.

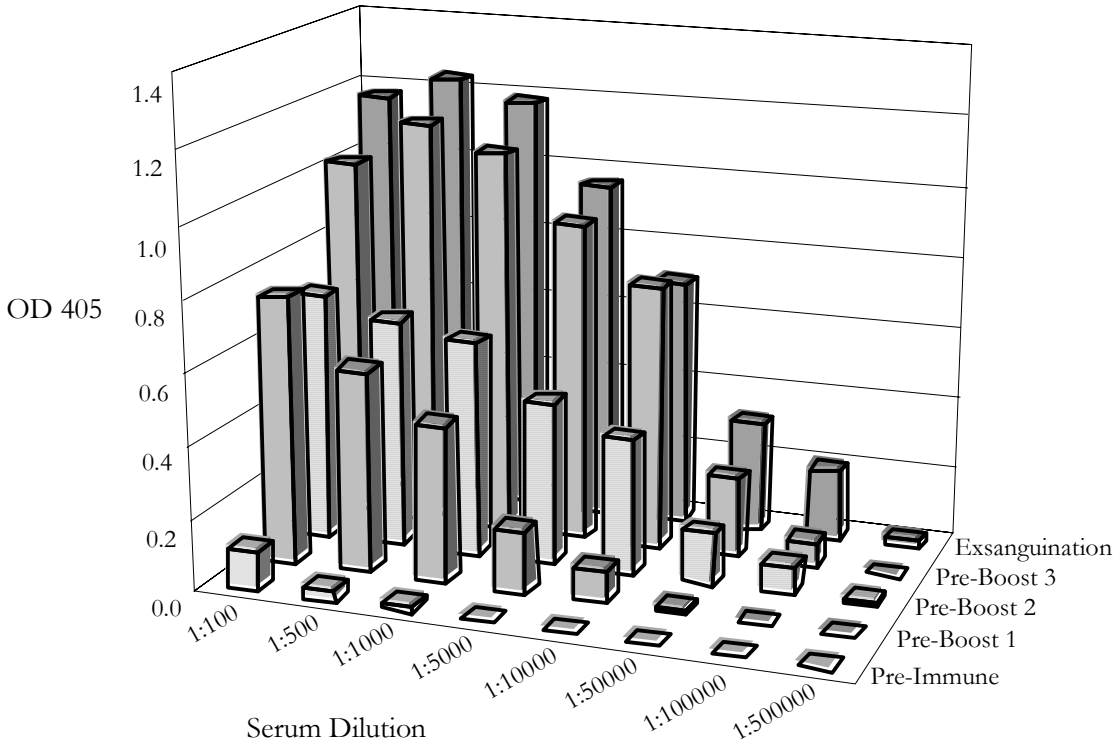
OD 405
1.4
1.2
1.0
0.8
0.6
0.4
0.2
0.0
1:100
1:500
1:1000
1:5000
1:10000
1:50000
1:100000
1:500000
Serum Dilution
Exsanguination
Pre-Boost 3
Pre-Boost 2
Pre-Boost 1
Pre-Immune

Total RNA was isolated from gill, spleen, head kidney and liver tissues of 3 fish from each of the time points, 8, 24, 48, 96, 120 and 168 hours post-stimulation as well as from 3 untreated control fish. The samples were analyzed in sets, with one set representing a group of seven fish, one sacrificed at each time point. Isolated RNA was reverse transcribed and the cDNA was PCR amplified with primers specific for IL-1β and Ef-1α. Amplification of elongation factor Ef-1α is used as a control to correct for any unequal loading of template in the PCR reaction because the levels of Ef-1α remain constant during the PMA stimulation. PCR amplification of IL-1β and Ef-1α were performed separately due to the difference in transcript levels, IL-1 β is present in very low levels and must be subjected to 35 cycles for detection while Ef-1α is present in much higher levels and is detected after 27 cycles. A duplex PCR amplifying both IL-1 β and Ef-1α would be inaccurate to use for densitometry analysis due to the extremely high levels of Ef-1α. After amplification, the IL-1β and Ef-1α PCR products were separated on a 1% agarose gel and visualized under UV light. Densitometry analysis was then performed with Total Lab 100 software. The intensity of the IL-1β band and the corresponding Ef-1α band were measured and the background was subtracted. The ratio of the IL-1β intensity to the Ef-1α intensity was calculated and the average ratio for each time point was determined. A comparison of these ratios across the time points allows for detection of an increase in IL-1β transcript levels, indicating immune system activation. To determine if the change in transcript levels is significant, statistical analysis was performed. A one-way ANOVA was performed to determine if there was a significant difference between the mean ratios for each time point and an LSD post hoc test was performed to determine which time points were significantly different from each other.

3.2.1 Analysis of Interleukin-1β Transcript Levels in PMA Stimulated Gill

Total RNA was isolated from gill tissue of 3 fish sacrificed at each of the time points, 8, 24, 48, 96, 120 and 168 hours after PMA stimulation, as well as from 3 untreated control fish. Reverse transcription was performed and cDNA was amplified separately for both IL-1β and Ef-1α. Amplification of IL-1β and the corresponding Ef-1α for the three fish sets analyzed are shown in Figure 3.3. All three sets show two distinct peaks of IL-1β transcript, one at the 8 hour time point and another at the 120 hour time point. Levels of IL-1β are decreased at the 24 hour time point in both set one and set two with the lowest levels at 48 hours. IL-1β transcript then begins to increase at 96 hours and reaches a maximum at 120 hours post-stimulation. In set three, the IL-1β transcript

Figure 3.3: RT-PCR analysis of IL-1β transcript levels in PMA stimulated gill. Total RNA was isolated from gill tissue of three fish from each of the time points 8, 24, 48, 96, 120, and 168 hours post stimulation, as well as from three untreated controls. The animals were grouped into sets for analysis, with one set consisting of seven fish, one from each time point and one untreated control. The RNA was reverse transcribed and the resulting cDNA was amplified for IL-1β as well as the control, elongation factor Ef-1α. These reactions were performed separately due to the difference in transcript levels of IL-1β and Ef-1α, with IL-1β requiring 35 cycles for amplification while Ef-1α required 27 cycles. Ef-1α is unaffected by the PMA stimulation and serves as a control to correct for any unequal sample loading during the RT-PCR procedure. The reactions were separated on a 1% agarose gel, stained with ethidium bromide and visualized under UV light. The RT-PCR results for all three gill sets analyzed are shown in this figure, along with the densitometry analysis. The IL-1β amplification product is shown in the upper gel for each set while the Ef-1α amplification product is shown in the bottom gel. The densitometry analysis shown in the bar graph represents the average IL-1β/Ef-1α ratio for set two and set three, with error bars representing the standard deviation of the means. Set one was not included in the analysis because there is no IL-1β present in the untreated control fish. The letters above the error bars represent the results of ANOVA and LSD post hoc analysis, where ‘a’ is significantly different from ‘b’ and ‘c’ is significantly different from ‘d’.

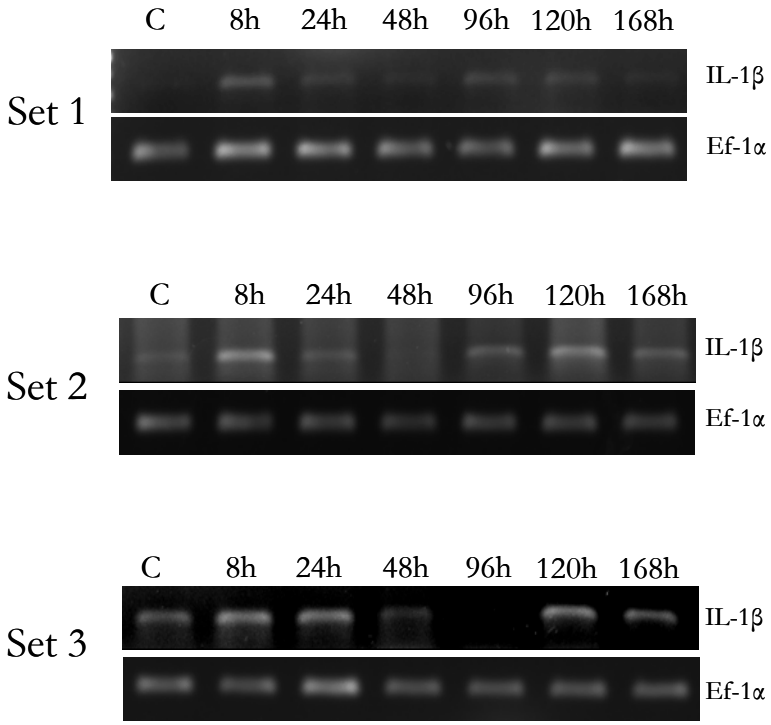
C
8h
24h
48h
96h
120h
168h
Set 1
IL-1β
Ef-1α
C
8h
24h
48h
96h
120h
168h
Set 2
IL-1β
Ef-1α
C
8h
24h
48h
96h
120h
168h
Set 3
IL-1β
Ef-1α

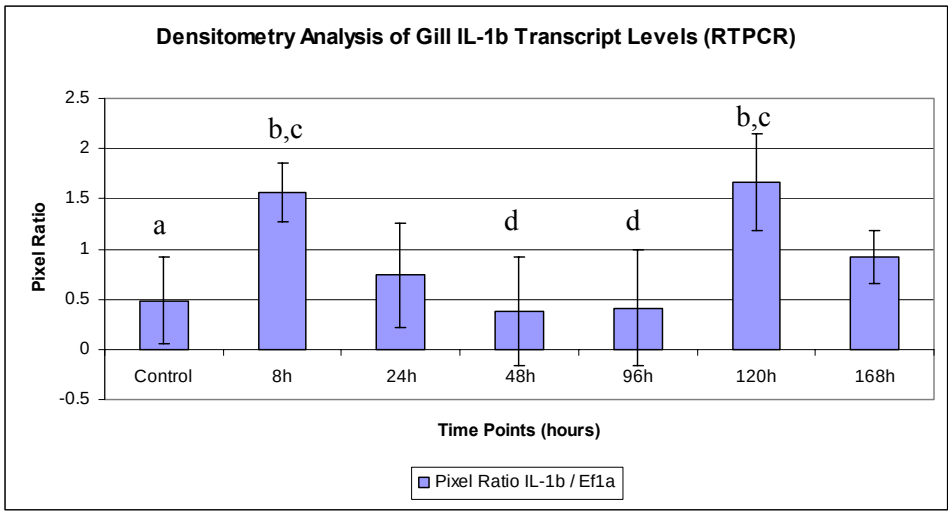
Densitometry Analysis of Gill IL-1b Transcript Levels (RTPCR)
Pixel Ratio
2.5
2
1.5
1
0.5
0
-0.5
a
b,c
d
d
b,c
Control
8h
24h
48h
96h
120h
168h
Time Points (hours)
Pixel Ratio IL-1b / Ef1a

decreases at 48 hours and is absent at 96 hours, but similar to the other sets, shows a high level at 120 hours post-stimulation. In set one, there is no IL-1β transcript detected in the control fish, however, in both set two and set three, there is a low level of IL-1β present in the control samples. Densitometry analysis was performed on these sets to verify an increase in IL-1β transcript levels after stimulation. The intensity of the IL-1β band and its corresponding Ef-1α band was measured for each time point and the ratio of the IL-1β volume to the Ef-1α volume was calculated. Figure 3.3 shows a bar graph representing the mean IL-1β / Ef-1α ratio for each time point, along with error bars representing the standard deviation of each average. The graph clearly demonstrates that while there is a low level of IL-1β transcript present in the control sample of set two and set three, the transcript level is elevated at both the 8 hour and 120 hour time points. In addition, this analysis also clearly demonstrates the decreased transcript levels at the 24 to 96 hour time points. ANOVA analysis indicates that there is a significant difference in the means of the time points for gill IL-1β transcript level ($p=0.034$), while LSD post hoc test demonstrates that the transcript level at 8 hours and 120 hours are significantly higher then the control ($p=0.034$ and $p=0.024$). Also, transcript level at 8 hours is significantly higher than 48 and 96 hours ($p=0.007$ and $p=0.026$). Likewise, transcript level at 120 hours is significantly higher than 48 and 96 hour time points ($p=0.05$ and $p=0.019$). Thus, an immune response has been activated in the gill of PMA treated fish.

3.2.2 Analysis of Interleukin-1β Transcript Levels in PMA Stimulated Spleen

As described above for gill, total RNA was isolated from spleen tissue of 3 fish from each of the time points, 8, 24, 48, 96, 120 and 168 hours post-stimulation as well as from 3 untreated control fish. The RNA was reverse transcribed and both IL-1β and Ef-1α were amplified separately. The amplification of these two transcripts are shown in figure 3.4 for all three sets analyzed. The control samples and the 8 hour time points for all sets show an absence of IL-1β transcript, with an increase at the later time points of 96, 120 and 168 hours post-stimulation. In set two, IL-1 β is also expressed transiently at the 24 hour time point. Densitometry analysis was performed by calculating the ratio of the intensity of the IL-1β band to the corresponding Ef-1α band. An average of this ratio was calculated for each time point and this is shown in figure 3.4, along with error bars, representing the standard deviation for each average. The densitometry analysis shows that the level of IL- β transcript is elevated at 96 hours after PMA stimulation. There is also transcript present at the 120 and 168 hour time points, but the error bars for these time points are very large. This occurs because while IL-1 β transcript is present at these time points in all three sets, it is present at very different levels. ANOVA

Figure 3.4: RT-PCR analysis of IL-1β transcript levels in PMA stimulated spleen. Total RNA was isolated from spleen tissue of three fish from each time point 8, 24, 48, 96, 120 and 168 hours post-stimulation as well as from three untreated control fish. The samples were analyzed in sets, as described above for gill IL-1β transcript analysis. RNA was reverse transcribed and amplified separately for both IL-1β and the control Ef-1α. PCR products were separated on a 1% agarose gel, stained with ethidium bromide and visualized under UV light. Amplification of IL-1β transcript along with the corresponding Ef-1α for all three sets is shown in this figure, along with the densitometry analysis of these results. The upper gel for each set is the IL-1β amplification product while the lower gel is the EF-1α amplification product. The densitometry analysis is summarized in the bar graph, which represents the average IL-1β/Ef-1α ratio for each time point, with error bars representing the standard deviation of these means. The letters above the error bars represent the results of ANOVA and LSD post hoc analysis, where 'a' is significantly different from 'b'. The three sets analyzed for spleen correspond to the three sets analyzed for gill.

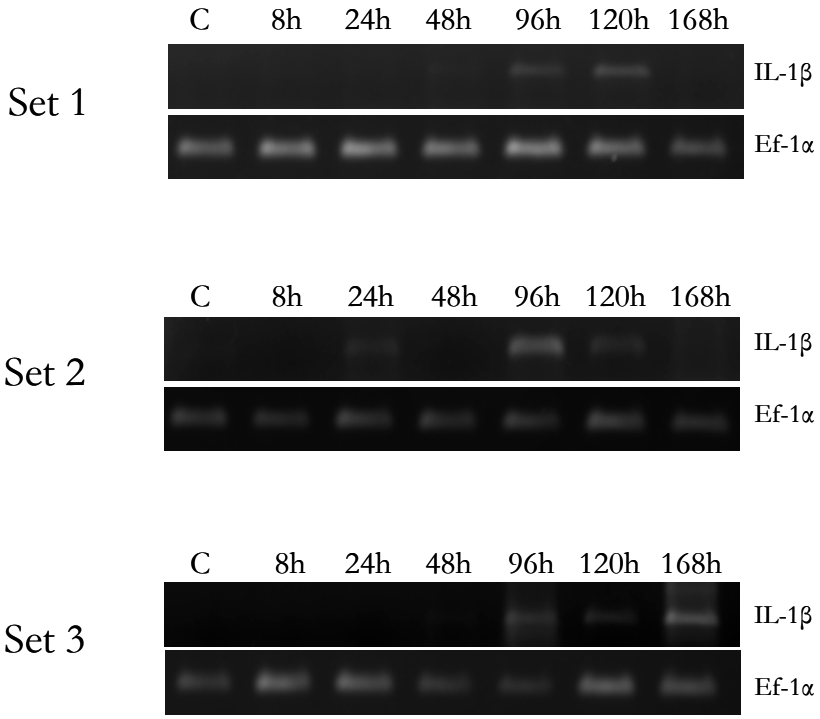
C 8h 24h 48h 96h 120h 168h
Set 1
IL-1β
Ef-1α
C 8h 24h 48h 96h 120h 168h
Set 2
IL-1β
Ef-1α
C 8h 24h 48h 96h 120h 168h
Set 3
IL-1β
Ef-1α

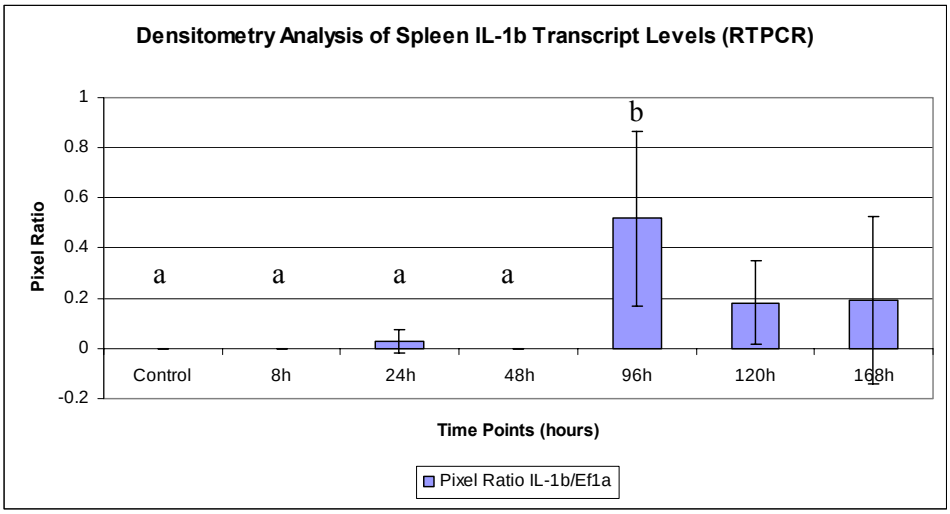
Densitometry Analysis of Spleen IL-1b Transcript Levels (RTPCR)
Pixel Ratio
1
0.8
0.6
0.4
0.2
0
-0.2
a
a
a
a
b
Control
8h
24h
48h
96h
120h
168h
Time Points (hours)
Pixel Ratio IL-1b/Ef1a

analysis indicates that there is a significant difference in the means of each time point (p=0.046) while LSD post hoc analysis indicates that the 96 hour time point is significantly higher than control, 8, 24 and 48 hour time points (p=0.006, p=0.006, p=0.008 and p=0.006). Thus, at the later time points, there is an immune response occurring in the spleen.

3.2.3 Analysis of Interleukin-1β Transcript Levels in PMA Stimulated Head Kidney

Total RNA was also isolated from head kidney tissue of 3 fish at each of the time points, 8, 24, 48, 96, 120 and 168 hours after PMA stimulation as well as from 3 untreated fish. The RNA was reverse transcribed and cDNA was amplified separately to measure levels of IL-1β transcript and Ef-1α transcript. Figure 3.5 shows the amplification of head kidney IL-1β, the corresponding Ef-1α, as well as the densitometry analysis of IL-1β transcript levels. Similar to the results in spleen, the IL-1β transcript is absent in the head kidney of control fish as well as in the early time points, with an increase at the later time points, beginning at 96 hours and reaching maximal levels at 120 hours after PMA treatment. While IL-1β transcript is clearly present in set two and set three at 96 and 168 hours post- stimulation, set one shows very low or no IL-1β at these time points. This causes large standard deviation for the average intensity ratio at the 96 and 168 hour time points for head kidney, making it difficult to show a significant increase in transcript level. ANOVA analysis indicates that there is no significant difference in the IL-1β transcript levels during PMA stimulation (p=0.163). The error bar for the 120 hour time point is very small, and LSD post hoc testing gives a p value of 0.06. Although this is not statistically significant, it is very close, and if the average IL-1β/Ef-1α ratio increased to a slightly higher value, it would have likely been a significant increase. Thus, although the IL-1β transcript is clearly increasing after PMA stimulation, this increase is small, and cannot be shown to be statistically significant.

3.2.4 Analysis of Interleukin-1β Transcript Levels in PMA Stimulated Liver

The transcript level of IL-1β was also analyzed in total liver RNA. As described above, RNA was isolated from 3 individuals at each of the time points 8, 24, 48, 96, 120 and 168 hours post-stimulation as well as from 3 untreated control fish. The RNA was reverse transcribed and cDNA was amplified separately with IL-1β and Ef-1α primers. Since the liver is not an immune organ, it is not expected to express IL-1β. As shown in figure 3.6, there is amplification of the Ef-1α control but not IL-1β. Densitometry analysis was not performed for these amplifications because IL-1β is not present.

Figure 3.5: RT-PCR analysis of IL-1β transcript levels in PMA stimulated head kidney. Total RNA was isolated from head kidney of three fish from each of the time points 8, 24, 48, 96, 120 and 168 hours post-stimulation as well as from three untreated control fish. RNA was reverse transcribed and amplified for both IL-1β and Ef-1α, in separate PCR reactions, as described above for gill. The resulting PCR products were separated on a 1% agarose gel, stained with ethidium bromide and visualized under UV light. This figure shows the amplification of IL-1β in the upper gel for each set as well as the corresponding Ef-1α in the lower gel, for all three sets. The densitometry analysis shown in the bar graph represents the average IL-1β/Ef-1α ratio for each time point, with error bars representing the standard deviation of each mean. The three sets analyzed for head kidney are the same sets analyzed for gill and spleen IL-1β transcript levels.

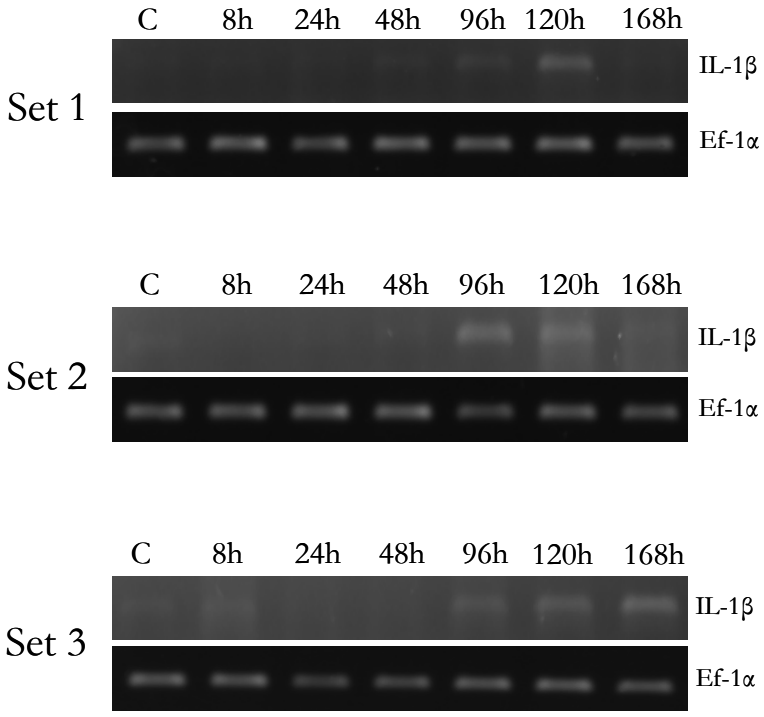
C 8h 24h 48h 96h 120h 168h
Set 1
IL-1β
Ef-1α
C 8h 24h 48h 96h 120h 168h
Set 2
IL-1β
Ef-1α
C 8h 24h 48h 96h 120h 168h
Set 3
IL-1β
Ef-1α

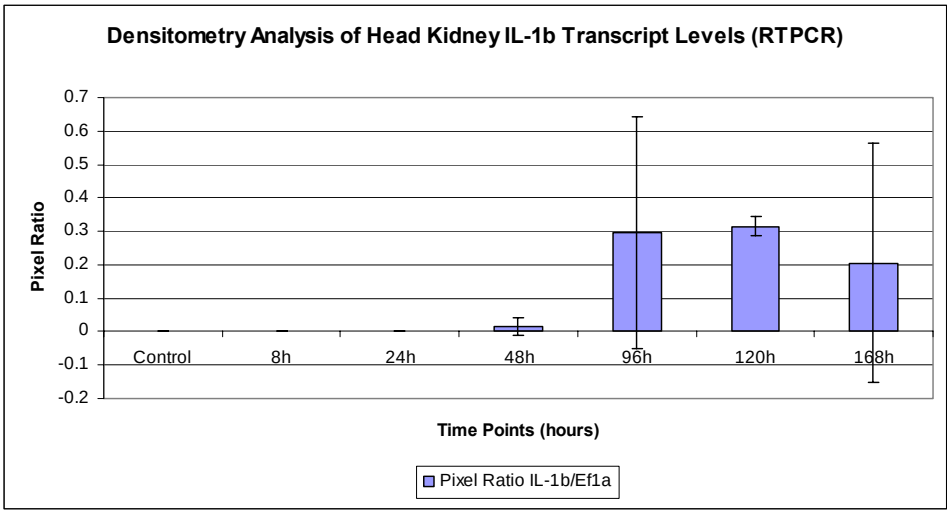
Densitometry Analysis of Head Kidney IL-1b Transcript Levels (RTPCR)
Pixel Ratio
0.7
0.6
0.5
0.4
0.3
0.2
0.1
0
-0.1
-0.2
Control
8h
24h
48h
96h
120h
168h
Time Points (hours)
Pixel Ratio IL-1b/Ef1a

Figure 3.6: RT-PCR analysis of IL-1β transcript levels in PMA stimulated liver. Total RNA was isolated from liver tissue of three fish from each of the time points 8, 24, 48, 96, 120 and 168 hours post-stimulation as well as from three untreated control fish. RNA was reverse transcribed and amplified for IL-1β and Ef-1α in separation reactions, as described above for gill. The resulting PCR products were separated on a 1% agarose gel, stained with ethidium bromide and visualized under UV light. This figure shows the IL-1β amplification, in the upper gel of each set, as well as the corresponding Ef-1α amplification, in the lower gel, for all three sets. There was no densitometry analysis performed on these results because there was no IL-1β detected. These three sets correspond to the three sets analyzed for IL-1β transcript in spleen, gill and head kidney.

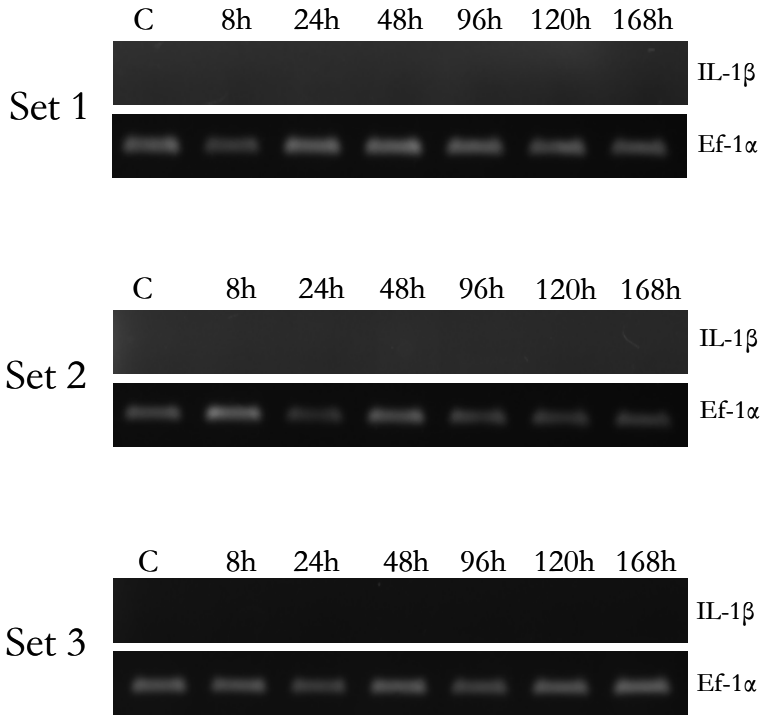
C 8h 24h 48h 96h 120h 168h
Set 1
IL-1β
Ef-1α
C 8h 24h 48h 96h 120h 168h
Set 2
IL-1β
Ef-1α
C 8h 24h 48h 96h 120h 168h
Set 3
IL-1β
Ef-1α

3.3 Analysis of Invariant Chain Transcript Levels in the PMA *in vivo* Time Course

Both northern blotting and RT-PCR were used to analyze S25-7 and INVX transcript levels during a PMA stimulated immune response. Total RNA was isolated from gill, spleen, head kidney, peripheral blood leukocytes and liver of six fish from each of the time points 8, 24, 48, 96, 120 and 168 hours post-stimulation as well from six untreated control fish. RT-PCR was performed to measure transcript levels in peripheral blood leukocytes due to the low level of isolated RNA. RNA isolated from the other tissues was subjected to northern blot analysis. For S25-7 transcript analysis, three RNA sets were separated on the same 1% agarose gel, while all six sets were separated on the same gel for INVX analysis. Combining multiple sets on one membrane limits variability by maintaining constant electrophoresis, probing and detection conditions for all sets, allowing for more accurate comparison of results between sets. After electrophoresis, the RNA was transferred onto a nylon membrane and probed with DIG-labeled probes for 40S ribosomal protein S11 transcript along with either S25-7 or INVX transcripts. S11 is used as a loading control because transcript levels will not be affected by the PMA stimulation and its size is significantly different from S25-7 and INVX which allows both control and experimental bands to be detected on the same blot. Again, this decreases the variability associated with comparison of two different blots. Densitometry analysis was performed on all blots using the Total Lab 100 software. Briefly, the intensity of the S25-7, INVX and S11 bands were measured and, after correcting for background, the ratio of the S25-7 or INVX signal to the corresponding S11 signal was calculated to correct for unequal RNA loading. The average ratio for each time point was calculated and these averages were analyzed by ANOVA and LSD post hoc testing to identify any significant changes in transcript levels.

3.3.1 Analysis of Invariant Chain Transcript Levels in PMA Stimulated Gill

As described above, total RNA was isolated from gill tissue of six fish from the time points 8, 24, 48, 96, 120 and 168 hours post-stimulation as well as from six untreated control fish and probed for both S25-7 and INVX. Representative S25-7 and INVX blots, along with densitometry analysis are shown in figure 3.7. A UV image of the 18S and 28S ribosomal RNA is also included for both sets of blots to show the quality of RNA isolation as well as equal sample loading. The signals for all three probes used are very different, with S25-7 giving a much more intense signal than S11, while S11 gives a

much more intense signal than INVX. The INVX signal was so low that x-ray film was used for detection. Since there is a constant amount of S11 transcript in both blots, these results indicate that the S25-7 transcript is present at a higher level in gill than the INVX transcript. As shown by densitometry analysis, there appears to be very little variation in the transcript level of S25-7 during the time course. The ANOVA analysis confirmed this result with a p value of 0.407. In the case of INVX, there may be a slight increase in transcript levels between control and 8 hours post-stimulation, with a subsequent decrease at later time points, such that after 8 hours there appears to be no difference between control and treated samples. However, ANOVA analysis indicates the difference in INVX transcript levels between control and 8 hours is not significant ($p=0.255$), which is likely due to the large error bar associated with the mean INVX/S11 ratio of the 8 hour time point. The difference in signal strength from the INVX and S11 probe resulted in a saturation of the S11 signal in many samples, as seen in figure 3.7, specifically in set one results. This makes it difficult to accurately measure the intensity of these signals to compare with INVX.

To verify the northern blot results, RT-PCR was also performed on gill RNA to confirm that INVX levels remain constant during the immune response. Figure 3.8 shows RT-PCR analysis performed on three sets of gill RNA along with the densitometry analysis. For this analysis, a duplex PCR was performed in which both INVX and the control transcript Ef-1α were amplified under the same conditions. ANOVA analysis of RT-PCR results confirm that there is no change in gill INVX transcript levels during immune system stimulation, even at the 8 hour time point ($p=0.931$). This analysis also confirms the large variability between samples within each time point, as shown by the large error bars, indicating that the variability within each time point is not due to the northern blot technique. The large variation in transcript levels between fish within the same time point makes it difficult to determine if there are any global changes in transcript level, however, since the means are all quite similar, it appears that both S25-7 and INVX transcript levels remain unchanged in gill tissue during an immune response.

3.3.2 Analysis of Invariant Chain Transcript Levels in PMA Stimulated Spleen

Again, as described above, total RNA was isolated from spleen tissue of six fish at each of the time points 8, 24, 48, 96, 120 and 168 hours post-stimulation as well as from six untreated control fish and

Figure 3.7: Northern blot analysis of S25-7 and INVX transcript levels in PMA stimulated gill. Total RNA was isolated from gill tissue of six fish sacrificed at each of the time points 8, 24, 48, 96, 120 and 168 hours post stimulation, as well as from six untreated control fish. RNA was separated on a 1% agarose gel, stained with ethidium bromide, visualized under UV light, transferred onto a nylon membrane and probed for either S25-7 or INVX with DIG-labeled probes. In addition, the blots were also probed for the 40S ribosomal protein S11 transcript. This transcript remains unchanged during PMA stimulation and serves as a loading control. A representative blot for both S25-7 and INVX is shown in this figure, along with densitometry analysis for both transcripts. To analyze changes in transcript levels, densitometry analysis was performed by measuring the intensity of the INVX, S25-7 and S11 bands. A ratio of INVX or S25-7 to the corresponding S11 signal was calculated and the average of ratio for each time point was plotted, along with error bars representing the standard deviation for each mean. The additional sets used for densitometry analysis are shown in appendix A, figure A.1. The sets used for S25-7 and INVX northern blot analysis are corresponding, such that set 1 in the S25-7 northern blot consists of the same fish as set 1 in the INVX northern blot.

(A) Northern blot analysis of S25-7 transcript levels in PMA stimulated gill. In the case of S25-7 analysis, three sets of RNA were separated on the same gel, transferred onto a nylon membrane, probed with DIG-labeled S25-7 and S11 probes and detected on the Flurochem 8000 imager. The upper band of the blot is the S25-7 transcript while the lower band is the S11 transcript. The UV image of the RNA gel is presented below the blot to show integrity of the 18S and 28S ribosomal RNA. Finally, the average S25-7/S11 ratio for each time point of all six sets, along with error bars, representing the standard deviation of each mean, is shown in the bar graph.

(B) Northern blot analysis of INVX transcript levels in PMA stimulated gill. For the analysis of INVX, all six sets of RNA were electrophesed on the same gel, transferred onto a nylon membrane, probed with DIG-labeled INVX and S11 probes and detected with x-ray film. The upper band of the blot is the INVX transcript while the lower band is the S11 transcript. The UV image of the RNA gel is shown below the blot, demonstrating 18S and 28S ribosomal RNA integrity. Finally, the bar graph represents the average INVX/S11 ratio for each time point, for five sets (set six was excluded from this analysis), along with the corresponding error bars for each mean.

A

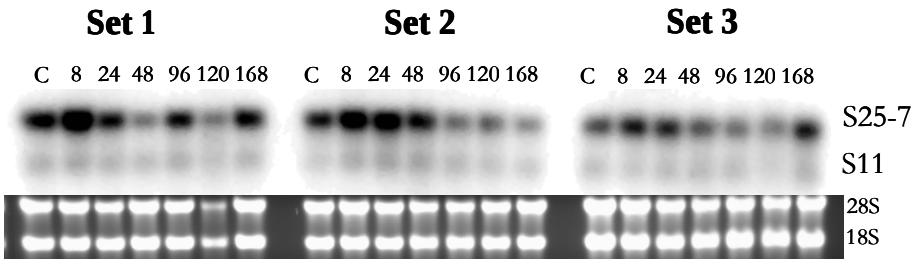
Set 1
Set 2
Set 3
C 8 24 48 96 120 168
C 8 24 48 96 120 168
C 8 24 48 96 120 168
S25-7
S11
28S
18S

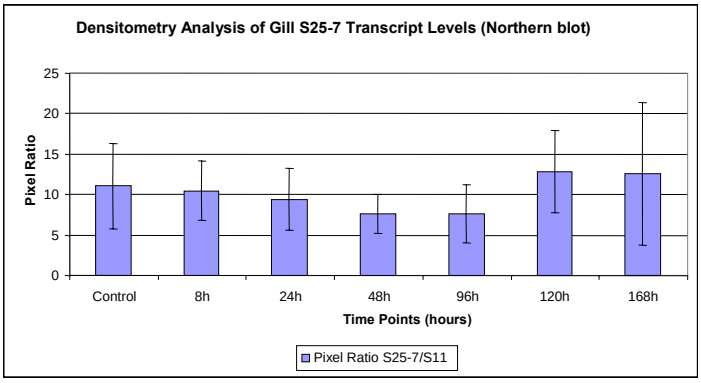
Densitometry Analysis of Gill S25-7 Transcript Levels (Northern blot)
Pixel Ratio
25
20
15
10
5
0
Control
8h
24h
48h
96h
120h
168h
Time Points (hours)
Pixel Ratio S25-7/S11

B

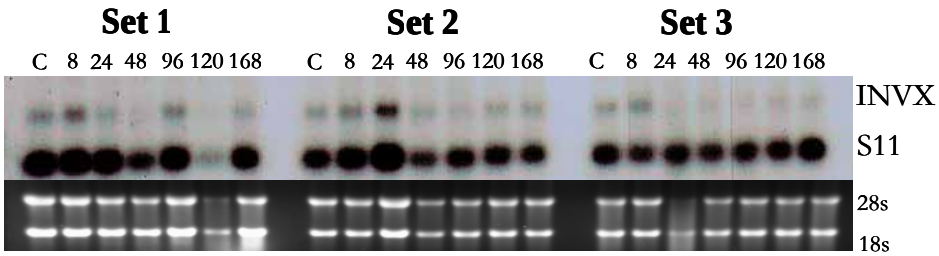
Set 1
Set 2
Set 3
C 8 24 48 96 120 168
C 8 24 48 96 120 168
C 8 24 48 96 120 168
INVX
S11
28s
18s

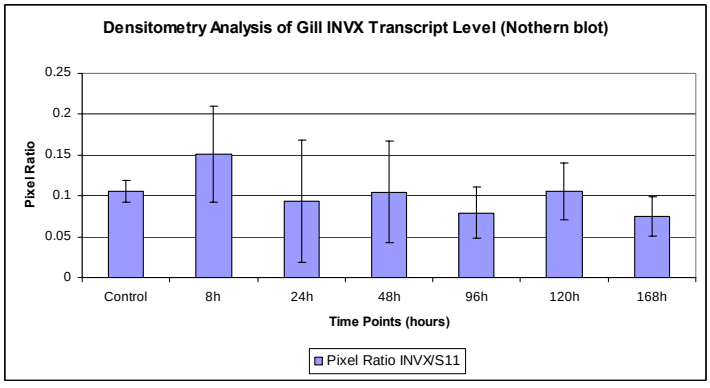
Densitometry Analysis of Gill INVX Transcript Level (Nothern blot)
Pixel Ratio
0.25
0.2
0.15
0.1
0.05
0
Control
8h
24h
48h
96h
120h
168h
Time Points (hours)
Pixel Ratio INVX/S11

Figure 3.8: RT-PCR analysis of INVX transcript levels in PMA stimulated gill. Total RNA was isolated from gill tissue of three fish sacrificed at each of the time points 8, 24, 48, 96, 120 and 168 hours post stimulation as well as from three untreated control fish. This RNA was reverse transcribed and subjected to a duplex PCR reaction in which both INVX and Ef-1α were amplified with 27 cycles in a thermocycler. The duplex PCR was performed to eliminate variations in PCR reaction, electrophoresis and visualization conditions between INVX and the corresponding Ef-1α control. The PCR products were separated on a 1% agarose gel, stained with ethidium bromide and visualized under UV light. Amplification of the three sets analyzed are shown in this figure, along with the densitometry analysis. The bar graph represents the average ratio of INVX/Ef-1α for each time point, with error bars representing the standard deviation of the means. The three sets analyzed by RT-PCR for INVX transcript correspond to the sets used for gill northern blot analysis, shown in figure 3.7.

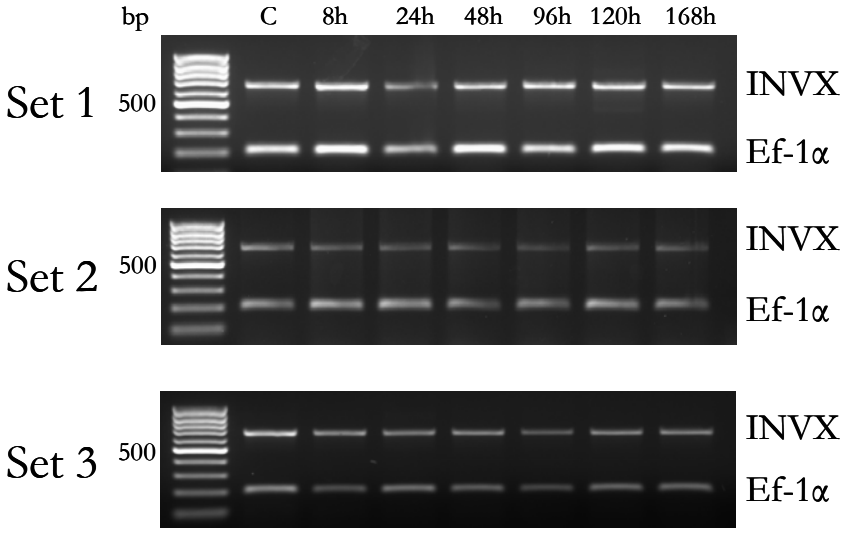
bp
C
8h
24h
48h
96h
120h
168h
Set 1
500
INVX
Ef-1α
Set 2
500
INVX
Ef-1α
Set 3
500
INVX
Ef-1α

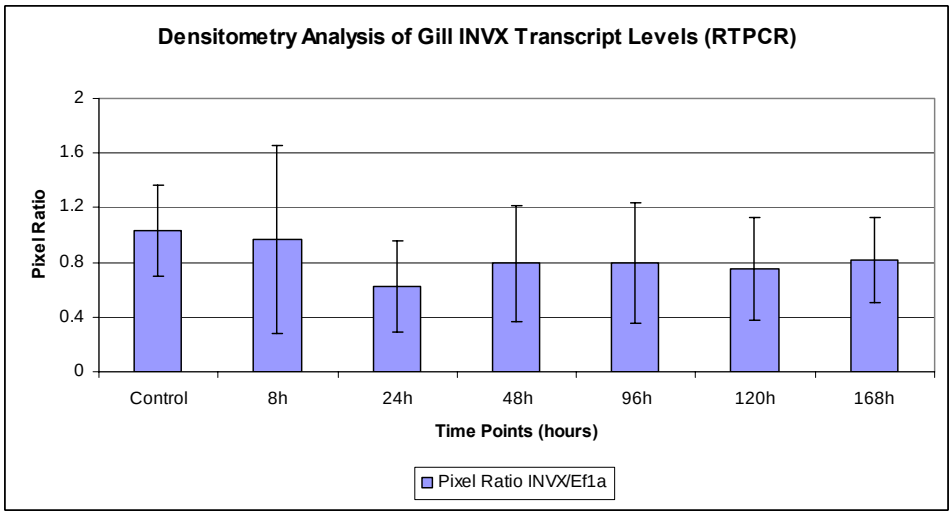
Densitometry Analysis of Gill INVX Transcript Levels (RTPCR)
Pixel Ratio
2
1.6
1.2
0.8
0.4
0
Control
8h
24h
48h
96h
120h
168h
Time Points (hours)
Pixel Ratio INVX/Ef1a

Figure 3.9: Northern blot analysis of S25-7 and INVX transcript levels in PMA stimulated spleen. Total RNA was isolated from spleen tissue of six fish from each of the time points 8, 24, 48, 96, 120 and 168 hours post stimulation as well as from six untreated control fish. RNA was separated on a 1% agarose gel, stained with ethidium bromide, visualized under UV light and transferred to a nylon membrane. The membrane was then probed with DIG-labeled probes for either S25-7 and S11 or INVX and S11. To analyze changes in transcript levels, densitometry analysis was performed by measuring the intensity of the INVX, S25-7 and S11 bands. A ratio of INVX or S25-7 to the corresponding S11 signal was calculated and the average of ratio for each time point was plotted, along with error bars representing the standard deviation for each mean. The additional sets used for densitometry analysis are shown in appendix A, figure A.2. The sets shown in this figure correspond to the sets analyzed for gill northern blotting.

(A) Northern blot analysis of S25-7 transcript levels in PMA stimulated spleen. As described above, three sets of RNA were separated on the same gel and transferred onto a nylon membrane for S25-7 and S11 probing. The bands were detected with the Fluorchem 8000. The upper band in the blot represents the S25-7 transcript while the lower band represents the S11 transcript. The UV image of the 18S and 28S ribosomal RNA is shown below the blot. Finally, the average S25-7/S11 ratio of each time point for all six sets is shown in the plot, along with error bars representing the standard deviation for these means.

(B) Northern blot analysis of INVX transcript levels in PMA stimulated spleen. As described above, all six sets of RNA were separated on the same gel and transferred onto a nylon membrane. The blot was probed for INVX and S11 and was detected with x-ray film. The upper band in the blot is the INVX transcript while the lower band is the S11 transcript. The UV image of the 18S and 28S ribosomal RNA is shown below the blot. Finally, the average INVX/S11 ratio of each time point for five sets is shown in the bar graph. Set three has been excluded from the analysis due to low RNA levels. The error bars for each time point represents the standard deviation of the means of the INVX/S11 ratio for that time point.

A

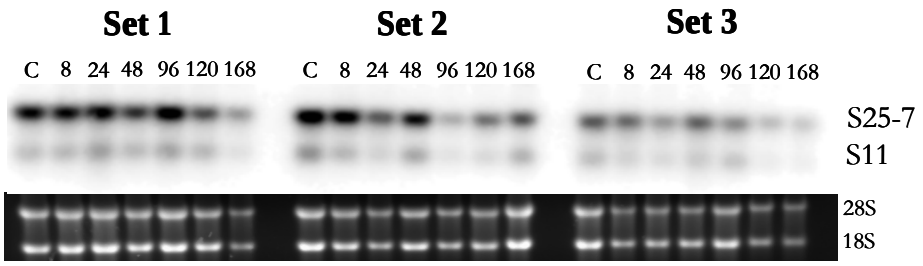
Set 1
Set 2
Set 3
C 8 24 48 96 120 168
C 8 24 48 96 120 168
C 8 24 48 96 120 168
S25-7
S11
28S
18S

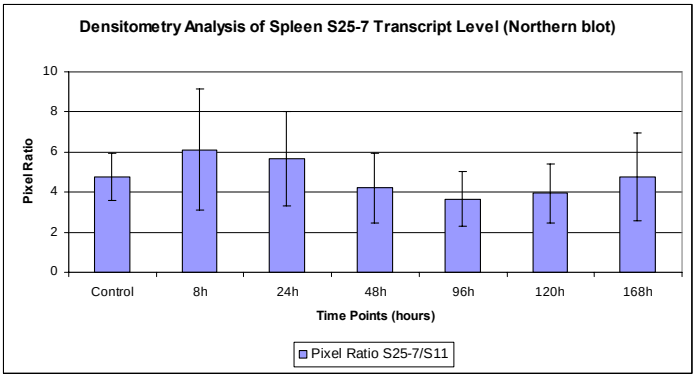
Densitometry Analysis of Spleen S25-7 Transcript Level (Northern blot)
Pixel Ratio
10
8
6
4
2
0
Control
8h
24h
48h
96h
120h
168h
Time Points (hours)
Pixel Ratio S25-7/S11

B

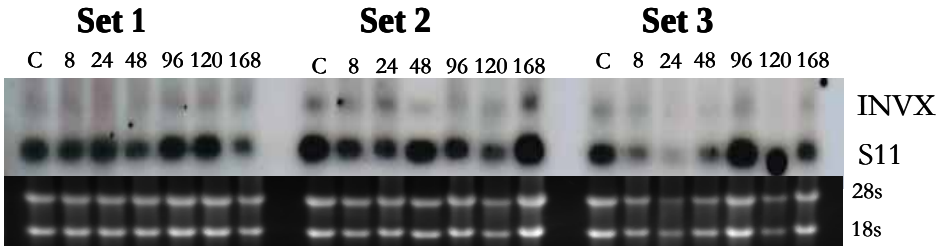
Set 1
Set 2
Set 3
C 8 24 48 96 120 168
C 8 24 48 96 120 168
C 8 24 48 96 120 168
INVX
S11
28s
18s

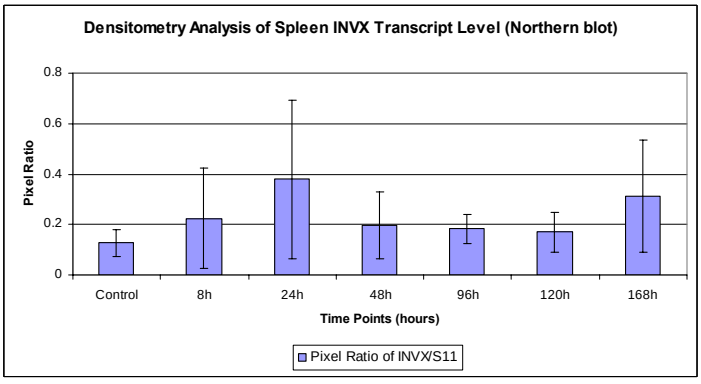
Densitometry Analysis of Spleen INVX Transcript Level (Northern blot)
Pixel Ratio
0.8
0.6
0.4
0.2
0
Control
8h
24h
48h
96h
120h
168h
Time Points (hours)
Pixel Ratio of INVX/S11

Figure 3.10: RT-PCR analysis of INVX transcript levels in PMA stimulated spleen. Total RNA was isolated from spleen tissue of three fish sacrificed at each of the time points 8, 24, 48, 96, 120 and 168 hours post stimulation as well as from three untreated control fish. The RNA was reverse transcribed and amplified for both INVX and Ef-1α in a duplex PCR reaction. The transcripts were amplified with 27 cycles and the products were separated on a 1% agarose gel, stained with ethidium bromide and visualized under UV light. The results of this amplification are shown in this figure. The upper band is the amplified INVX fragment while the lower band is the Ef-1α fragment. Densitometry analysis of INVX levels was performed and unequal template loading was corrected for by calculating the ratio of INVX signal to Ef-1α signal. The average of the ratio for each time point is shown in the bar graph, with error bars representing the standard deviation of the means for each time point. The average of all three sets was taken for the densitometry analysis. The three sets analyzed by RT-PCR for INVX transcript corresponds to the three sets shown in figure 3.9 for spleen northern blot analysis.

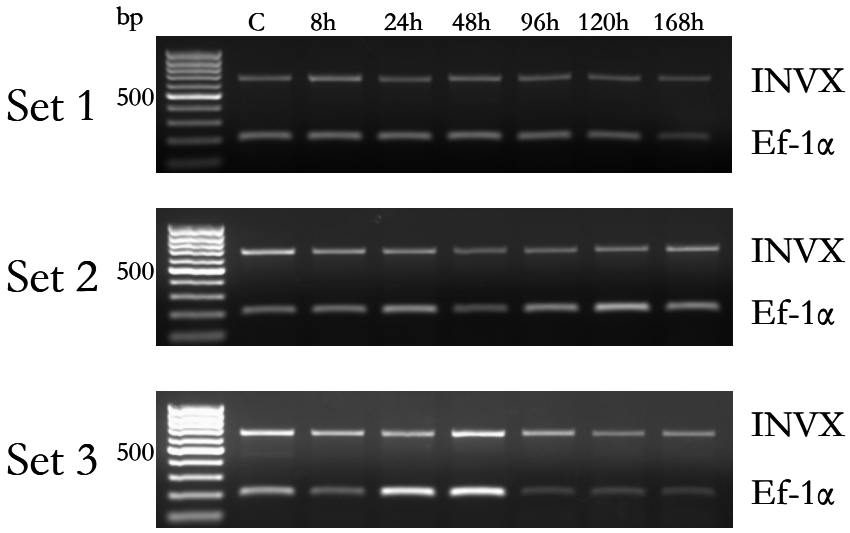
bp
C
8h
24h
48h
96h
120h
168h
Set 1
500
INVX
Ef-1α
Set 2
500
INVX
Ef-1α
Set 3
500
INVX
Ef-1α

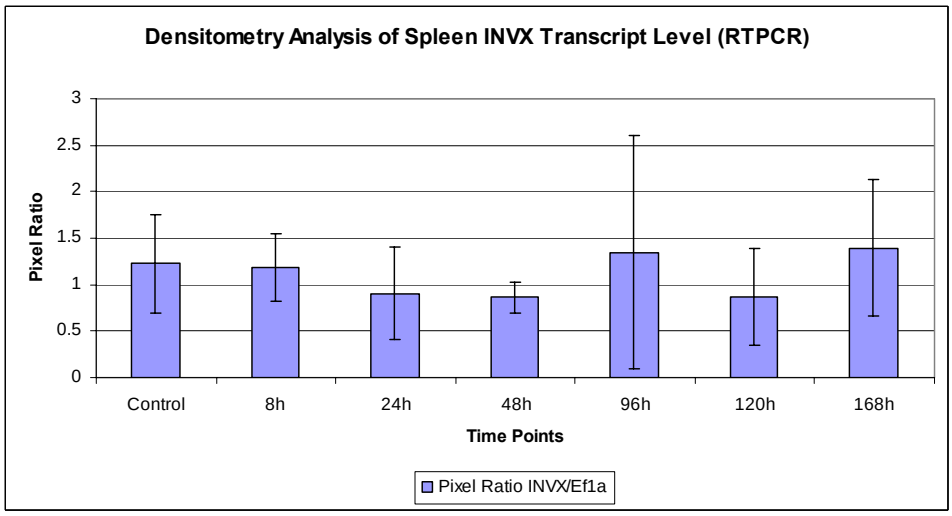
Densitometry Analysis of Spleen INVX Transcript Level (RTPCR)
Pixel Ratio
3
2.5
2
1.5
1
0.5
0
Control
8h
24h
48h
96h
120h
168h
Time Points
Pixel Ratio INVX/Ef1a

probed for S25-7 and INVX. Representative S25-7 and INVX blots, along with densitometry analysis and a UV image of the 18S and 28S rRNA are shown in figure 3.9. The transcript levels of S25-7 are again much higher in spleen than the levels of INVX transcript, similar to the case for gill. However, the levels of S25-7 appear to be lower in spleen than in gill, as shown by the S25-7/S11 ratio values in the two tissues. In contrast, INVX transcript appears to be at a similar low level in both spleen and gill and while INVX bands are seen more clearly in gill, the S11 control bands are not as saturated in spleen. This gives rise to similar ratio values even though the bands are seen more clearly in gill. Similar to gill, the S25-7 transcript levels appear to remain constant in the spleen during immune system stimulation, with perhaps a slight increase at 8 hours, followed by a slight decrease at 96 hours. However, as was the case for gill, the large variability within each time point causes large error bars, making it difficult to show statistical significance for these changes (ANOVA: $p=0.314$). Similarly, it appears that the INVX transcript may increase at 8 hours, but is insignificant due to the extremely large error bars associated with the 8 hour time point (ANOVA: $p=0.314$). It is very difficult to analyze the INVX transcript levels in spleen by northern blotting due to the extremely large error bars associated with the 8, 24 and 168 hour time points. These errors are due to difficulty in comparing the extremely low signal from the INVX transcript with the large signal from the S11 transcript.

To analyze the low levels of INVX, RT-PCR was also performed on spleen RNA, as described above for gill. The results, shown in figure 3.10, indicate that INVX transcript levels remain quite constant during the time course. However, in contrast to the northern blot results, there does not appear to be any increase in INVX transcript levels at 8 hours, as the control has a higher average INVX/S11 ratio, although the large error bar associated with the control makes comparisons difficult. It is possible that there may be a slight decrease at 24 hours post-stimulation, but this is also not statistically significant (ANOVA: $p=0.894$). Taken together, it appears that the transcript levels of both S25-7 and INVX in the spleen remain fairly constant during immune system stimulation.

3.3.3 Analysis of Invariant Chain Transcript Levels in PMA Stimulated Head Kidney

As described above, total RNA was isolated from head kidney of six fish from each of the time points 8, 24, 48, 96, 120 and 168 hours post stimulation as well as from 6 untreated control fish. The RNA was separated, transferred onto a nylon membrane and probed for S25-7 and INVX. Representative blots for both S25-7 and INVX, along with densitometry analysis and a UV image of

Figure 3.11: Northern blot analysis of S25-7 and INVX transcript levels in PMA stimulated head kidney. Total RNA was isolated from head kidney tissue from six fish sacrificed at each of the time points 8, 24, 48, 96, 120 and 168 hours post stimulation as well as from six untreated control fish. The RNA was separated on a 1% agarose gel, stained with ethidium bromide, visualized under UV light and transferred onto a nylon membrane. The membrane was then probed with DIG-labeled probes for either S25-7 and S11 or INVX and S11. Densitometry analysis was performed to examine transcript levels by measuring the signal from each band. To correct for any unequal RNA loading, the ratio of S25-7 signal to S11 signal or INVX signal to S11 signal was calculated. The average ratio for each time point was plotted along with error bars representing the standard deviation of each mean. The sets shown in this figure correspond to the sets analyzed for gill and spleen northern blotting.

(A) Northern blot analysis of S25-7 transcript levels in PMA stimulated head kidney. As described for gill, three sets of RNA were separated on the same gel and transferred onto a nylon membrane. The membrane was probed for both S25-7 and S11 and the bands were detected with the Fluorchem 8000. The upper band of the blot is the S25-7 transcript while the lower band is the S11 control band. The 18S and 28S ribosomal RNA are shown in the UV image, just below the blot. Finally, the densitometry analysis of S25-7 transcript levels in head kidney is represented by the bar graph. The average S25-7/S11 ratio for each time point is plotted, along with error bars representing the standard deviation of the means. The letters represent the results of ANOVA and LSD post hoc analysis, where ‘a’ is significantly different from ‘b’ and ‘c’ is significantly different from ‘d’. The additional sets used for densitometry analysis are shown in appendix A, figure A.3.

(B) Northern blot analysis of INVX transcript levels in PMA stimulated head kidney. As described for gill, all six sets of RNA were separated on the same gel and transferred onto a nylon membrane. The membrane was probed for both INVX and S11 and was detected with x-ray film. The INVX transcript is not detected in this tissue, only the lower S11 band can be seen. The UV image of the 18S and 28S ribosomal RNA is shown below the blot. Densitometry analysis was not performed for this tissue because INVX was not detected.

A

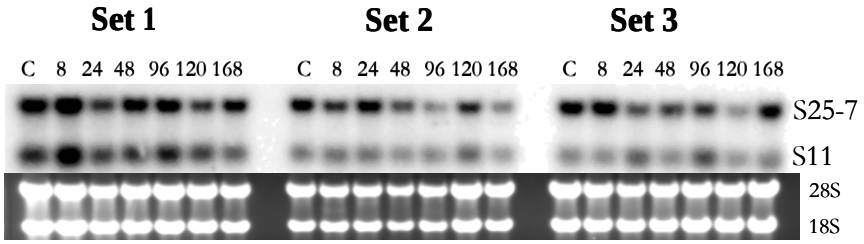
Set 1
Set 2
Set 3
C 8 24 48 96 120 168
C 8 24 48 96 120 168
C 8 24 48 96 120 168
S25-7
S11
28S
18S

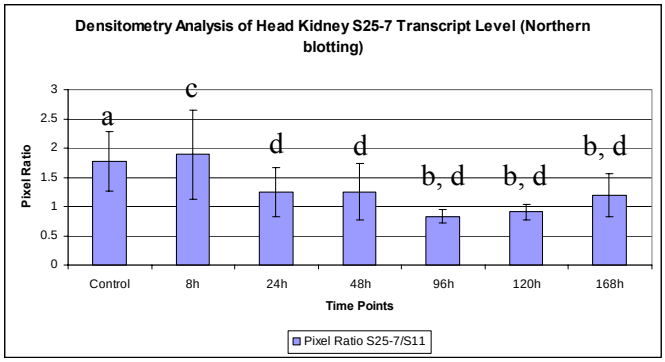
Densitometry Analysis of Head Kidney S25-7 Transcript Level (Northern blotting)
Pixel Ratio
3
2.5
2
1.5
1
0.5
0
a
c
d
d
b, d
b, d
b, d
Control
8h
24h
48h
96h
120h
168h
Time Points
Pixel Ratio S25-7/S11

B

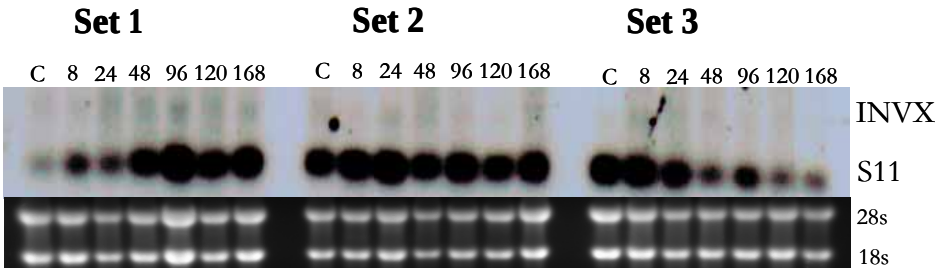
Set 1
Set 2
Set 3
C 8 24 48 96 120 168
C 8 24 48 96 120 168
C 8 24 48 96 120 168
INVX
S11
28s
18s

Figure 3.12: RT-PCR analysis of INVX transcript levels in PMA stimulated head kidney. Total RNA was isolated from head kidney tissue of three fish sacrificed at each of the time points 8, 24, 48, 96, 120 and 168 hours post stimulation as well as from three untreated control fish. The RNA was reverse transcribed and subjected to duplex PCR reaction to amplify both INVX and Ef-1α. The PCR products were separated on a 1% agarose gel, stained with ethidium bromide and visualized under UV light. The results of the amplification, along with densitometry analysis are shown in this figure. The upper band is the amplified INVX transcript and the lower band is the Ef-1α band. Densitometry analysis of INVX levels was performed and unequal template loading was corrected for by calculating the ratio of INVX signal to Ef-1α signal. The average of the ratio for each time point is shown in the bar graph, with error bars representing the standard deviation of the means for each time point. All three sets were included in the densitometry analysis. The sets used for RT-PCR analysis of INVX transcript levels correspond to the sets used for northern blot analysis of INVX transcript in head kidney.

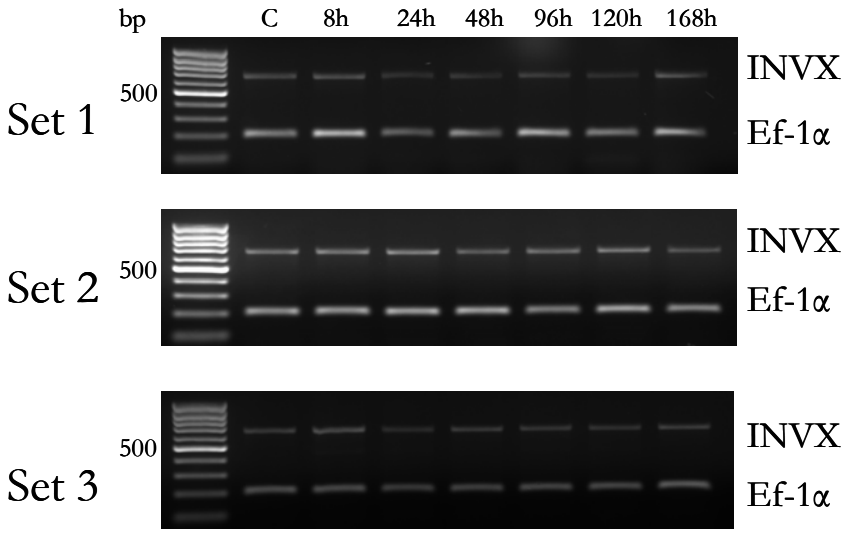
bp
C
8h
24h
48h
96h
120h
168h
Set 1
500
INVX
Ef-1α
Set 2
500
INVX
Ef-1α
Set 3
500
INVX
Ef-1α

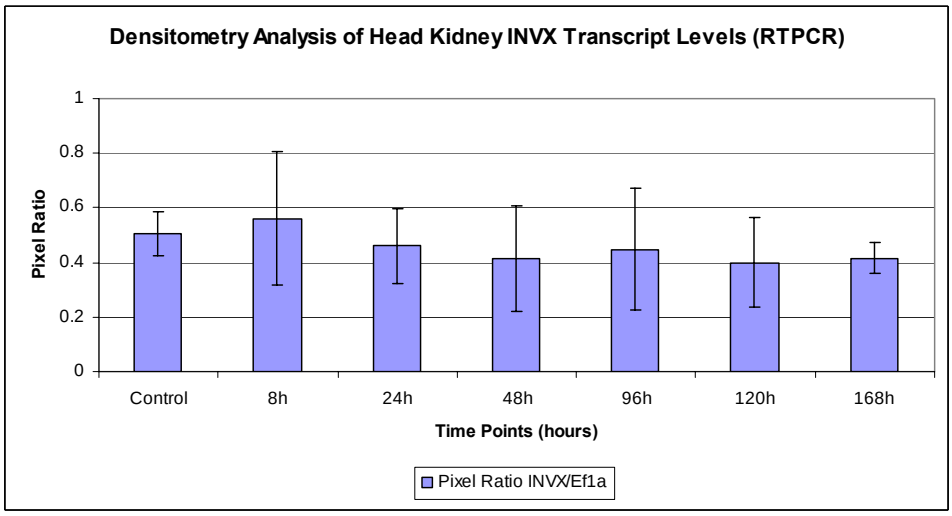
Densitometry Analysis of Head Kidney INVX Transcript Levels (RTPCR)
Pixel Ratio
1
0.8
0.6
0.4
0.2
0
Control
8h
24h
48h
96h
120h
168h
Time Points (hours)
Pixel Ratio INVX/Ef1a

the 18S and 28S rRNA are shown in figure 3.11. Again, as indicated by the decreased pixel ratio values, the levels of S25-7 transcript appear to be lower in head kidney than in both spleen and gill. Likewise, INVX transcript cannot be detected by northern blot analysis, and was subsequently analyzed by RT-PCR. This demonstrates that INVX transcript is present at a lower level in head kidney than S25-7 transcript and also is present at lower levels than found in spleen or gill. From the densitometry analysis, it appears that S25-7 transcript levels may be increasing slightly at the 8 hour time point, but similar to gill and spleen results, this increase is not statistically significant due to the large error bars associated with the S25-7/S11 means. However, the late time points, 96, 120 and 168 hours all have very small error bars and all appear to be lower than the control and early time points, indicating that S25-7 transcript levels may be decreasing during immune stimulation within head kidney. ANOVA analysis verifies that there is a significant difference in the means of this time course ($p=0.001$) while LSD post hoc testing indicates that the 96, 120 and 168 hour time points are significantly lower than the control time point ($p=0.001$, $p=0.002$ and $p=0.036$). Furthermore, the 24, 48, 96, 120 and 168 hour time points are all significantly lower than the 8 hour time point ($p=0.019$, $p=0.019$, $p=0.000$, $p=0.001$, and $p=0.012$). Although the error bars for the 8 hour time point appears to overlap with the error bar for the 24 and 48 hour time points, LSD post-hoc testing indicates that these time points are significantly different. This is because the analysis was performed for the entire set and was not a pair-wise comparison. Thus, although the level of S25-7 transcript is low in head kidney tissue, the transcript appears to be decreasing upon immune system stimulation.

To measure INVX transcript levels, RT-PCR analysis was performed with a duplex reaction to amplify both INVX and Ef-1α, as described above for both gill and spleen. The results of this amplification for the three sets analyzed are shown in figure 3.12. The densitometry analysis indicates that INVX transcript levels remains constant during immune system stimulation in head kidney, as confirmed by ANOVA analysis ($p=0.903$).

3.3.4 Analysis of Invariant Chain Transcript Levels in PMA Stimulated Liver

As a negative control, liver was also analyzed for S25-7 and INVX transcript expression, as this is not an immune tissue and is not expected to express INVX or S25-7. As described above, total RNA was isolated from liver tissue of six fish from each of the time points 8, 24, 48, 96, 120 and 168 hours post-stimulation as well as from six untreated control fish. The RNA was separated and transferred onto a nylon membrane and probed separately for S25-7 and INVX. Representative blots for both S25-7 and INVX, along with densitometry analysis and a UV image of the 18S and 28S rRNA are

Figure 3.13: Northern blot analysis of S25-7 and INVX transcript levels in PMA stimulated liver. Total RNA was isolated from liver tissue of six fish sacrificed at each of the time points 8, 24, 48, 96, 120 and 168 hours post stimulation as well as from six untreated control fish. The RNA was separated on a 1% agarose gel, stained with ethidium bromide, visualized under UV light and transferred onto nylon membrane. The RNA was then probed with either DIG-labeled S25-7 and S11 probes or INVX and S11 probes. A representative blot for both S25-7 and INVX are shown in this figure. The sets used for both S25-7 and INVX northern blotting correspond to the sets used for head kidney, spleen and gill northern blot analysis.

(A) Northern blot analysis of S25-7 transcript levels in PMA stimulated liver. As described above, three sets of RNA were separated on the same gel and transferred onto a nylon membrane. The membrane was probed for both S25-7 and S11 and the bands were detected on the Fluorchem 8000. The upper band in the blot is the S25-7 transcript while the lower band is the S11 transcript. The 18S and 28S bands are shown in the UV image of the RNA, under the blot. Finally, densitometry analysis was performed to analyze S25-7 transcript levels. The ratio of S25-7 signal to S11 signal was calculated and the average ratio for each point was plotted, along with error bars representing the standard deviation for each mean. All six sets were used for densitometry analysis. The additional sets are shown in appendix A, figure A.4.

(B) Northern blot analysis of INVX transcript levels in PMA stimulated liver. As described above, all six sets were separated on the same gel and transferred onto a nylon membrane. The membrane was probed for both INVX and S11 and the bands were detected with x-ray film. INVX transcript was not detected in liver RNA, only the lower S11 transcript can be seen. The 18S and 28S ribosomal RNA is shown in the UV image below the blot. No densitometry analysis was performed because INVX was not detected in this tissue.

A

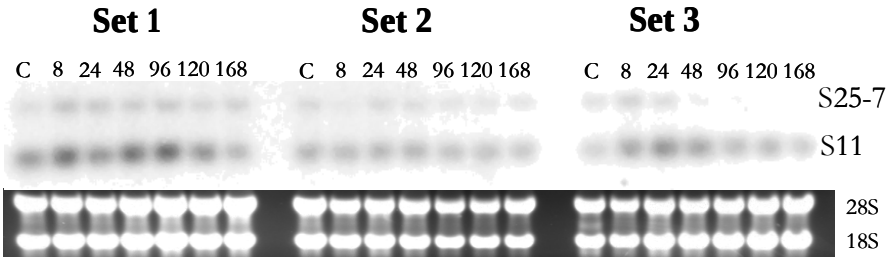
Set 1
Set 2
Set 3
C 8 24 48 96 120 168
C 8 24 48 96 120 168
C 8 24 48 96 120 168
S25-7
S11
28S
18S

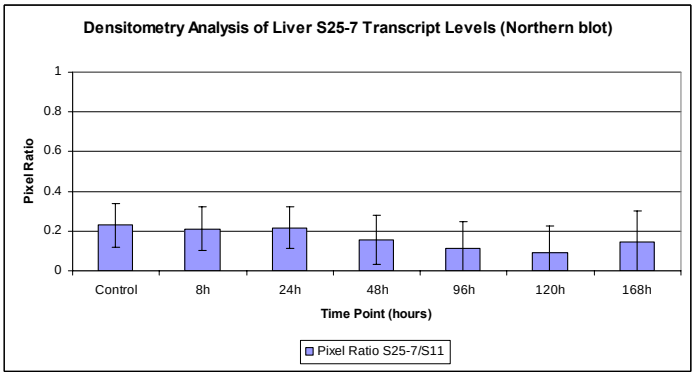
Densitometry Analysis of Liver S25-7 Transcript Levels (Northern blot)
Pixel Ratio
1
0.8
0.6
0.4
0.2
0
Control
8h
24h
48h
96h
120h
168h
Time Point (hours)
Pixel Ratio S25-7/S11

B

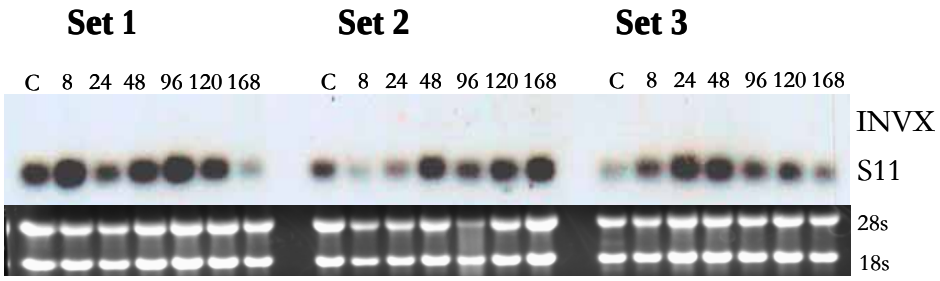
Set 1
Set 2
Set 3
C 8 24 48 96 120 168
C 8 24 48 96 120 168
C 8 24 48 96 120 168
INVX
S11
28s
18s

Figure 3.14: RT-PCR analysis of INVX transcript levels in PMA stimulated liver. Total RNA was isolated from liver tissue of three fish sacrificed at each of the time points 8, 24, 48, 96, 120 and 168 hours post stimulation as well as from three untreated control fish. The RNA was reverse transcribed and subjected to a duplex PCR to amplify both INVX and Ef-1α. The PCR products were separated on a 1% agarose gel, stained with ethidium bromide and visualized under UV light. Amplification of the three sets analyzed are shown in this figure, along with the densitometry analysis. The upper band in each gel is the INVX transcript while the lower band in the Ef-1α transcript. The ratio of INVX signal to Ef-1α signal was calculated for all time points, and the average INVX/Ef-1α for each time point was plotted along with error bars representing the standard deviation for each mean. The sets analyzed for INVX transcript by RT-PCR correspond to the sets analyzed by northern blotting.

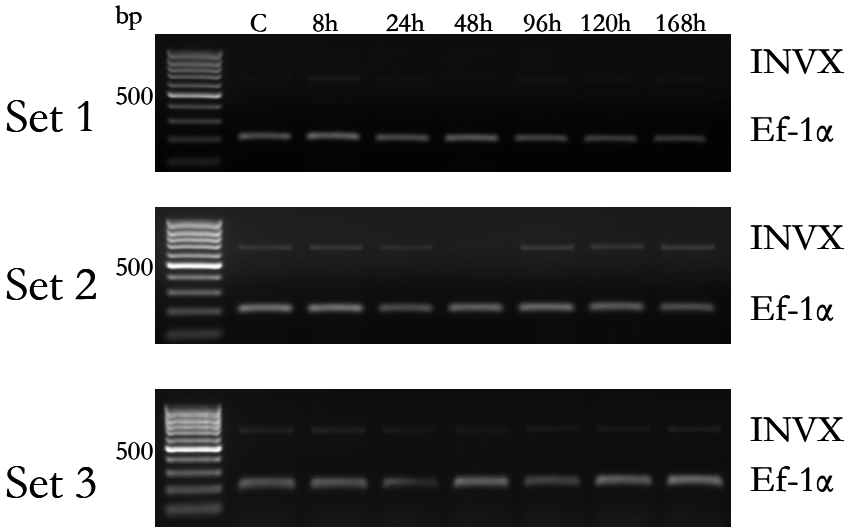
bp
C
8h
24h
48h
96h
120h
168h
Set 1
500
INVX
Ef-1α
Set 2
500
INVX
Ef-1α
Set 3
500
INVX
Ef-1α

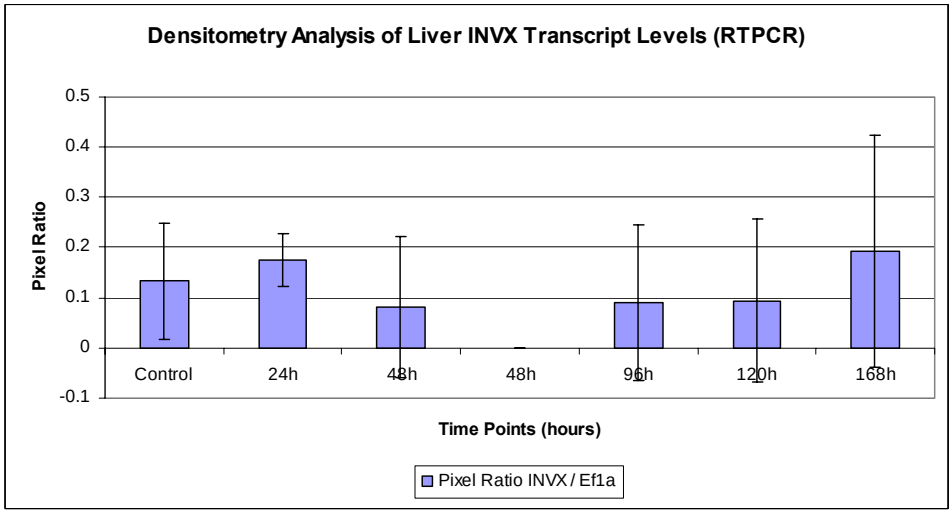
Densitometry Analysis of Liver INVX Transcript Levels (RTPCR)
Pixel Ratio
0.5
0.4
0.3
0.2
0.1
0
-0.1
Control
24h
48h
48h
96h
120h
168h
Time Points (hours)
Pixel Ratio INVX / Ef1a

shown in figure 3.13. As expected, there was no INVX signal; however, there was a very low signal from S25-7. The S25-7/S11 ratio was much lower than the other tissues analyzed, and is quite variable within each time point, as indicated by the large error bars relative to the small means. ANOVA analysis indicates that there is no significant difference between S25-7 transcript levels at each of the time points examined ($p=0.370$). The likely source of this signal is leukocytes within liver tissue. Indeed, when RT-PCR was performed on liver RNA to analyze INVX levels, a low level was also detected. As shown in figure 3.14, the level of INVX transcript is also very low with large variability within each time point. ANOVA analysis also confirms that there is no significant change in INVX transcript levels in the liver during immune system stimulation ($p=0.705$). Since the signals for both S25-7 and INVX are likely due to leukocytes within the liver, these results also indirectly demonstrate a higher level of S25-7 transcript in leukocytes than INVX, as INVX cannot be detected by northern blotting while S25-7 can.

3.3.5 Analysis of Invariant Chain Transcript Levels in PMA Stimulated Peripheral Blood Leukocytes

Total RNA was isolated from peripheral blood leukocytes of six fish from each of the time points 8, 24, 48, 96, 120 and 168 hours post-stimulation as well as from six untreated control fish. The level of isolated RNA was too low to perform northern blot analysis. Instead, RT-PCR was performed to measure S25-7 and INVX transcript levels. Although RNA was isolated from six sets, only four sets showed non-degraded RNA, and thus only 4 sets were included for the analysis. A separate PCR reaction was performed for INVX, S25-7 and the control Ef-1α, each reaction was run on a 1% agarose gel and visualized under UV light. A representative gel for INVX, S25-7 and Ef-1α RT-PCR results are shown in figure 3.15, along with densitometry analysis. The other three sets used for densitometry analysis are shown in appendix A. Densitometry analysis of RT-PCR results indicates that S25-7 and INVX are present at similar levels in leukocytes. While there was a marked difference in S25-7 and INVX transcript levels in the other tissues analyzed, it is likely that the separate PCR reactions makes it difficult to compare these transcript levels in peripheral blood leukocytes. If a duplex PCR reaction with INVX and Ef-1α as well as S25-7 and Ef-1α had been performed, it would have been much easier to compare the levels of S25-7 and INVX, as there would be no variability of PCR conditions or gel loading and visualizing between the invariant chain transcript and the control transcript. However, the amplified S25-7 and Ef-1α band are very close in size and cannot be

Figure 3.15: RT-PCR analysis of S25-7 and INVX transcript levels in PMA stimulated peripheral blood leukocytes. Total RNA was isolated from peripheral blood leukocytes collected from six fish sacrificed at each of the time points 8, 24, 48, 96, 120 and 168 hours post stimulation as well as from six untreated control fish. The RNA was reverse transcribed and amplified separately for INVX, S25-7 and Ef-1α. The PCR products were separated on a 1% agarose gel, stained with ethidium bromide and visualized under UV light. Due to RNA degradation in some samples, only four sets could be analyzed for invariant chain transcript levels. A representative image for INVX, S25-7 and Ef-1α is shown in this figure, along with densitometry analysis for both S25-7 and INVX transcripts. The upper gel is the INVX PCR product, the middle gel is S25-7 and the lower gel is Ef-1α. Densitometry analysis was performed by calculating the ratio of INVX or S25-7 signal to the corresponding Ef-1α signal. The average ratio for S25-7 and INVX for the four set analyzed were plotted, along with error bars representing the standard deviation for each mean. The additional three sets used for the densitometry analysis are shown in appendix A, figure A.5.

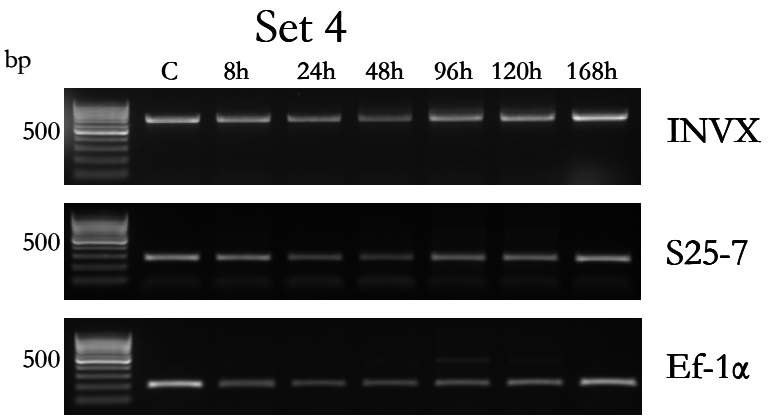
Set 4
bp
C
8h
24h
48h
96h
120h
168h
500
INVX
500
S25-7
500
Ef-1α

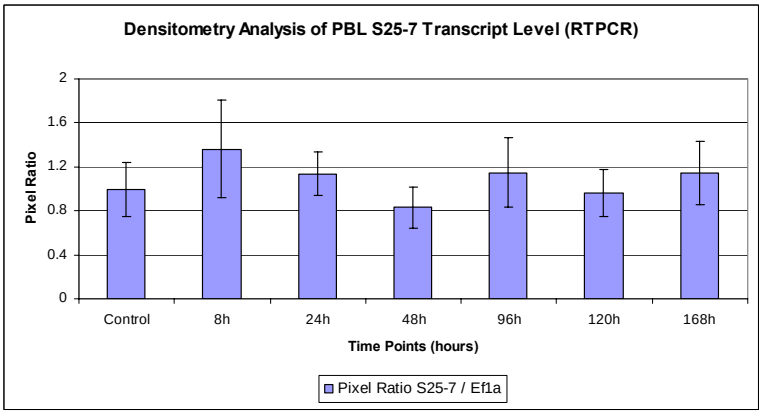
Densitometry Analysis of PBL S25-7 Transcript Level (RTPCR)
Pixel Ratio
2
1.6
1.2
0.8
0.4
0
Control
8h
24h
48h
96h
120h
168h
Time Points (hours)
Pixel Ratio S25-7 / Ef1a

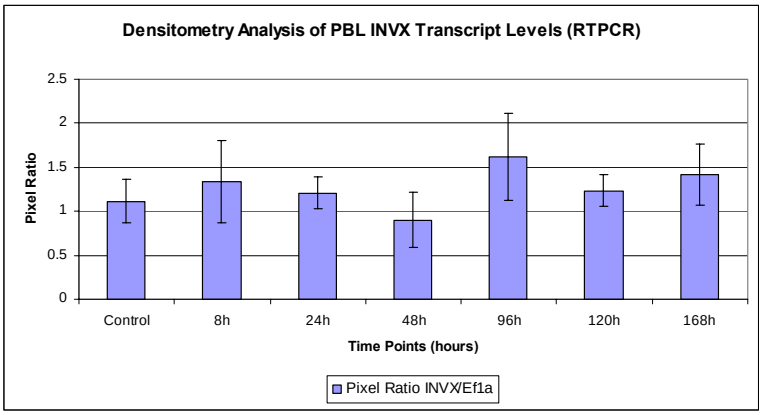
Densitometry Analysis of PBL INVX Transcript Levels (RTPCR)
Pixel Ratio
2.5
2
1.5
1
0.5
0
Control
8h
24h
48h
96h
120h
168h
Time Points (hours)
Pixel Ratio INVX/Ef1a

resolved from each other on an agarose gel. Thus, it cannot be conclusively determined if S25-7 and INVX are present at different levels in peripheral blood leukocytes.

Both S25-7 and INVX appear to increase slightly at 8 hours post-stimulation, followed by a decrease at 24 and 48 hours and a subsequent increase at 96 hours. However, as was the case for the northern blot analysis, there is great variability between individuals within each time point, resulting in large error bars, making it very difficult to show significant differences across time points. ANOVA analysis indicates that there is no significant difference in the levels of either S25-7 or INVX ($p=0.093$ and $p=0.244$) transcript in peripheral blood leukocytes during immune system stimulation.

3.4 Analysis of Invariant Chain Protein Expression in the PMA *in vivo* Time Course

Total cellular protein was isolated from gill, spleen, head kidney and liver of six fish from each of the time points 8, 24, 48, 96, 120 and 168 hours post-stimulation as well as from six untreated control fish. The S25-7 and INVX protein level was analyzed by western blot analysis. For each blot, one set of one tissue was run on a 12% polyacrylamide gel and transferred onto a nitrocellulose membrane. Western blotting was performed to analyze both S25-7 and INVX protein levels in all tissues for all six sets. However, due to poor western blot results, only four sets were used for protein expression analysis in gill and spleen. As described above for northern blot analysis, densitometry analysis was also performed on the western blots to measure changes in protein levels. However, in this case there is no antibody against a control protein that will remain unaffected during the immune system stimulation. Instead, a 50 kDa protein found on the ponceau stained membranes was used as a control. Further complicating the densitometry analysis is the fact that both S25-7 and INVX migrate as doublets. In order to quantify the signals for these proteins, the signal from both bands of the doublet was added together, and the ratio of this value to the corresponding 50 kDa band was calculated to control for unequal protein loading. ANOVA analysis and LSD post hoc tests were performed to identify statistically significant changes in S25-7 and INVX proteins levels during immune system stimulation.

3.4.1 Analysis of Invariant Chain Protein Levels in PMA Stimulated Gill

Protein was isolated from gill tissue of four fish from each time point 8, 24, 48, 96, 120 and 168 as well as from four untreated control fish and subjected to western blot analysis for S25-7 and INVX protein expression levels. Representative western blots, along with the corresponding ponceau staining of the nitrocellulose membrane to show equal sample loading, as well as densitometry analysis for both S25-7 and INVX are shown in figure 3.16. The other three sets of blots are shown in appendix A. In the case of S25-7, it appears the protein level may increase slightly between control and the 8 and 24 hour time points, but this increase is not statistically significant due to the large error bars associated with the average S25-7 / 50 kDa ratio for each time point (ANOVA: $p=0.778$). The large variability of S25-7 protein levels between individual fish can be clearly seen within the control fish. In two of the sets analyzed, the level of S25-7 is very low in the control sample, while in the two other sets S25-7 levels are quite high. It is difficult to determine any change in protein levels between treatment and control when the variability within the untreated controls is so high. INVX protein levels in gill are similar to S25-7, indicating that the difference in transcript level of these two genes may not be reflected in the level of expressed protein. INVX also appears to increase slightly between the untreated control and the 8 hour time point, with this increase being larger than the one seen for S25-7. However, as is the case for S25-7, the large error bars and the variability within the control fish make it difficult to show a significant increase (ANOVA: $p=0.184$). Thus, while there may appear to be a very slight increase in both S25-7 and INVX protein levels at 8 hours after immune system stimulation, this increase is not statistically significant and may be due to random variability between fish and not dependent on the immune system stimulation. From these results, it appears that S25-7 and INVX protein levels in the gill remain fairly constant during immune system stimulation. Interestingly, both invariant chain proteins show degradation at the 168 hour time point. This may be evidence of the stepwise degradation of the invariant chain as it travels through the cell for class II antigen loading.

3.4.2 Analysis of Invariant Chain Protein Levels in PMA Stimulated Spleen

Protein was isolated from spleen tissue of four fish from each of the time points 8, 24, 48, 96, 120 and 168 hours post-stimulation as well as from four untreated control fish. The protein was denatured and run as single sets for SDS-PAGE and western blot analysis of S25-7 and INVX protein expression. Representative western blots for both S25-7 and INVX, along with ponceau staining as well as densitometry analysis are shown in figure 3.17. The expression of both S25-7 and INVX are

Figure 3.16: Western blot analysis of S25-7 and INVX protein levels in PMA stimulated gill. Total protein was isolated from gill tissue of six fish sacrificed at each of the time points 8, 24, 48, 96, 120 and 168 hours post stimulation as well as from six untreated control fish. The protein was denatured, 100µg of each sample was separated on a 12% polyacrylamide gel and transferred onto a nitrocellulose membrane. The membrane was ponceau stained to check for equal protein loading and probed with either anti-rtINVX antibody or anti-rTg antibody, followed by anti-rabbit IgG HRP conjugated antibody. The protein was detected by the addition of the ECL-plus substrate followed by visualization with the Fluorchem 8000 imager. The blots were then subjected to densitometry analysis. Since there is no antibody against a housekeeping protein, the 50kDa protein seen on the ponceau stain was used as a control. The intensity of this band was measured, and used to correct for unequal protein loading. Both S25-7 and INVX migrate as doublets in the western blot, thus, for the densitometry analysis the intensity of both bands of the doublet was added together. The ratio of this value to the 50kDa signal was calculated and the average ratio for each time point was plotted on a bar graph, with error bars representing the standard deviation for each mean. Due to difficulty detecting blots, only four sets were used for the densitometry analysis. The additional three sets used are shown in appendix A, figure A.6.

(A) Western blot analysis of S25-7 protein levels in PMA stimulated gill. The doublet of S25-7 protein is shown in the blot, migrating just above 36kDa. The ponceau stain of this membrane is shown just below the western blot. The densitometry analysis of S25-7 protein levels is shown, with the average S25-7/50kDa ratio for each time point plotted in a bar graph along with the error bars.

(B) Western blot analysis of INVX protein levels in PMA stimulated gill. The doublet of INVX protein is shown in the blot, migrating slightly above 36 kDa. The ponceau stain of this membrane is shown just below the western blot. The densitometry analysis is represented by a bar graph of the average INVX/50kDa ratio for each time point along with the corresponding error bars.

A

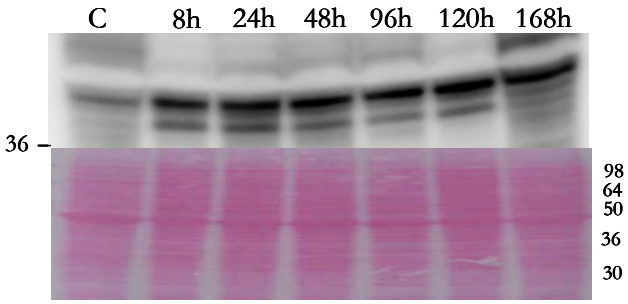
C
8h
24h
48h
96h
120h
168h
36
98
64
50
36
30

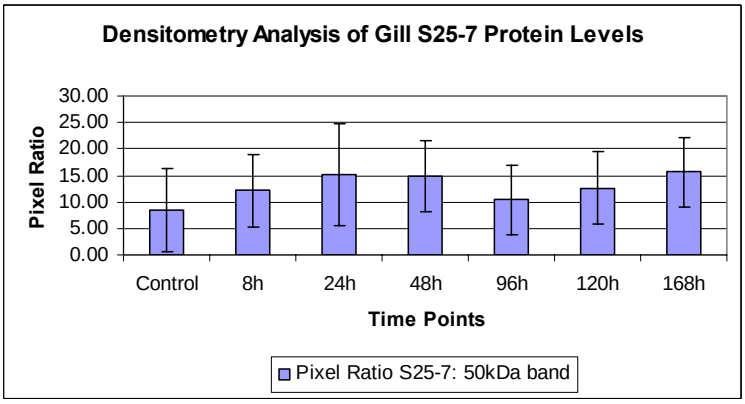
Densitometry Analysis of Gill S25-7 Protein Levels
Pixel Ratio
30.00
25.00
20.00
15.00
10.00
5.00
0.00
Control
8h
24h
48h
96h
120h
168h
Time Points
Pixel Ratio S25-7: 50kDa band

B

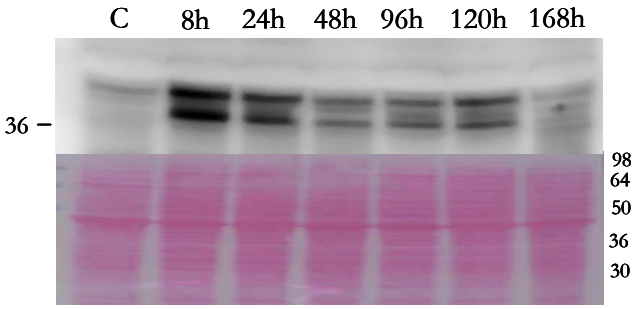
C
8h
24h
48h
96h
120h
168h
36
98
64
50
36
30

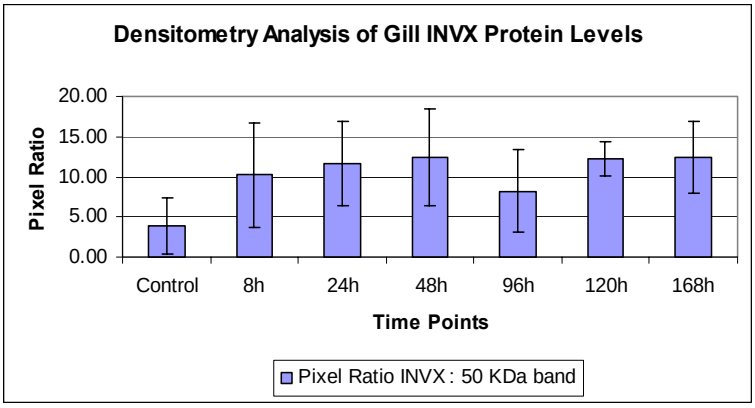
Densitometry Analysis of Gill INVX Protein Levels
Pixel Ratio
20.00
15.00
10.00
5.00
0.00
Control
8h
24h
48h
96h
120h
168h
Time Points
Pixel Ratio INVX : 50 KDa band

Figure 3.17: Western blot analysis of S25-7 and INVX protein levels in PMA stimulated spleen. Protein was isolated from spleen tissue of six fish sacrificed at each of the time points 8, 24, 48, 96, 120, and 168 hours post stimulation as well as from six untreated control fish. The protein was denatured, 100µg of each sample was separated on a 12% polyacrylamide gel and transferred onto a nitrocellulose membrane. The membrane was the ponceau stained to visualize total cellular proteins. The membrane was then probed with either anti-rtINVX antibody or anti-rTg antibody followed by anti-rabbit IgG HRP conjugated antibody. The blot was detected by incubation with the ECL-plus substrate followed by detection on the Fluorchem 8000 imager. The blots were subjected to densitometry analysis in the same way as described above for gill western blot analysis. Again, only four sets were used for densitometry analysis due to difficulties analyzing blots with the Total Lab 100 software. The additional blots used for densitometry analysis is shown in appendix A, figure A.6.

(A) Western blot analysis of S25-7 protein levels in PMA stimulated spleen. The doublet of S25-7 protein is shown in the blot running just above 36kDa. The ponceau stain of this membrane is shown below the blot. The densitometry analysis consisting of a bar graph representing the average S25-7/50kDa ratio for each time point, along with error bars representing the standard deviation for each time point is shown below the ponceau stain.

(B) Western blot analysis of INVX protein levels in PMA stimulated spleen. The doublet of INVX protein is shown in the blot running slightly above 36kDa. The ponceau stain of this membrane is shown below the blot. The densitometry analysis, consisting of a bar graph representing the average INVX/50kDa ratio for each time point, along with error bars representing the standard deviation for each time point is shown below the ponceau stain.

A

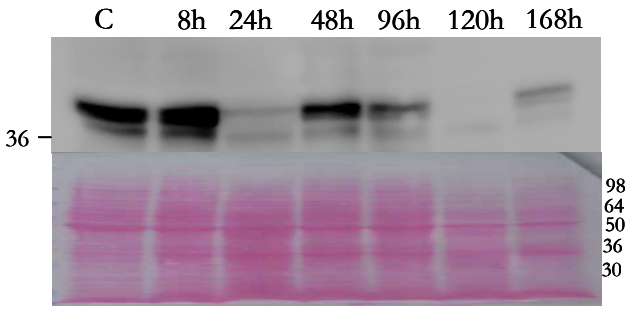
C
8h
24h
48h
96h
120h
168h
36
98
64
50
36
30

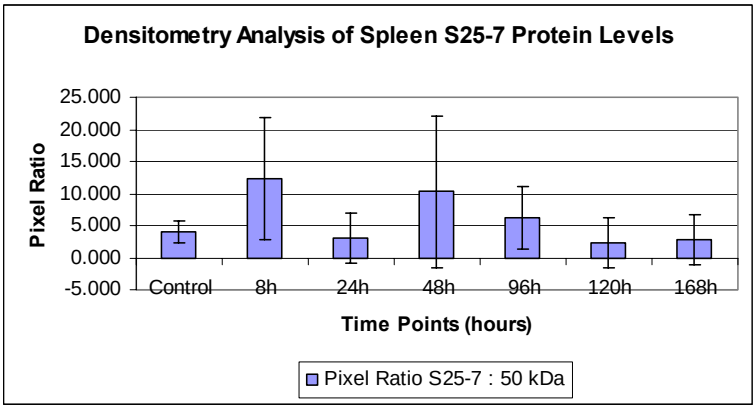
Densitometry Analysis of Spleen S25-7 Protein Levels
Pixel Ratio
25.000
20.000
15.000
10.000
5.000
0.000
-5.000
Control
8h
24h
48h
96h
120h
168h
Time Points (hours)
Pixel Ratio S25-7 : 50 kDa

B

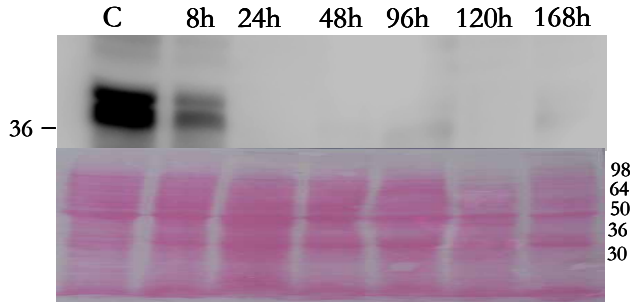
C
8h
24h
48h
96h
120h
168h
36
98
64
50
36
30

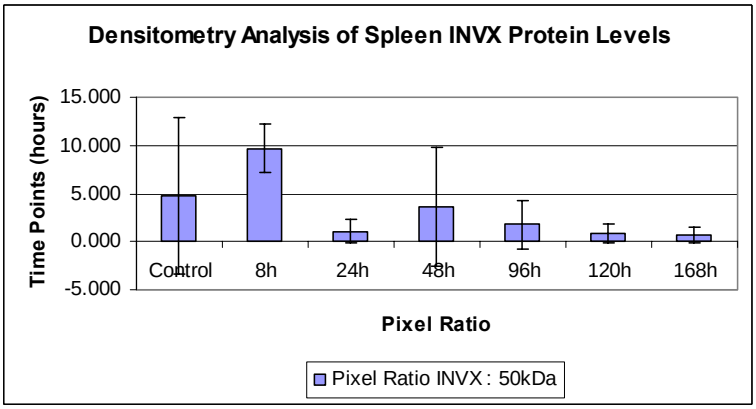
Densitometry Analysis of Spleen INVX Protein Levels
Time Points (hours)
15.000
10.000
5.000
0.000
-5.000
Control
8h
24h
48h
96h
120h
168h
Pixel Ratio
Pixel Ratio INVX : 50kDa

extremely variable within the spleen. All four sets show one or two time points with a very high level of S25-7 and INVX, for the representative blots, these time points are control and 8 hours for INVX and control, 8, 48 and 96 hours for S25-7. The other time points have very low or undetectable S25-7 and INVX. The ponceau staining of the membranes show approximately equal sample loading, indicating that this large variability in protein expression is not due to errors in sample loading. This pattern is consistent for all spleen blots, as shown in appendix A, figure A.7. As a control, six untreated fish were sacrificed and analyzed for S25-7 and INVX, and again, the levels of the protein vary from undetectable to very high, with INVX:50KDa densitometry values ranging 1.17 to 10.73 and S25-7:50KDa densitometry ratios ranging from 1.17 to 34.32 (data not shown). Thus, it is impossible to draw conclusions about any changes in spleen S25-7 and INVX protein levels during an immune response due to the large degree of variability of spleen S25-7 and INVX protein expression between fish.

3.4.3 Analysis of Invariant Chain Protein Levels in PMA Stimulated Head Kidney

Total cellular protein was isolated from head kidney tissue of six fish from each of the time points 8, 24, 48, 96, 120 and 168 hours post-stimulation as well as from six untreated control fish. S25-7 and INVX protein levels were analyzed by western blotting. Each set was separated on a 12% polyacrylamide gel, transferred to a nitrocellulose membrane and probed for either INVX or S25-7. Representative blots for both S25-7 and INVX, along with ponceau staining of the membrane are shown in figure 3.18. Neither INVX nor S25-7 could be detected in head kidney by western blot analysis, thus no densitometry analysis was performed. Although transcript for both genes could be detected at low levels in head kidney, either there is no translation of the transcripts, or the protein is present at such low levels that it is undetectable with the western blotting methods used.

3.4.4 Analysis of Invariant Chain Protein Levels in PMA Stimulated Liver

Protein was also isolated from liver tissue of six fish from each of the time points 8, 24, 48, 96, 120 and 168 hours post-stimulation, as well as from six untreated control fish and analyzed by western blot analysis for S25-7 and INVX protein expression. Representative blots for both S25-7 and INVX, along with the corresponding ponceau stain are shown in figure 3.19. Neither INVX nor S25-7 was detected in liver tissue and no densitometry analysis was performed. Again, although there was a small amount transcript detected for both S25-7 and INVX, either these are not translated or the amount of protein translated is too small to be detected by the western blotting method.

Figure 3.18: Western blot analysis of S25-7 and INVX protein levels in PMA stimulated head kidney. Total protein was isolated from head kidney tissue of six fish sacrificed at each of the time points 8, 24, 48, 96, 120 and 168 hours post stimulation as well as from six untreated control fish. The protein was denatured, 100µg of each sample was separated on a 12% polyacrylamide gel and transferred onto a nitrocellulose membrane. The membrane was ponceau stained to visualize integrity of separated protein and to verify equal sample loading. The blot was then probed with either anti-rtINVX antibody or anti-rTg antibody followed by anti-rabbit IgG HRP conjugated antibody. The blot was detected by incubation with the substrate ECL-plus followed by visualization with the Fluorchem 8000. Since neither S25-7 nor INVX were detected in this tissue, no densitometry analysis was performed.

(A) Western blot analysis of S25-7 protein levels in PMA stimulated head kidney. The western blot is shown, with no detectable bands, along with the ponceau staining of this blot.

(B) Western blot analysis of INVX protein levels in PMA stimulated head kidney. The western blot is shown, with no detectable bands, along with the ponceau staining of this blot.

A

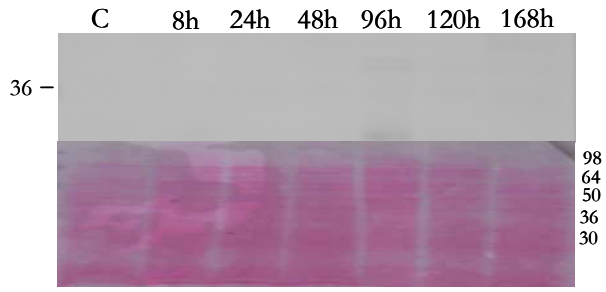
C
8h
24h
48h
96h
120h
168h
36
98
64
50
36
30

B

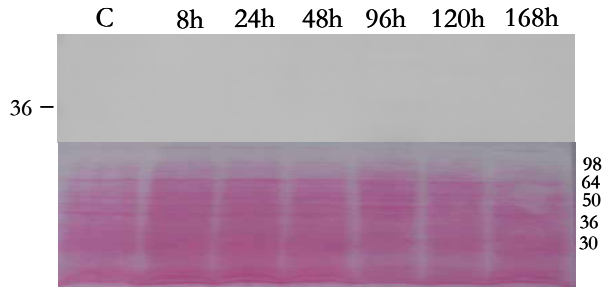
C
8h
24h
48h
96h
120h
168h
36
98
64
50
36
30

Figure 3.19: Western blot analysis of S25-7 and INVX protein levels in PMA stimulated liver. Total protein was isolated from liver tissue of six fish sacrificed at each of the time points 8, 24, 48, 96, 120 and 168 hours post stimulation as well as from six untreated control fish. The protein was denatured, 100µg of each sample was separated on a 12% polyacrylamide gel and transferred onto a nitrocellulose membrane. The membrane was ponceau stained to visualize integrity of separated protein and to verify equal sample loading. The blot was then probed with either anti-rtINVX antibody or anti-rTg antibody followed by anti-rabbit IgG HRP conjugated antibody. The blot was detected by incubation with the substrate ECL-plus followed by visualization with the Fluorchem 8000. Since neither S25-7 nor INVX were detected in this tissue, no densitometry analysis was performed.

(A) Western blot analysis of S25-7 protein levels in PMA stimulated liver. The western blot is shown, with no detectable bands, along with the ponceau staining of this blot.

(B) Western blot analysis of INVX protein levels in PMA stimulated liver. The western blot is shown, with no detectable bands, along with the ponceau staining of this blot.

A

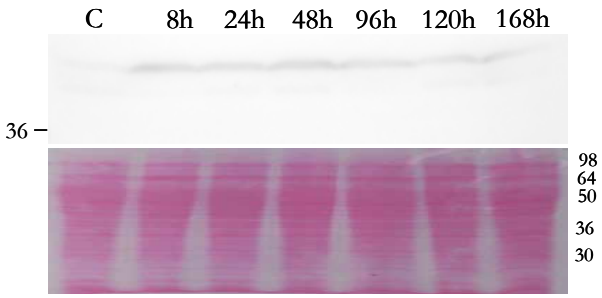
C
8h
24h
48h
96h
120h
168h
36
98
64
50
36
30

B

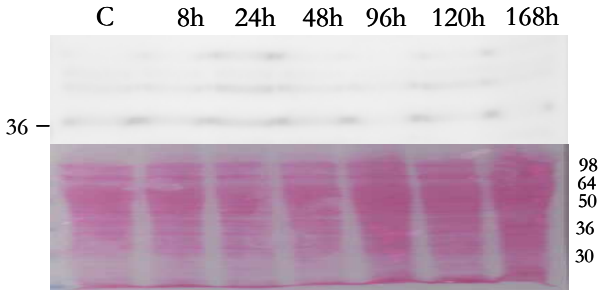
C
8h
24h
48h
96h
120h
168h
36
98
64
50
36
30

3.5 Analysis of Invariant Chain Expression in the Macrophage-Like Cell Line RTS11

In addition to the *in vivo* time course, an *in vitro* time course was also performed to analyze S25-7 and INVX expression in the macrophage-like cell line RTS11. These cells were plated at a concentration of $2x10^7$ cells per well and treated with 2µg PMA per 1mL of media. Cells were incubated at 18°C and samples were collected at each of the time points 8, 24, 48, 96, 120 and 168 hours post-stimulation. In addition, a DMSO-treated control was also collected after 168 hours of incubation. The collected cells for each time point were split in two aliquots and used for both western blot and RT-PCR analysis.

3.5.1 Analysis of Invariant Chain Transcript Levels in PMA Stimulated RTS11

Total RNA was isolated from cells collected at each of the time points 8, 24, 48, 96, 120 and 168 hours post-stimulation as well as from the DMSO-treated control. The RNA was reverse transcribed and amplified with primers specific for INVX, S25-7 and Ef-1α. These PCR reactions were performed separately and run on separate 1% agarose gels. To control for unequal sample loading, densitometry analysis was performed for both S25-7 and INVX by calculating the ratio of INVX / Ef-1α and S25-7 / Ef-1α. The *in vitro* time course was performed in triplicate. Representative results for all three PCR reactions as well as densitometry analysis for both S25-7 and INVX transcript expression is shown in figure 3.20. As described above for peripheral blood leukocyte analysis, the use of separate PCR reactions for INVX, S25-7 and Ef-1α makes it difficult to compare expression levels of S25-7 and INVX.

Similar to the results of the *in vivo* time course, there appears to be very little change in the levels of S25-7 transcript after stimulation, with only a slight decrease at 48 hours, which is not statistically significant, as confirmed by ANOVA analysis ($p=0.713$). INVX transcript levels appear to be at the highest level in the control samples, with a continual decrease from 8 hours to 24 hours followed by an increase at 96, 120 and 168 hours after stimulation. In the case of INVX, ANOVA analysis indicates that there is a significant change in transcript levels ($p=0.021$), while LSD post hoc analysis indicates that INVX transcript in the control sample is significantly higher than 48, 96 and 120 hour time points ($p=0.001$, $p=0.004$ and $p=0.037$). Furthermore, INVX transcript level the 8 hour time

Figure 3.20: RT-PCR analysis of S25-7 and INVX transcript levels in the macrophage-like cell line RTS11. Cells were plated at a concentration of $2x10^7$ cells / well, treated with 2μg/mL PMA and incubated at 18°C. Samples were then collected at each of the time points 8, 24, 48, 96, 120, and 168 hours post stimulation. In addition, a control well was treated with DMSO and collected after 168 hours. The collected cells were split in half, such that approximately 10^7 cells were analyzed for invariant chain transcript and 10^7 cells analyzed for invariant chain protein levels for each time point. The time course was performed in triplicate.

For transcript analysis, total RNA was isolated from cells of each time point and the RNA was reverse transcribed. The resulting cDNA was then amplified separately for INVX, S25-7 and Ef-1α. The PCR products were separated on a 1% agarose gel, stained with ethidium bromide and visualized under UV light. A representative set of PCR products are shown in this figure along with the densitometry analysis for both S25-7 and INVX. The bar graphs represent the average INVX/Ef-1α and S25-7/Ef-1α ratios for each time point, with error bars representing the standard deviation for each mean. The letters represent the results of ANOVA and LSD post hoc testing, where 'a' is significantly different from 'b', 'c' is significantly different from 'd' and 'e' is significantly different from 'f'. The additional sets used for densitometry analysis are shown in appendix A, figure A.8.

Set 1

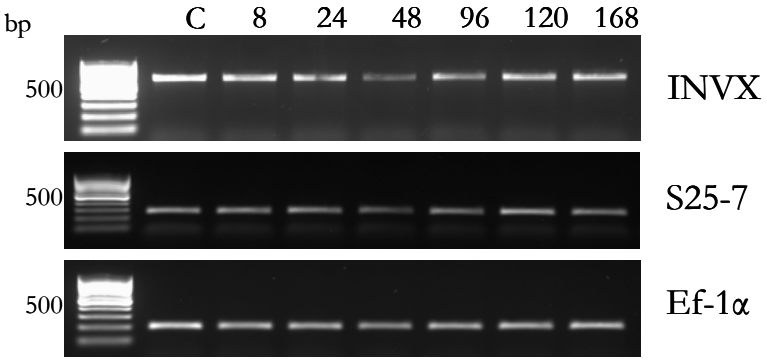
bp
C
8
24
48
96
120
168
500
INVX
500
S25-7
500
Ef-1α

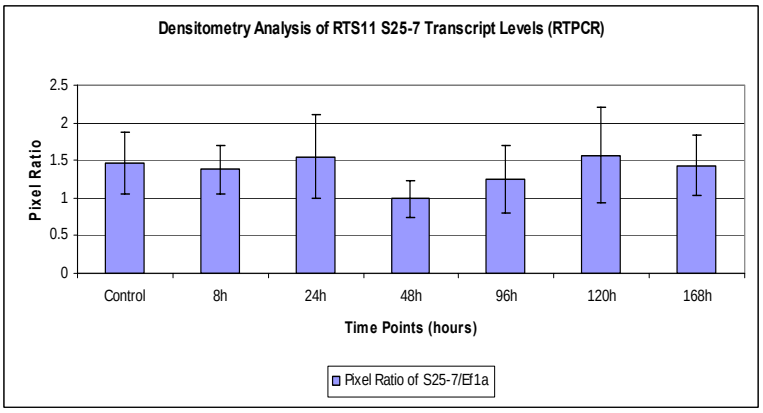
Densitometry Analysis of RTS11 S25-7 Transcript Levels (RTPCR)
Pixel Ratio
2.5
2
1.5
1
0.5
0
Control
8h
24h
48h
96h
120h
168h
Time Points (hours)
Pixel Ratio of S25-7/Ef1a

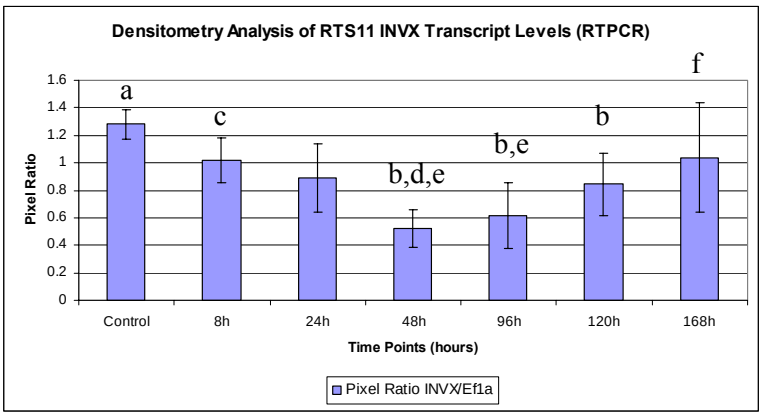
Densitometry Analysis of RTS11 INVX Transcript Levels (RTPCR)
Pixel Ratio
1.6
1.4
1.2
1
0.8
0.6
0.4
0.2
0
a
c
b,d,e
b,e
b
f
Control
8h
24h
48h
96h
120h
168h
Time Points (hours)
Pixel Ratio INVX/Ef1a

point is significantly higher than 48 hour time point (p=0.022). Finally, the 168 hour time point is significantly higher than the 48 and 96 hour time points (p=0.017 and p=0.044). Although the 8 hour and 168 hour time points have very similar values, only the 168 hour time point is significantly different from the 96 hour time point. Similar to the results in head kidney, this is due to the comparison of the entire time course instead of a pair-wise comparison. These results demonstrate that while S25-7 transcript levels appear to remain unchanged during PMA stimulation, INVX transcript decreases upon stimulation and then increases again at the later time points.

3.5.2 Analysis of Invariant Chain Protein Levels in PMA Stimulated RTS11

Total protein was isolated from cells collected at 8, 24, 48, 96, 120, and 168 hours post-stimulation as well as from DMSO-treated control cells. This protein was separated on a 12% polyacrylamide gel, transferred onto a nitrocellulose membrane and probed for either INVX or S25-7. Representative blots for both S25-7 and INVX, along with ponceau staining of these blots as well as densitometry analysis is shown in figure 3.21. Again, as found with the *in vivo* time course western blotting, there is a great deal of variability within each time point. However, for INVX, only 3 replicates were analyzed while only 2 replicates were analyzed for the S25-7 western blot densitometry. If more samples had been analyzed, it is likely that the error bars would be decreased in size. Comparison of the ratios of S25-7 / 50 kDa and INVX / 50 kDa indicate that S25-7 appears to be present in a higher amount than INVX. S25-7 appears to be present in high levels in the control samples, which corresponds to the high levels of transcript in these samples. The levels appear to decrease at the 24 and 48 hour time points, although the large error bars indicate that this decrease is not significant. INVX protein levels appear to remain constant during the time course. ANOVA analysis indicates that there is no significant change in the levels of S25-7 or INVX protein during PMA stimulation (p=0.230 and p=0.883).

Figure 3.21: Western blot analysis of S25-7 and INVX protein levels in the macrophage-like cell line RTS11. Total protein was isolated from 10^7 RTS11 cells collected at each of the time points 8, 24, 48, 96, 120 and 168 hours after PMA stimulation as well as from a DMSO treated control. The protein was denatured, 100µg of each sample was separated on a 12% polyacrylamide gel and transferred onto a nitrocellulose membrane. The membrane was ponceau stained to verify protein integrity as well as equal sample loading across the membrane. The blot was then probed with either anti-rtINVX antibody or anti-rTg antibody, followed by anti-rabbit IgG HRP conjugated antibody. The blot was incubated with ECL-plus substrate followed by detection with the Fluorchem 8000 imager. Densitometry analysis was performed on these blots in a similar manner to that described above for gill western blot anlaysis. The sum of the S25-7 and INVX doublet bands were calculated and the ratio of this sum to the 50kDa band on the ponceau was determined. The additional blots used for this densitometry analysis is shown in appendix A, figure A.9.

(A) Western blot analysis of S25-7 protein levels in PMA stimulated RTS11 cells. The doublet in the blot running just above 36kDa represents the S25-7 protein. The ponceau staining of this membrane is shown below the blot. The densitometry analysis of S25-7 protein levels is also shown, where each bar represents the average S25-7 / 50kDa ratio for each time point, with error bars representing the standard deviation for each mean. The densitometry analysis is the average of two S25-7 blots.

(B) Western blot analysis of INVX protein levels in PMA stimulated RTS11 cells. The doublet in the blot running slightly above 36kDa represents the INVX protein. The ponceau staining of this membrane is shown below the blot. The densitometry analysis of INVX protein levels is also shown, where each bar represents the average INVX / 50kDa ratio for each time point, with error bars representing the standard deviation for each mean. The densitometry analysis is an average of three INVX blots.

A

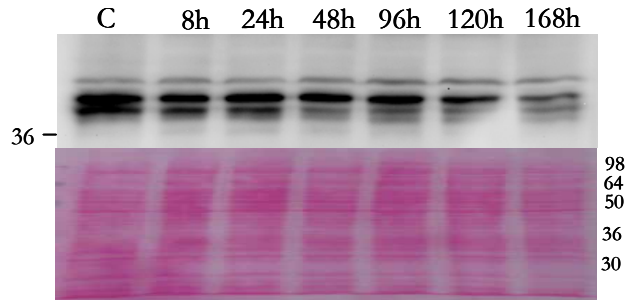
C
8h
24h
48h
96h
120h
168h
36
98
64
50
36
30

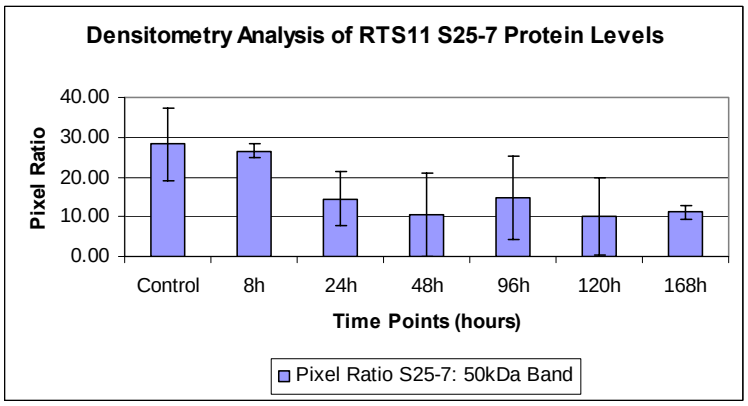
Densitometry Analysis of RTS11 S25-7 Protein Levels
Pixel Ratio
40.00
30.00
20.00
10.00
0.00
Control
8h
24h
48h
96h
120h
168h
Time Points (hours)
Pixel Ratio S25-7: 50kDa Band

B

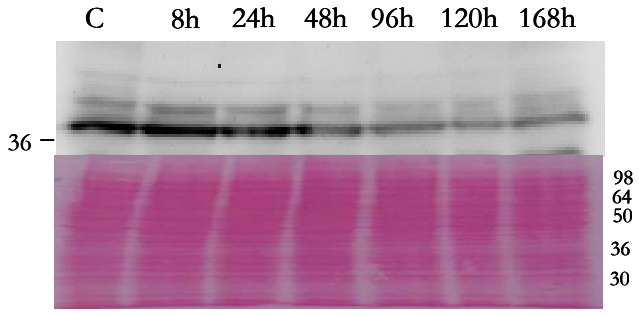
C
8h
24h
48h
96h
120h
168h
36
98
64
50
36
30

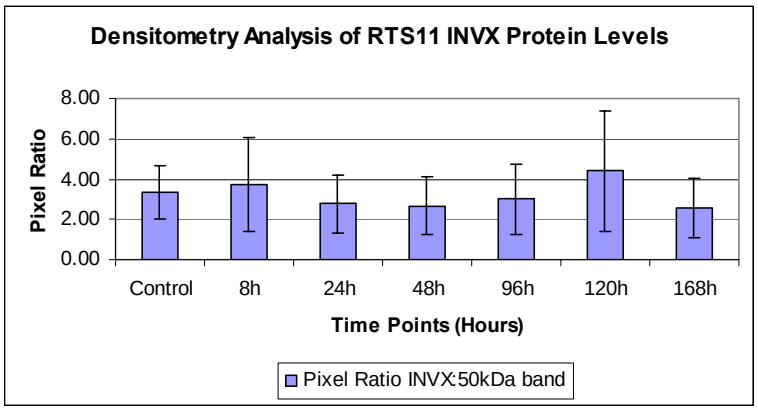
Densitometry Analysis of RTS11 INVX Protein Levels
Pixel Ratio
8.00
6.00
4.00
2.00
0.00
Control
8h
24h
48h
96h
120h
168h
Time Points (Hours)
Pixel Ratio INVX:50kDa band

Chapter 4
Discussion

4.1 Overview of Experimental Results

The purpose of this research was to simulate an immune response and study the resulting effect on the expression of the rainbow trout invariant chain genes S25-7 and INVX. The immune system was activated both *in vivo*, by treating live animals with PMA as well as *in vitro*, by similarly stimulating the macrophage-like cell line RTS11. To identify successful immune system activation *in vivo*, the transcript levels of the cytokine IL-1β were examined because this gene is expressed by activated macrophage (Janeway *et al*, 2001). The level of IL-1β transcript increased significantly upon PMA treatment in both gill and spleen, with an immediate increase at 8 hours post-treatment in gill tissue. These levels decreased from 24 hours to 96 hours post-treatment but increased again at 120 hours. In the spleen, IL-1β transcript was not detected at early time points, but was elevated at later time points, with the highest levels found at 96 hours post-stimulation. Similar to spleen, the IL-1β transcript was also absent at early time points in head kidney, with an increase beginning approximately 96 hours post-stimulation. However, this increase was lower than the increase in both gill and spleen, and was not statistically significant. Regardless, these results demonstrate the presence of activated macrophage in the immune organs of PMA-stimulated fish, indicating successful immune activation. The level of IL-1β was not examined in RTS11 because previous studies show that PMA treatment induces RTS11 activation, as shown by the induction of homotypic aggregation, a characteristic of activated immune cells (DeWitte-Orr *et al*, 2007).

After demonstrating the ability of PMA to induce immune system activation *in vivo*, the expression of S25-7 and INVX was examined. Northern blot analysis indicates that S25-7 transcript is present in all tissues examined, including gill, spleen, head kidney, peripheral blood leukocytes and liver. However, the level of S25-7 varies greatly in these tissues, with the highest level being found in gill. Of the immune tissues, head kidney shows the lowest levels of S25-7 transcript. In addition, the liver, a non-immune tissue, also shows very low S25-7 transcript levels, although this is likely caused by leukocytes present in the liver from circulating blood. It is difficult to make comparisons between of the level of S25-7 transcript found in peripheral blood leukocytes and the expression in

other tissues because S25-7 transcript was detected by RT-PCR analysis in leukocytes, which cannot be compared to the northern blot results. Although all tissues examined differ in the level of S25-7 expressed, there appears to be very little change in this transcript during immune system activation in most tissues. Gill, spleen, liver and peripheral blood leukocytes show no significant change in the S25-7 transcript level after PMA treatment. However, an exception occurs within head kidney, as S25-7 is significantly decreased at the later time points, beginning 24 hours post-stimulation.

Similarly, INVX transcript is detected in all tissues analyzed with the highest levels found in gill and spleen tissue, while head kidney shows the lowest expression level of the immune tissues. Furthermore, there is a small amount of INVX transcript detected in the liver tissue of some individuals, and as explained above, is likely due to blood leukocytes circulating through this tissue. INVX transcript is present in all of these tissues at a much lower level than S25-7 transcript and could only be detected in head kidney and liver by RT-PCR. However, similar to S25-7, INVX transcript levels remain constant during immune system activation in all tissues analyzed.

In contrast to transcript levels, protein levels of S25-7 and INVX appear to be very similar within the same tissue. Both proteins appear to be expressed at similar levels in gill tissue, and while these proteins seem to be slightly increased after PMA stimulation, it is not significant. In addition, both proteins are present in spleen, although the levels vary greatly between similarly treated individuals. The large variation of S25-7 and INVX expression even within untreated controls make it difficult to separate PMA induced protein up-regulation from the natural variation of the fish used for this study. However, for each individual analyzed, the levels of S25-7 and INVX protein are very similar within spleen tissue. Neither INVX nor S25-7 protein is detected in head kidney or liver tissue, which corresponds with the very low transcript levels in these tissues.

The PMA induced activation of RTS11 causes no change in the transcript levels of S25-7, as shown by RT-PCR analysis. In contrast, INVX transcript decreases 48 hours after PMA stimulation with a subsequent increase at 168 hours post-stimulation. In contrast to the *in vivo* results, S25-7 protein appears to be at a higher level than INVX protein in the RST11 cells. Both S25-7 and INVX protein levels remains unchanged upon immune system activation.

4.2 Implications for the Teleost Immune System

The expression pattern of invariant chain, at both the transcript and protein level, provides valuable insight into immune functions carried out within various organs of rainbow trout, as the presence of

these proteins indicates an ability to present antigens via the MH class II antigen presentation pathway. To begin, peripheral blood leukocytes consist of a mixture of various immune cells, including B cells and macrophage circulating in the blood stream (Shanchez *et al*, 1995; Kollner *et al*, 2001). In addition, although dendritic cells have not yet been identified in teleosts, a sequence similar to the dendritic cell surface marker CD83 has recently been identified in rainbow trout, indicating the presence of this cell type in the teleost immune system (Ohta *et al*, 2004). B cells, macrophage and dendritic cells are thought to be the antigen presenting cells of the teleost immune system and as such, are expected to express both MH class II and invariant chain. The detection of invariant chain transcript, along with MH class II transcript and protein, in this cell population indicates the presence of circulating cells capable of presenting extracellular antigen to activate a $CD4^+$ T cell response (Nath *et al*, 2006).

The rainbow trout invariant chain genes show the highest level of expression in gill tissue, at both transcript and protein level. The gills represent an entry site for any pathogens located in the water, thus, to prevent infection, this site must be constantly monitored by the immune system. Although very little is known about the immune system effector cells found in gill tissue, much more is known about the mammalian lungs, a corresponding site of pathogen entry. The lungs contain a high number of alveolar macrophage, capable of non-specific removal of foreign material (Martin *et al*, 2005). These cells endocytose and degrade foreign pathogens, and can present antigenic fragments to activate memory T cells located within the lungs (Woodland and Scott, 2005). In addition, there is also a population of dendritic cells found within the connective tissue surrounding the blood vessels of the lungs (Lambrecht *et al*, 2001). These cells have an immature phenotype and are capable of rapid endocytosis and degradation of antigens. These cells play an essential role in the activation of an adaptive immune response. Upon infection of the rat lung, additional dendritic cells are recruited by a number of chemokines secreted by activated lung epithelial cells. Dendritic cells are directly activated by pathogens through the binding of the TLR on the dendritic cell surface. This causes a number of changes in the dendritic cell, including the up-regulation of CD80 and CD86, which are required for T cell activation, as well as the up-regulation of receptors for chemokines synthesized in secondary lymph organs (Lambrecht *et al*, 2001). Furthermore, mature dendritic cells down-regulate receptors for chemokines expressed at sites of infection. In this way antigen loaded dendritic cells can migrate from the site of infection to the lymph tissue, where they activate circulating T cells, and these activated cells in turn migrate to the site of infection.

Previous work has shown that MH class II α and β are present in the gill tissue of rainbow trout, with both transcript and protein being detected (Nath *et al*, 2006). This, together with the detection of S25-7 and INVX, indicate that the gill contains immune cells capable of processing and presenting extracellular antigen. In contrast to other tissues examined, S25-7 and INVX are constitutively expressed in gill as both proteins were detected in the gill tissue of all analyzed individuals. This indicates that antigen presentation occurs continuously in this tissue, allowing for constant immune surveillance. Although the cells carrying out this surveillance have not yet been identified, it likely performed by macrophage and dendritic cells, similar to the mammalian lung. Analysis of the expression pattern of the recently cloned rainbow trout CD83 homologue demonstrates the presence of this transcript in gill tissue, indicating the presence of a dendritic cell population (Ohta *et al*, 2004). Furthermore, indirect evidence of a macrophage population in gill tissue comes from the detection of inducible nitric oxide synthetase transcript in rainbow trout gill, as this enzyme is produced predominately by macrophage (Campos-Perez *et al,* 2000). Also, the detection of a rapid up-regulation of IL-1β transcript demonstrates the presence of activated macrophage within the gill. It is likely that gill macrophage are primarily responsible for non-specific elimination of foreign pathogens while dendritic cells process antigens for the activation of T cells. In teleosts, $CD8^+$ T cells have been identified and a CD4 homologue has recently been cloned, indicating the existence of $CD4^+$ T cells in these fish (Laing *et al*, 2006, Fischer *et al*, 2003). The CD8 and CD4 transcript are undetected in non-stimulated gill tissue, indicating that, similar to the human lung, antigen loaded dendritic cells leave the gill and migrate to a secondary lymphoid tissue to activate circulating T cells (Fischer *et al*, 2003, Moore *et al*, 2005). Once activated, T cells likely migrate back to the site of infection in the gill. After treating rainbow trout with a DNA vaccine against infectious hematopoietic necrosis virus (IHNV), both TCR-β and CD8-α transcript are detected in gill tissue (Purcell *et al*, 2006). Unfortunately, there has been no corresponding study of CD4 transcript upon immune system stimulation. Although the migration of dendritic cell out of the gill would be expected to result in a decrease of invariant chain, it is likely that additional dendritic cells, B cells or macrophage are simultaneously migrating to the site of infection, resulting in a constant level of invariant chain.

Once antigen has been captured at the initial site of infection, antigen presenting cells must interact with lymphocytes in order to activate an adaptive immune response. This interaction occurs within the secondary lymphoid organs. The spleen is one such organ in both mammals and fish (Brendolan *et al*, 2007). The spleen consists of red pulp, which is responsible for the destruction of erythrocytes,

and white pulp, which is the location of lymphocyte activation. In the human spleen, the white pulp compartment consists of a T cell zone and a B cell zone, or follicle (Mebius and Krall, 2005). The follicle is surrounded by a marginal zone and the entire compartment is surrounded by a perifollicular zone. The perifollicular zone is a blood filled site due to open spleenic circulation and is the entry site for all antigens, antigen presenting cells and lymphocytes from the circulation. In defense against blood borne pathogens, the perifollicular zone has a population of macrophage. In addition, this zone also contains endothelial like fibroblasts which secrete a number of chemokines to attract lymphocytes from the blood (Crivellato *et al*, 2004). Upon infection, antigen loaded dendritic cells migrate through the blood from the site of infection and enter the spleen. These cells activate a population of memory B cells found in the marginal zone, resulting in the rapid production of IgM antibodies. The dendritic cells then migrate into the B and T cells zones. Both $CD8^+$ and $CD4^+$ T cells are activated in the T cell zone, with the activated $CD8^+$ T cell leaving the spleen to migrate to the site of infection. The activated $CD4^+$ T cells migrate to the periphery of the T cell zone to help activate B cells at the periphery of the B cell follicle. Thus the spleen is an important immune organ, required to co-localize various immune effectors cells to induce an adaptive immune response to eliminate pathogen infection.

In teleosts, the spleen is also composed of red and white pulp, although the white pulp is poorly developed (Press and Evensen, 1999). The white pulp consists of two compartments, the melanomacrophage compartment, which is responsible for erythrocyte destruction and the ellipsoid compartment, which contains macrophage that are responsible for degrading blood borne pathogens. Both of these compartments are capable of retaining antigen, which may allow for the activation of lymphocytes attracted from circulation. The rainbow trout CD83 homologue transcript is detected in spleen, indicating that dendritic cells may also be involved in the activation lymphocytes in the teleost spleen (Ohta *et al*, 2004). Similarly, while T cells have not been identified within the spleen, the CD8α and β transcript, as well as the CD4 transcript have been detected in rainbow trout spleen (Moore *et al*, 2005, Laing *et al*, 2006). In addition, two populations of Ig-bearing cells have been identified in the spleen of rainbow trout, likely representing the B cells (Sanchez *et al*, 1995). Thus, it appears that the teleost spleen contains the same populations of cells as the mammalian spleen, and is likewise capable of activating an adaptive immune response. The presence of macrophage, B cells, and most likely, dendritic cells within the spleen indicates that the invariant chain proteins should also be found here. Furthermore, examination of the spleen-derived macrophage like cell line RTS11 demonstrates the presence of S25-7 and INVX, at both the transcript and protein level, indicating the

presence of antigen presenting macrophage within spleen. Finally, in this study, northern blot analysis indicates that all fish studied expressed both S25-7 and INVX transcript in the spleen tissue. However, there was a great variability in the detection of these proteins within the spleen. Although all fish express the invariant chain transcripts, the variation at the protein level indicates that there may be a different rate of invariant chain translation or proteolysis within the spleen antigen presenting cells between individuals. Some fish have no detectable invariant chain protein, but this may be due to an inability to detect weak signals on a blot with very strong signals. It is possible that a lower intensity band may be detected by a longer exposure time or by increasing the amount of primary or secondary antibody. However, other samples with high signal intensity would be supersaturated under these detection conditions and the high intensity signal would overshadow the low signal. It is unclear how the variation in invariant chain protein level may affect antigen presentation.

In teleost fish, the major function of the head kidney is blood cell differentiation, similar to the role played by the mammalian bone marrow (Press and Evensen, 1999). The hematopoietic stem cell population of the bone marrow is capable of differentiating into either the common lymphoid progenitor, which gives rise to B cells, T cells and NK cells, or the common myeloid progenitor, which gives rise to platelets, erythrocytes, monocytes, neutrophils, eosinophils or basophils (Kaushansky, 2006). A complex array of factors control this differentiation pathway to ensure the maintenance or up-regulation of specific cell populations. After differentiation in the bone marrow, cells enter the bloodstream and migrate throughout the body to carry out effector functions.

Immature T cells migrate from the bone marrow to the thymus, where cellular maturation continues as positive and negative selection produce a T cell population capable of recognizing self MHC dimers but incapable of recognizing self antigens (Janeway *et al*, 2001). In teleosts, B cell maturation, including negative selection of non-self reactive B cells, occurs entirely within the bone marrow. Once differentiation and selection has occurred, mature B and T cells migrate through the bloodstream and the lymphatic system, frequently entering secondary immune tissues, such as the spleen or lymph nodes. As described above, lymphoid cells are activated in these tissues by loaded antigen presenting cells and these activated cells then migrate to the site of infection to eliminate pathogen.

In the mammalian immune system, the process of differentiation and negative selection of non-self reactive cells occurs in a physically distinct location from the activation of mature cells. In contrast,

both lymphoid differentiation and activation is thought to occur in head kidney (Kaattari and Irwin, 1985). However, the absence of invariant chain proteins together with the very low levels of transcript indicate that MH class II antigen presentation may not be occurring in this tissue. Likewise, although MH class II transcript is detected in the head kidney, it is also present at a lower level than spleen or gill (Nath *et al*, 2006). Invariant chain and MH class II transcripts may be expressed at a low level by differentiating immune cells, but the absence of invariant chain protein indicates that no antigen presentation, and thus, no lymphoid activation is occurring within this tissue. As a result, it appears that the teleost head kidney may be performing only hematopoietic functions, similar to mammalian bone marrow, and the physical separation of differentiation and activation may be similar in both mammalian and teleost immune systems. This separation may be important for controlling the factors cell populations are subjected to, as differentiating cells should not be exposed to antigen presenting cells and activation cytokines before negative selection removes self-reactive cells.

Neither teleost nor mammalian liver are thought to be involved in the immune response. Although a very low level of invariant chain transcript is detected, it is likely due to circulating leukocytes that have entered the liver. As expected, no invariant chain proteins are detected, which indicates no MH class II antigen presentation is occurring in this tissue.

4.3 Regulation of Invariant Chain During an Immune Response

The mammalian invariant chain has been shown to be up-regulated at both the transcript and protein level in response to IFN-γ treatment in a number of cell types, including macrophage, endothelial cells, fibroblasts and keratinocytes (Paulnock-King *et al*, 1985, Collins *et al*, 1984, Albanesi *et al*, 1998). This provides indirect evidence for the up-regulation of invariant chain during an immune response as IFN-γ is synthesized and secreted from a number of activated immune effector cells, including $CD8^+$ and $CD4^+$ T cells as well as natural killer cells (Janeway *et al*, 2001). The increased invariant chain expression after IFN-γ stimulation is due to an up-regulation of the transcription factor CIITA, which increases the transcription rate of the MHC class II and the accessory genes (Ting and Zhu, 1999). In addition, invariant chain is also directly up-regulated by the binding of IFN-γ to the IFN responsive element in the invariant chain promoter region (Barr and Saunders, 1991). This up-regulation of the MHC class II genes allows for an increased rate of antigen presentation during an immune response (Collins *et al*, 1984).

In contrast, the teleost invariant chain homologues were not up-regulated during an immune response. In gill and spleen, the major sites of antigen presentation, there was no change in INVX or S25-7 transcript or protein levels, although the up-regulation of the IL-1β transcript demonstrated the induction of an immune response. This may indicate that the teleost invariant chains are constitutively expressed at a high level, which would allow for a rapid response to pathogenic challenge. However, this would also require a high expression of MH class II. Unfortunately, the response of MH class II to an artificial immune challenge has not been studied, making it difficult to determine the relationship between MH class II and invariant chain expression. If MH class II remains unchanged during an immune response, it is likely that both invariant chain and MH class II are expressed at a constitutive level, allowing rapid response to pathogenic challenge, as there is no lag time required for the transcription and translation of these genes. However, if MH class II is up-regulated, it leads to the question of how a steady level of invariant chain is able to chaperone the increasing level of MH class II dimers.

Two studies have been performed recently in which teleosts were subjected to a live pathogen challenge. Rainbow trout were challenged with the infectious hematopoietic necrosis virus (IHNV) and Japanese flounder were challenged with the intracellular bacteria *Edwardsiella tarda* (Matsuyama *et al,* 2007, Hansen and LePatra, 2002). In both cases MH class II transcript were significantly decreased after infection. Interestingly, infected Japanese flounder also showed a significant down-regulation of invariant chain transcript. The interpretation of these results in terms of the regulation of MH class II genes after infection is difficult because these pathogens may have evolved the ability to down-regulate MH class II as an immune system evasion mechanism, which may not occur for all pathogens. However, the down-regulation of both invariant chain and MH class II may indicate a co-regulatory expression pattern between these two genes, as occurs in the mammalian immune system. Furthermore, this may provide indirect evidence that both MH class II and the associated invariant chains are constitutively expressed in specific immune tissues, and while immune system stimulation does not cause an up-regulation of these genes, some pathogens may have evolved the ability to down-regulate these genes, likely by interfering with a transcription factor that may be required for coordinated expression.

Furthermore, in this study, the results of IL-1β transcript analysis demonstrate an initial expression peak at the 8 hour time point followed by a reduction at the 24 to 48 hour time points with a second increase at 120 hours post stimulation. This pattern is also seen in the invariant chain results, although

statistical analysis does not show a significant change. When rainbow trout were infected with IHNV, the MH class II transcript was decreased at 72 hours post infection but returned to control levels by 192 hours post infection (Hansen and La Patra, 2002). In addition, exposure to cold temperatures also caused a downregulation of MH class II (Nath et al, 2006). When rainbow trout were kept at 2°C for 5 days, MH class II was downregulated at both the transcript and protein level which was maintained after 10 days at the low temperature. Furthermore, incubation of rainbow trout leukocytes with the stress hormone cortisol caused a decrease in IL-1β transcript (Zou et al, 2000). The down-regulation of IL-1B likely causes an inhibition of the innate immune response, which is seen by a decrease of MH class II within innate antigen presenting cells. However, activation of the adaptive immune response causes the upregulation of MH class II at the later time points. Taken together, these results indicate that after immune system stimulation, there is a transient down-regulation of IL-1β, MH class II and invariant chain, which is overcome at later time points.

Another major difference between the regulation of teleost and mammalian invariant chain can be seen in the comparison of the homologues p41 and S25-7. In mammals, p33 is constitutively expressed, while p41 is induced upon IFN-γ stimulation (Albanesi *et al*, 1998). However, not only is S25-7 transcript expressed in non-stimulated tissues, it is expressed at a higher level than INVX. This high level of S25-7 expression indicates that it is likely performing the majority of the invariant chain functions during an immune response, similar to the up-regulated p41. The thyroglobulin domain of S25-7 likely carries out the same protease inhibition roles as the p41 thyroglobulin domain and this inhibition may increase the half life of the MH class II dimer and invariant chain as it travels through the endosomal pathway, leading to an increased presentation of antigen at the cell surface. Although S25-7 transcript is present at higher levels than INVX, western blot analysis indicates that both appear to be present at the same protein level, which may be due to a different rate of translation between the two transcripts. However, no conclusive comment can be made about the protein levels of the two invariant chain isoforms because comparison of western blots is not reliable without an internal standard. To determine conclusively if there is a difference in the protein levels of S25-7 and INVX, both need to be detected on the same blot, or an antibody to a housekeeping protein should be used to probe both S25-7 and INVX blots, similar to the S11 probe in the northern blots.

In contrast to results shown in other tissues, S25-7 transcript level in head kidney is significantly decreased during immune system activation. However, since neither INVX nor S25-7 protein is detected in head kidney and the transcript is very low to begin with, the purpose of this down-

regulation is unclear, as no antigen presentation occurs within this tissue. In addition, RTS11 INVX transcript level also decreases after PMA stimulation, although levels return to untreated control levels by the last time point analyzed. The effect of this down-regulation is also unclear because there is no corresponding down-regulation at the INVX protein level. Furthermore, stable S25-7 transcript and protein levels indicate antigen presentation can still occur. It is interesting that in these two cases of down-regulation, only one invariant chain isoform is affected. This indicates that different factors are responsible for controlling the expression of these two genes. As described above, the promoter regions of MHC class II genes and invariant chain contain some similar elements while the invariant chain promoter also has unique elements, allowing for independent expression of invariant chain. A similar situation likely occurs within the promoter regions of S25-7 and INVX, in which there are some common elements and some unique elements, giving rise to both coordinated and independent regulation of expression. This is an alternative method of control compared to the mammalian invariant chain in which the expression of p33 and p41 is controlled at the post-transcriptional level by alternative splicing. In contrast, the separate invariant chain genes in rainbow trout are controlled at the transcriptional level by unique promoter elements.

4.4 The Challenge of Individual Variability

A major challenge with using animals to study the immune system lies within the variability of gene expression between individuals. In this study, all fish have a different genetic background, resulting in variability in the expression level of S25-7 and INVX. Spleen samples collected from non-stimulated fish vary from no expression of either invariant chain protein to high expression of both, with corrected INVX signals ranging from 1.17 to 10.73 and corrected S25-7 signals ranging from 1.17 to 34.32. Furthermore, this same pattern can be seen in the untreated control samples of the PMA time course. In gill western blot analysis, the corrected INVX signal of the untreated control samples varies from 1.9 to 9.13, while the time point means vary from 3.95 to 12.46. Similarly, the corrected S25-7 signal of the control samples varies from 3.07 to 20.04, while the time point means vary from 8.35 to 15.59. Finally, the corrected S25-7 transcript signal of untreated controls varies from 5.74 to 20.54 while the time point means vary from 7.64 to 12.81. These results demonstrate that the level of protein and transcript varies almost as much, and in some cases more so, within each group than between groups. This makes it difficult to determine if changes across time are due to immune system stimulation or simply due to individual variability.

There are two possible solutions to the problem of individual variability. First off, the analysis of invariant chain expression could be confined to peripheral blood leukocytes. In this case, blood samples could be collected from the same fish at various time points, allowing an analysis of the immune response within one individual over a specific time period after an immune challenge. In this way, even if each individual showed different levels of invariant chain, a general pattern of response from each individual over time could demonstrate any changes in expression. A major problem associated with this method of immune system analysis is the stress to the animals from repeated sample collections. Studies of the stress response in rainbow trout demonstrate decreased peripheral white blood cells after extended net confinement (Ruane *et al*, 1999). Thus, the repeated catch and anesthetization of the fish would likely affect the immune system response. In addition, to analyze both protein and transcript level, a significant amount of blood would have to be collected. This would require a long time lapse between each time point and would not allow for the analysis of the immune response over a short period of time.

A second solution to the problem of individual variability would be to utilize cell lines for immune system analysis. This would eliminate the variability in the genetic background, resulting in a consistent expression of invariant chain. Thus, changes in invariant chain expression would be due solely to the activation of an immune response. Furthermore, cell lines are not susceptible to a stress response, are easier to maintain and prevent the need to sacrifice live animals. In addition, since the function and regulation of the immune response in teleost is only beginning to be elucidated, cell lines will allow for a more simplified analysis of immune effector cell responses. Once the immune system has become more defined, whole animal studies would be useful to understand how the system works as a whole *in vivo*, including how various cells work together and how cells migrate to various sites within the animal during an immune response. However, for the initial studies, it is very difficult to understand the basic functions of the immune system in such a complex setting.

4.5 Future Research

The results from this study represent a preliminary glimpse at the regulation of invariant chain. A great deal of work is still required for a more complete understanding of teleost invariant chain regulation and function. The regulation of invariant chain expression is likely carried out at a number of levels, including post-translational, post-transcriptional and transcriptional. However, in the mammalian immune system, the majority of work has focused on the translational control of invariant

chain. To determine if the teleost invariant chain genes are controlled in a similar manner, it would be useful to analyze promoter regions and proteins capable of binding to these regions. To begin, the promoter regions of all invariant chain genes could be cloned and sequenced. The promoter regions of both S25-7 and INVX could be compared to the promoter region of mammalian invariant chain to look for conserved regions. Furthermore, the promoter sequences could be compared between S25-7 and INVX, as well as with the promoter region of MH class II genes to look for similar sequences, which may indicate a co-regulation of these genes. Once a region of interest has been identified, further analysis could be performed to confirm promoter capabilities. To begin, the putative promoter elements could be subjected to gel mobility shift analysis and DNase footprinting to demonstrate the ability of protein factors to bind these regions as well as to identify the precise protein binding sequences. Furthermore, reporter assays could be performed to determine the ability of the putative promoter region to activate expression of a reporter gene within various cell lines and mutational analysis of this promoter region would provide information regarding essential nucleotides required for transcription initiation.

Once the promoter elements have been identified, yeast one-hybrid analysis could be performed to identify proteins capable of interacting with these sequences. In this strategy, a rainbow trout cDNA library could be cloned into a vector, upstream of a transcriptional activation domain sequence. This vector would be transfected into cells containing a reporter gene downstream of the invariant chain promoter region. By identifying which clones can activate transcription, the sequence of invariant chain transcription factors can be identified. The functions of these identified factors could then be examined *in vitro*, by knocking out the endogenous protein with siRNA and examining the resulting expression of either the invariant chain genes themselves, or the expression of a reporter construct. In addition, a search could be performed for homologous sequences of transcription factors known to be involved in mammalian invariant chain expression. These sequences could be used in yeast one-hybrid analysis to confirm interaction with the invariant chain promoter region, and could be co-expressed along with an invariant chain reporter construct to determine if there is an up-regulation of reporter gene expression.

Furthermore, to examine the regulation of invariant chain during an immune response, cell lines could be stimulated with a variety of cytokines and the effect on invariant chain expression could be analyzed. The sequences of IFNγ and TNF have recently been cloned from rainbow trout (Zou *et al*, 2005, Zou *et al*, 2003). These genes could be recombinantly expressed and used to stimulate a cell

line to determine the effects on invariant chain expression. Furthermore, teleost homologous of other mammalian cytokines known to be involved in the immune response could be similarly cloned, expressed and used to stimulate immune cell lines to examine the effect on invariant chain expression. Finally, immune cell lines could also be exposed to live fish pathogens to determine the response of invariant chain. This would provide a simplified picture of invariant chain regulation within specific cell types.

In addition to understanding the regulatory control of invariant chain expression, an understanding of its function within the MH class II antigen presentation pathway is essential. To begin, the ability of invariant chain to bind MH class II dimers could be demonstrated by co-immunoprecipitation of either the invariant chain proteins or MH class II. To determine if invariant chain is capable of directing transport of the MH class II dimer, a non-immune cell line could be transfected with an expression vector encoding both MH class II α and β chains. Flow cytometry could be performed to determine the amount of MH class II dimers present at the cell surface and subcellular fractionation along with western blot analysis could determine the intracellular location of MH class II. This same cell line could then be co-transfected with the invariant chain sequence and the same analysis of MH class II localization could be performed. The results of Ii^- and Ii^+ cells could then be compared to determine if invariant chain has an effect on the MH class II transport path and surface expression.

A number of mutational studies of the rainbow trout invariant chain would also lead to a more complete understanding of the function of these proteins. Further analysis of the transportation ability of invariant chain could be performed by mutating the putative endosomal targeting sequences and looking at the intracellular localization of these mutated proteins. Furthermore, to determine if trimerization is important for targeting, the putative trimerization domain could be mutated and the intracellular localization of invariant chain could be examined. The invariant chain lacking the trimerization domain could also be expressed along with MH class II to determine the effect on MH class II transport. Finally, the putative CLIP region could also be mutated or deleted and the ability of the mutant invariant chain to interact with MH class II could be examined by co-immunoprecipitation. This would indicate the exact residues involved in peptide binding groove interaction.

Finally, yeast two-hybrid analysis could be performed to identify proteins capable of interacting with invariant chain. Similar to the yeast one-hybrid, a cDNA library from rainbow trout could be cloned upstream of a transcriptional activator while the region of interest from invariant chain could

be cloned upstream of a DNA binding domain. The expression of the reporter gene will indicate which cDNA sequences encode proteins capable of interacting with invariant chain. These sequences could then be analyzed for similarity to known mammalian proteins. This could be performed with the thyroglobulin domain, in an attempt to identify an interaction with a protease, similar to the interaction of the p41 thyroglobulin domain and cathepsin L. In addition, the cytosolic region of invariant chain could be analyzed for any protein interactions, as it is known to interact with NF-κB in the mammalian immune system. Finally, the macrophage inhibitory factor (MIF) has been sequenced from rainbow trout (Jin and Shoa, unpublished). This could also be used in the yeast two hybrid assay with various regions of the invariant chain to identify an interaction between invariant chain and MIF. Furthermore, if an interaction between MIF and invariant chain is shown to occur, yeast two hybrid may be used to identify other proteins that invariant chain is capable of interacting with to facilitate the MIF signaling cascade within macrophage.

Lastly, in a step towards DNA vaccination, a modified invariant chain vector could be synthesized in which the CLIP region is replaced with a known antigenic peptide. An immune cell line could be transfected with this vector, incubated for a sufficient time to allow expression and processing of the invariant chain, after which surface MH class II proteins could be isolated and levels of antigenic peptide could be measured. This could be compared with surface expression of the antigen when cells are incubated with the antigenic peptide alone, or transfected with a vector encoding just the antigenic peptide. If the modified invariant chain vector increases surface antigen, it could then be used *in vivo* in combination with vaccines targeting the MH class I antigen presentation pathway to analyze the ability of DNA vaccines to elicit a sustained protective immunity against a number of different pathogens.

4.6 Conclusions

The expression pattern of invariant chain transcript and protein provides insight into the immune functions carried out within the various tissues of rainbow trout. The majority of MH class II antigen presentation occurs primarily within the gill and spleen in rainbow trout. The gill represents a site of constant immunosurveillance, as it is a primary site of antigen entry while the spleen functions as a secondary immune tissue in which antigen presenting cells can interact with and activate B cells and T cells of the adaptive immune response. The lack of detectable invariant chain protein within the head kidney indicates that this tissue is not functioning as a secondary immune tissue. Furthermore,

INVX and S25-7 are differentially regulated at the transcriptional level, allowing for unique control of each gene, similar to the use of alternative splicing of mammalian invariant chain to produce either p33 or p41. Finally, these results also indicate that invariant chain expression is not up-regulated during an immune system response, in contrast to the up-regulation of the homologous mammalian genes. Thus, it appears that the teleost immune system has evolved a unique method of immune system regulation upon pathogenic challenge.

Appendix A

Figures

Figure A.1: Northern blot analysis of S25-7 and INVX transcript levels in PMA stimulated gill, additional sets. Total RNA was isolated from gill tissue, separated and transferred onto a nylon membrane. The membrane was probed for either (A) S25-7 and S11 or (B) INVX and S11. The densitometry analysis of these sets is included in the average S25-7/S11 and INVX/S11 pixel ratio shown in figure 3.7. The blot for S25-7 is a separate membrane from the blot shown in figure 3.7 while INVX is the bottom half of the same membrane shown in figure 3.7.

A

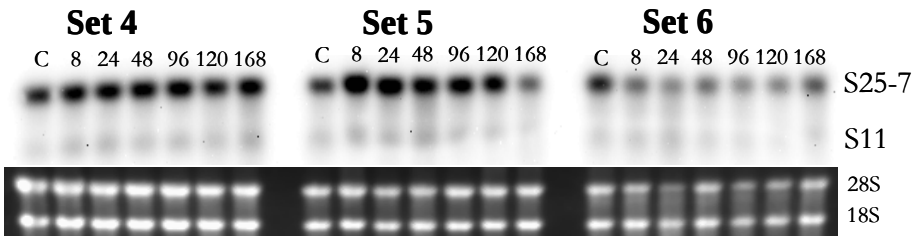

B

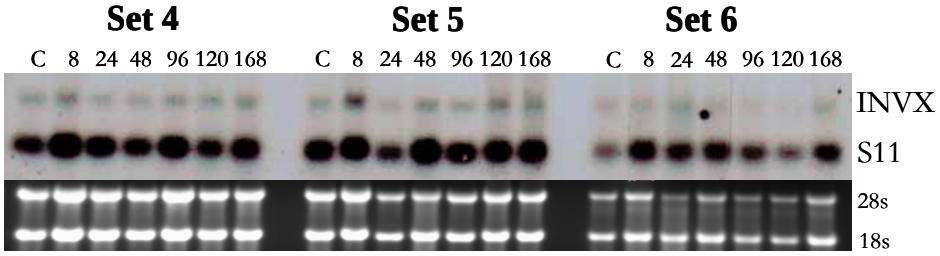

Figure A.2: Northern blot analysis of S25-7 and INVX transcript levels in PMA stimulated spleen, additional sets. Total RNA was isolated from spleen tissue, separated and transferred onto a nylon membrane. The membrane was probed for either (A) S25-7 and S11 or (B) INVX and S11. The densitometry analysis of these sets is included in the average S25-7/S11 and INVX/S11 pixel ratio shown in figure 3.9. The blot for S25-7 is a separate membrane from the blot shown in figure 3.9A while INVX is the bottom half of the same membrane shown in figure 3.9B.

A

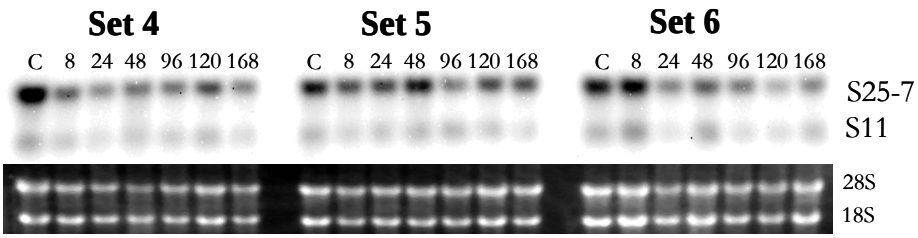

B

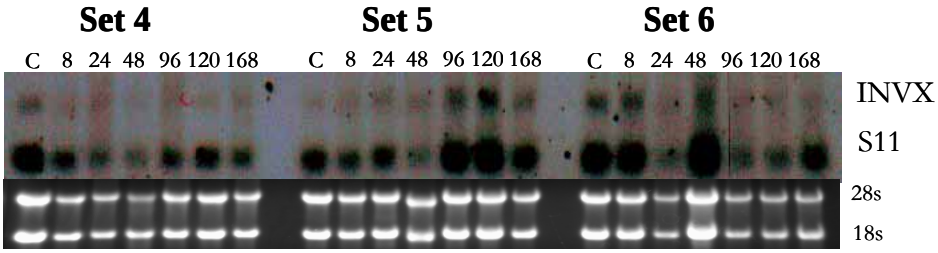

Figure A.3: Northern blot analysis of S25-7 transcript levels in PMA stimulated head kidney, additional sets. Total RNA was isolated from head kidney tissue, separated, transferred onto a nylon membrane and probed for S25-7 and S11. The densitometry analysis of these sets is included in the average S25-7/S11 pixel ratio shown in figure 3.13. The blot for S25-7 is a separate membrane from the blot shown in figure 3.11A.

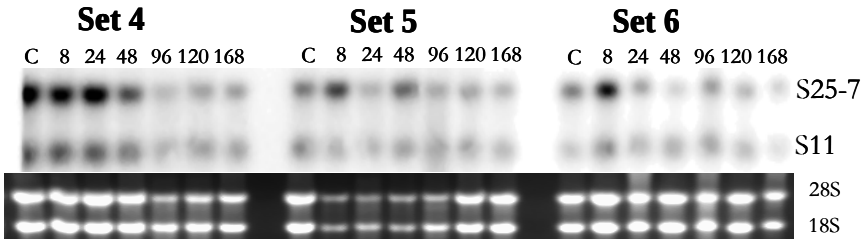

Figure A.4: Northern blot analysis of S25-7 transcript levels in PMA stimulated liver, additional sets. Total RNA was isolated from liver tissue, separated, transferred onto a nylon membrane and probed for S25-7 and S11. The densitometry analysis of these sets is included in the average S25-7/S11 pixel ratio shown in figure 3.13. The blot for S25-7 is a separate membrane from the blot shown in figure 3.13A.

Figure A.5: RT-PCR analysis of S25-7 and INVX transcript levels in PMA stimulated PBLs, additional sets. Total RNA was isolated from four sets of PBLs. This RNA was reverse transcribed and amplified for INVX, S25-7 and Ef-1α. The PCR reactions were performed separately and separated on separate 1% agarose gels. The UV images of the additional PBL sets used for densitometry analysis in figure 3.15 are shown below.

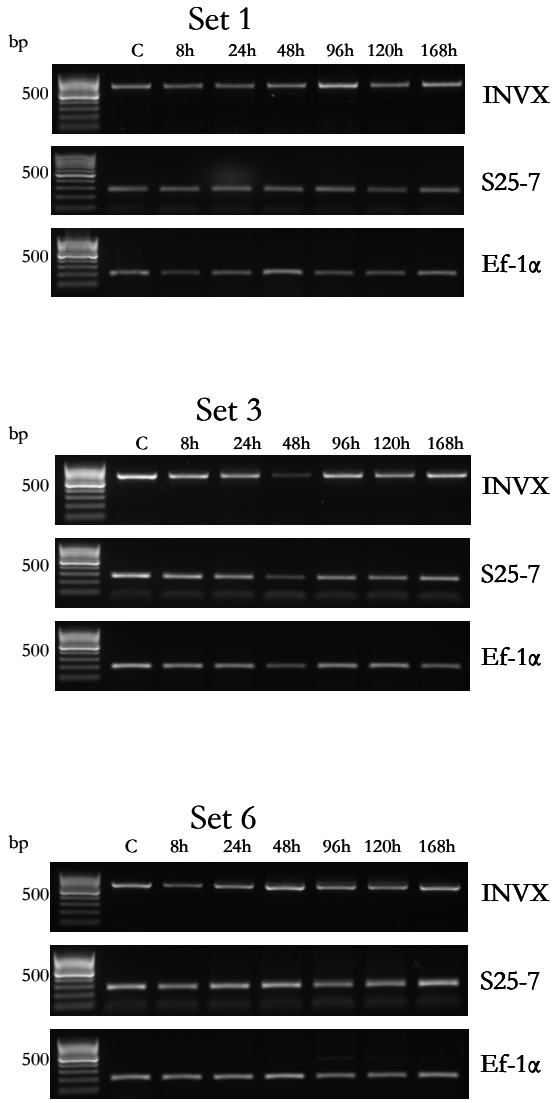

Figure A.6: Western blot analysis of S25-7 and INVX protein levels in PMA stimulated gill, additional sets. Protein was isolated from gill tissue of six sets of fish, although only four sets were used for densitometry analysis. The protein was analyzed by western blotting with either anti-rtINVX antibody or anti-rTg antibody, followed by anti-rabbit IgG HRP conjugated antibody. The additional three sets used for the S25-7 and INVX densitometry analysis shown in figure 3.16 are shown below.

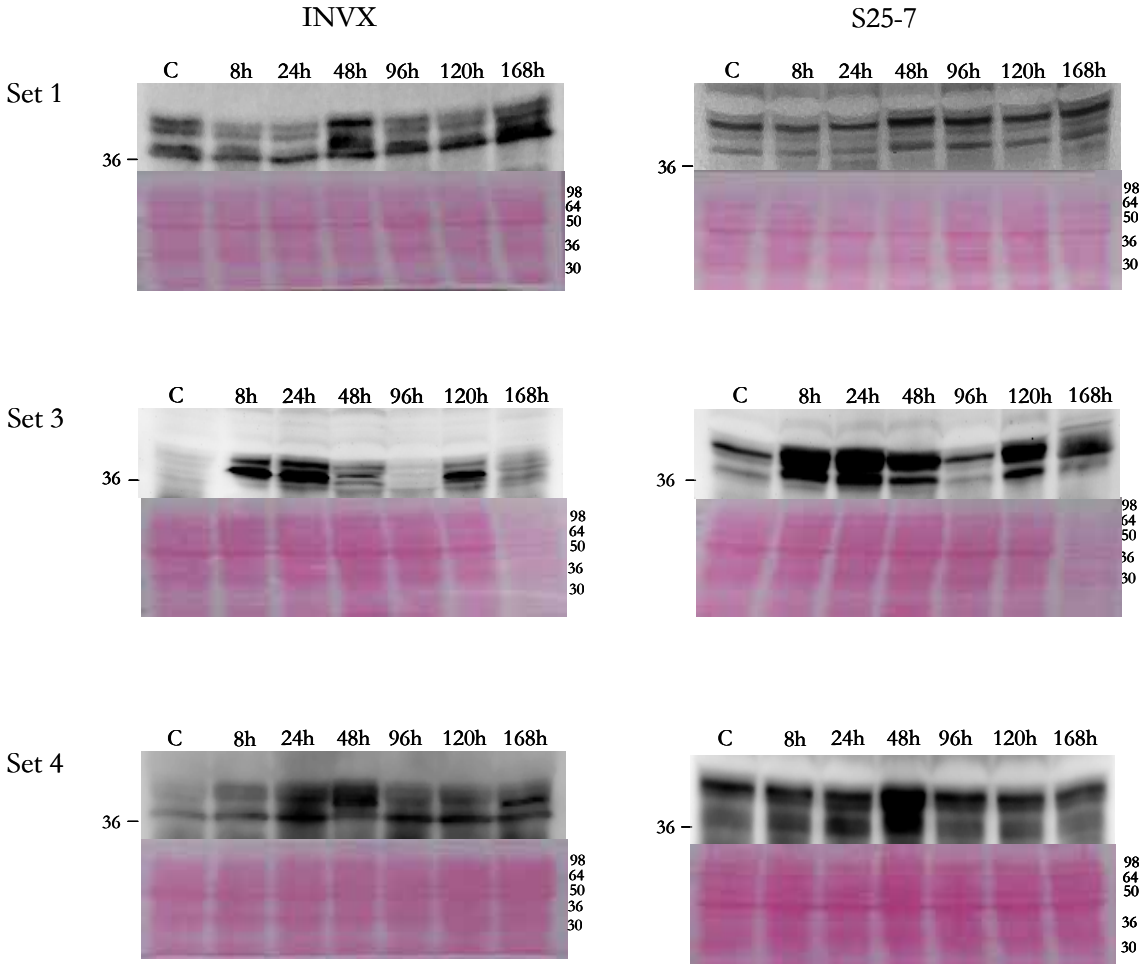

Figure A.7: Western blot analysis of S25-7 and INVX protein levels in PMA stimulated spleen, additional sets. Protein was isolated from spleen tissue of six sets of fish, although only four sets were used for densitometry analysis. The protein was analyzed by western blotting with either anti-rtINVX antibody or anti-rTg antibody, followed by anti-rabbit IgG HRP conjugated antibody. The additional three sets used for the S25-7 and INVX densitometry analysis shown in figure 3.17 are shown below.

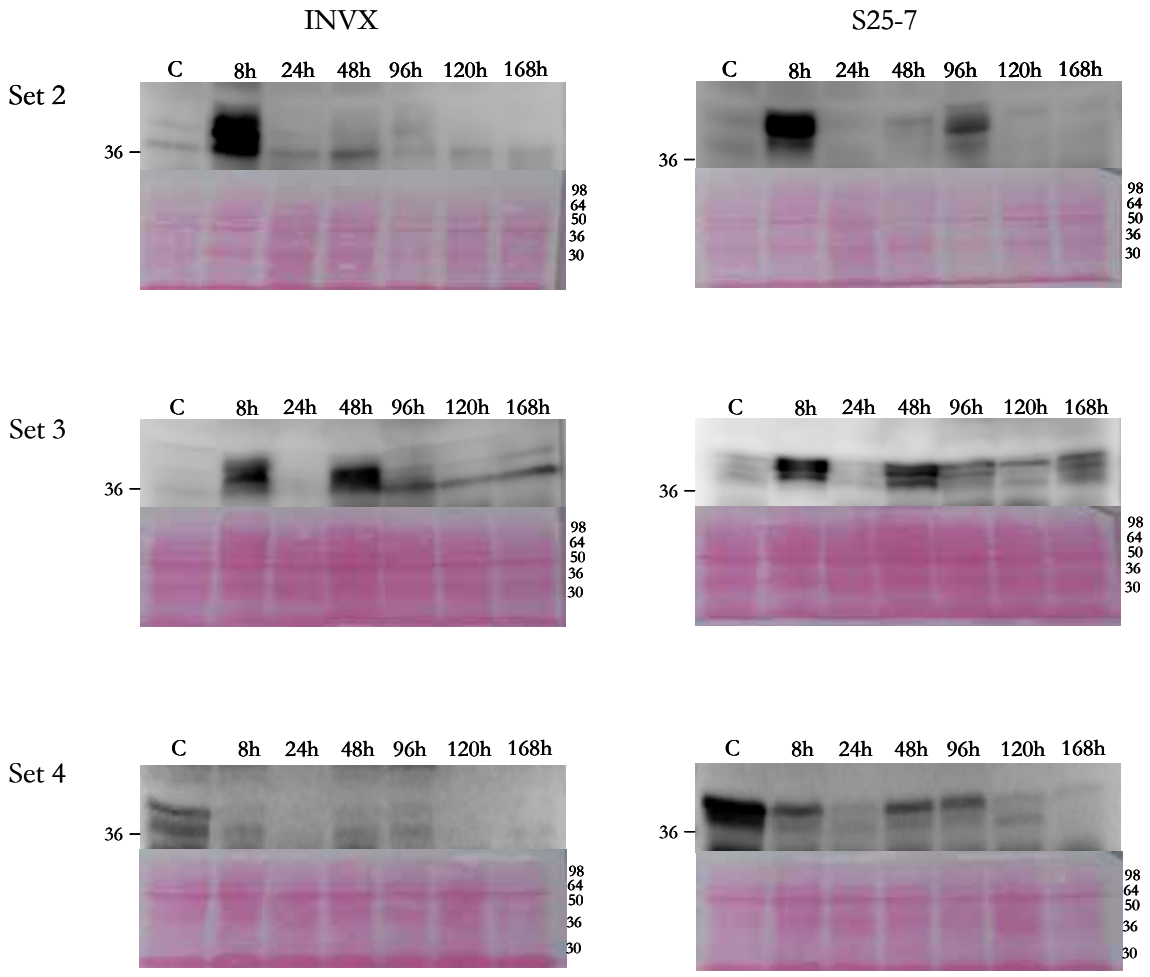

Figure A.8: RT-PCR analysis of S25-7 and INVX transcript levels in PMA stimulated RTS11, additional sets. Total RNA was isolated from three replicates of an RTS11 time course, reverse transcribed and amplified for INVX, S25-7 and Ef-1α. The PCR reactions were performed separately and separated on separate 1% agarose gels. The UV image of the additional RTS11 sets used for densitometry analysis in figure 3.20 is shown below.

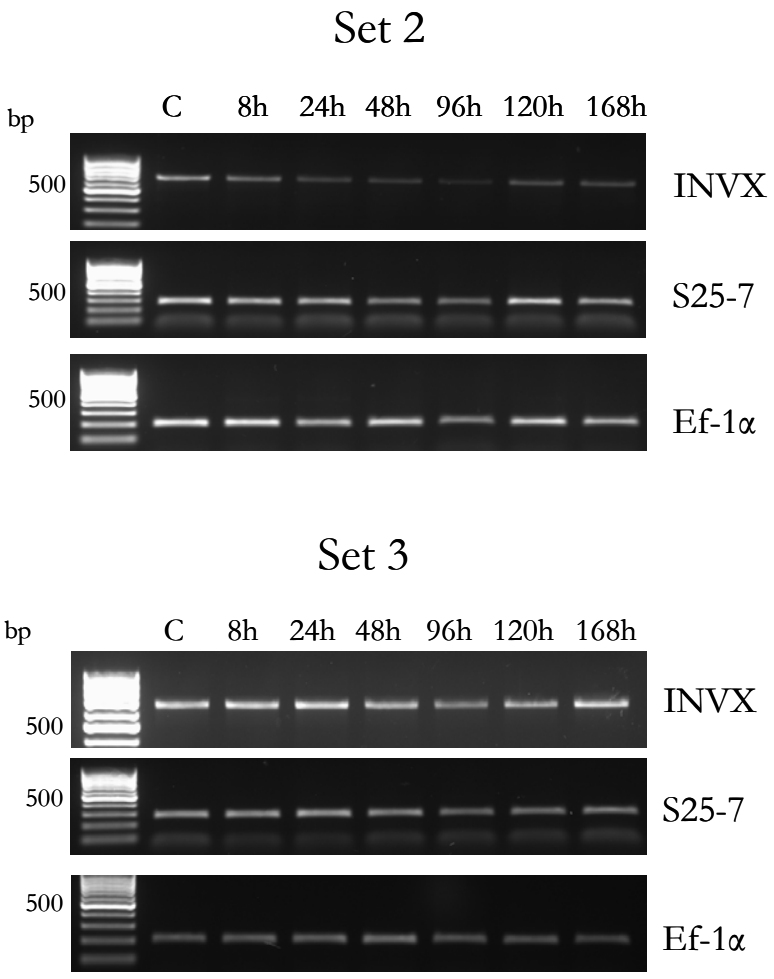

Figure A.9: Western blot analysis of S25-7 and INVX protein levels in PMA stimulated RTS11, additional sets. Protein was isolated from three replicates of an RTS11 time course. The protein was analyzed by western blotting with either anti-rtINVX antibody or anti-rTg antibody, followed by anti-rabbit IgG HRP conjugated antibody. The additional sets used for the S25-7 and INVX densitometry analysis shown in figure 3.21 are shown below.

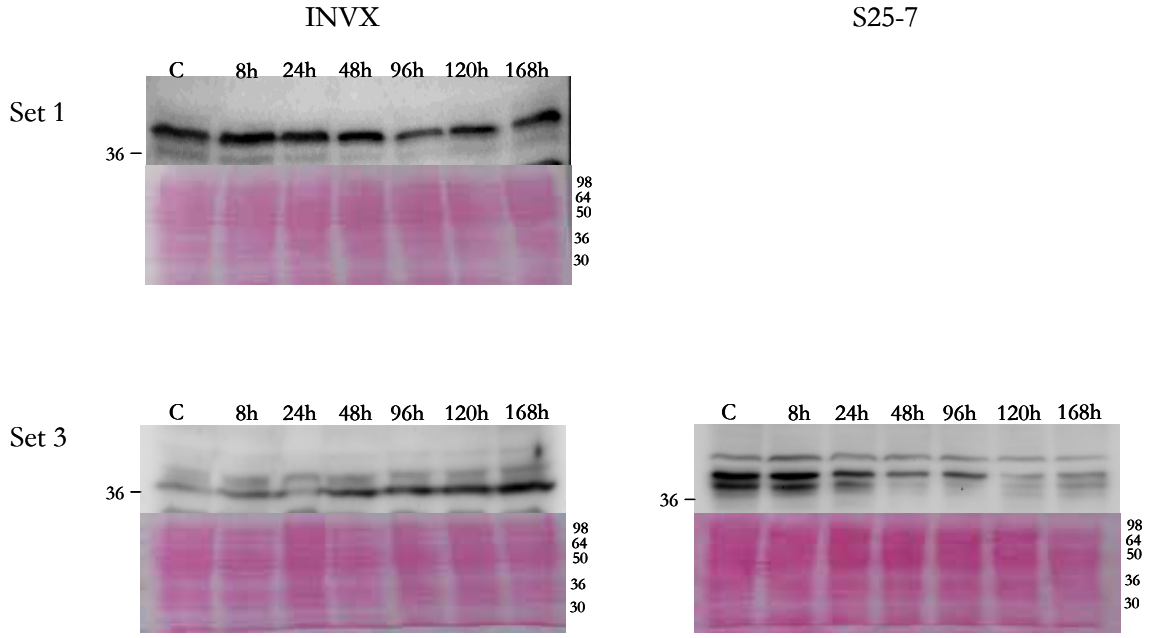

Appendix B
Tables

Table B.1: Densitometry analysis for RT-PCR analysis of IL-1β transcript level in PMA stimulated gill. The corrected intensity for the IL-1β band as well as the corresponding Ef-1α band is listed in the table. The ratio of IL-1β/Ef-1α for each sample and the average ratio for each time point along with the standard deviation of each average are shown.

		Control	8h	24h	48h	96h	120h	168h
Set 2	**IL-1β**	1041569	6136599	1722720	0	3399725	5539378	2861160
	Ef1α	5797194	4537203	4621456	3290412	4153138	4199831	3884870
	IL/E	0.179668	1.352507	0.372766	0	0.818592	1.318953	0.736488
Set 3	**IL-1β**	4958159	9041557	10018578	3737134	0	10233636	5716026
	Ef1α	6266396	5113571	9079721	4927889	4440567	5100691	5169024
	IL/E	0.79123	1.768149	1.103402	0.758364	0	2.006323	1.105823
	Avg IL/E	0.485	1.560	0.738	0.379	0.409	1.663	0.921
	St Dev	0.432	0.294	0.517	0.536	0.579	0.486	0.261

Table B.2: Densitometry analysis for RT-PCR analysis of IL-1β transcript level in PMA stimulated spleen. The corrected intensity for the IL-1β band as well as the corresponding Ef-1α band is listed in the table. The ratio of IL-1β/Ef-1α for each sample and the average ratio for each time point along with the standard deviation of each average are shown.

		Control	8h	24h	48h	96h	120h	168h
Set 1	**IL-1β**	0	0	0	0	1472691	2407652	0
	Ef1α	5803340	7663336	8106870	6713371	8904626	6801315	3980902
	IL/E	0	0	0	0	0.165385	0.353998	0
Set 2	**IL-1β**	0	0	561527.3	0	3122690	203823	0
	Ef1α	6457439	4706813	6848286	5793612	5929417	8365632	5700087
	IL/E	0	0	0.081995	0	0.526644	0.024364	0
Set 3	**IL-1β**	0	0	0	0	4096447	2417998	6184867
	Ef1α	7267659	14716220	13039309	6029999	4754531	14305411	10692877
	IL/E	0	0	0	0	0.861588	0.169027	0.57841
	Avg IL/E	0.000	0.000	0.027	0.000	0.518	0.182	0.193
	St Dev	0.000	0.000	0.047	0.000	0.348	0.165	0.334

Table B.3: Densitometry analysis for RT-PCR analysis of IL-1β transcript level in PMA stimulated head kidney. The corrected intensity for the IL-1β band as well as the corresponding Ef-1α band is listed in the table. The ratio of IL-1β/Ef-1α for each sample and the average ratio for each time point along with the standard deviation of each average are shown.

		Control	8h	24h	48h	96h	120h	168h
Set 1	**IL-1β**	0	0	0	307469.5	1334126	2428969	0
	Ef1α	5475829	7117126	5345413	6700807	6296603	7008797	5548820
	IL/E	0	0	0	0.045885	0.21188	0.34656	0
Set 2	**IL-1β**	0	0	0	0	2911309	1713789	0
	Ef1α	5837247	5838845	6537015	6701408	4313660	5946107	5045697
	IL/E	0	0	0	0	0.674905	0.28822	0
Set 3	**IL-1β**	0	0	0	0	0	1857199	3026010
	Ef1α	5969791	5832765	3886834	4534722	5669924	5987727	4896484
		0	0	0	0	0	0.310168	0.617996
	Avg IL/E	0	0	0	0.015	0.296	0.315	0.206
	St Dev	0	0	0	0.026	0.345	0.029	0.357

Table B.4 Densitometry analysis for northern blot analysis of S25-7 transcript level in PMA stimulated gill. The corrected intensity for the S25-7 band as well as the corresponding S11 band for all samples analyzed is listed in the table. The ratio of S25-7/S11 for each sample and the average ratio for each time point along with the standard deviation of each average are shown.

		Control	8h	24h	48h	96h	120h	168h
Set 1	**S25-7**	61074.5	72653	42867	21611	40460	21752	44869.5
	S11	7051	5694	5174.5	7137	6008	2446	5505
	S25-7/S11	8.661821	12.75957	8.284279	3.028023	6.734354	8.892886	8.150681
Set 2	**S25-7**	41506.5	63307	52799	43012	23441.5	25205	19471
	S11	2020	4529	3390	4417.5	5459.5	3897	5634
	S25-7/S11	20.54777	13.97814	15.57493	9.736729	4.293708	6.467796	3.455982
Set 3	**S25-7**	32376	43382	39374	28821	23431.5	23002	40206.5
	S11	5637	3027	3921.5	3731	5302.5	1279	4141
	S25-7/S11	5.743481	14.33168	10.04055	7.724739	4.418953	17.98436	9.70937
Set 4	**S25-7**	36271.5	43646.5	43557.5	47683.5	49542	39769	44724
	S11	3241.5	6193	5993	5121	6433	4239	5702
	S25-7/S11	11.18973	7.047715	7.268063	9.311365	7.701228	9.381694	7.843564
Set 5	**S25-7**	32339	55079.5	51837.5	47380.5	44949.5	38598	22470
	S11	4373	6443	4666	6337	3207	2278.5	822.5
	S25-7/S11	7.395152	8.548735	11.10962	7.476803	14.01606	16.94009	27.31915
Set 6	**S25-7**	40595	28191.5	19998	23980	19591	18353.5	27387.5
	S11	3194	4511	4774.5	2785.5	2289	1068	1442
	S25-7/S11	12.70977	6.249501	4.188501	8.608867	8.558759	17.18493	18.99272
Avg S25-7/S11		11.041	10.486	9.411	7.648	7.621	12.809	12.579
St Dev		5.295	3.624	3.858	2.426	3.575	5.105	8.853

Table B.5: Densitometry analysis for northern blot analysis of S25-7 transcript level in PMA stimulated spleen. The corrected intensity for the S25-7 band as well as the corresponding S11 band for all samples analyzed is listed in the table. The ratio of S25-7/S11 for each sample and the average ratio for each time point along with the standard deviation of each average are shown

		Control	8h	24h	48h	96h	120h	168h
Set 1	**S25-7**	43961	43430	43709	34549	52258	28737	16703
	S11	6369	6318	9613.5	7300	9753	7593.5	2214.5
	S25-7/S11	6.902339	6.874011	4.546627	4.73274	5.358146	3.784421	7.54256
Set 2	**S25-7**	52094	45669	28542	38328	13406	23300	25889.5
	S11	12460	6545	2836	9946	3424.5	3458	9231
	S25-7/S11	4.180899	6.977693	10.06417	3.853609	3.914732	6.737999	2.804626
Set 3	**S25-7**	26394	25363	17234.5	26831	19599	12593	10679
	S11	6104	2252	2851	3777.5	6500	3173	1899
	S25-7/S11	4.32405	11.26243	6.045072	7.102846	3.015231	3.968799	5.623486
Set 4	**S25-7**	63465	29520	20825	25374	24345	31138.5	21148
	S11	12026	8273.5	5747.2	8223.5	8303	10801.5	5611
	S25-7/S11	5.277316	3.568018	3.623504	3.085548	2.932073	2.882794	3.769025
Set 5	**S25-7**	39763	31932	33183	42213	21960	30074.5	31992.43
	S11	11093.5	6277	8161	9651	12595	8306.5	4758
	S25-7/S11	3.584351	5.087144	4.066046	4.373951	1.743549	3.620598	6.723924
Set 6	**S25-7**	44478.5	47451.5	22627	29770.5	23993	12564	20470.5
	S11	10378	16072	3975	14496.5	4830.5	4758	9739
	S25-7/S11	4.285845	2.952433	5.692327	2.053634	4.966981	2.640605	2.10191
	Avg S25-7/S11	4.759133	6.120289	5.672958	4.200388	3.655119	3.939203	4.760922
	St Dev	1.182338	3.012032	2.344043	1.715195	1.361986	1.467103	2.200736

Table B.6: Densitometry analysis for northern blot analysis of S25-7 transcript level in PMA stimulated head kidney. The corrected intensity for the S25-7 band as well as the corresponding S11 band for all samples analyzed is listed in the table. The ratio of S25-7/S11 for each sample and the average ratio for each time point along with the standard deviation of each average are shown.

		Control	8h	24h	48h	96h	120h	168h
Set 1	**S25-7**	56440	65020	34913	48447	46841	28793.5	41564
	S11	47282	63994.5	37170	35919	46251	36626	28855
	S/S11	1.193689	1.016025	0.939279	1.348785	1.012756	0.786149	1.440444
Set 2	**S25-7**	41747.5	30997	43939	26152	15862.1	31129	17192
	S11	20955.5	24729	24852.5	18913	20521.5	27431.5	18645
	S/S11	1.992198	1.253468	1.767991	1.382753	0.77295	1.13479	0.92207
Set 3	**S25-7**	44627.5	47276	27512	33888	34562.5	21194.5	46611
	S11	21410	21784	33949.22	25069	38290	23090	25521
	S/S11	2.084423	2.170217	0.810387	1.351789	0.902651	0.917908	1.826378
Set 4	**S25-7**	32908	36568	38977.5	22611	7811.74	10493.5	10151.85
	S11	18897	23091	22748.5	18682.5	9464	13390.5	10695.5
	S/S11	1.74144	1.583647	1.71341	1.210277	0.825416	0.783653	0.94917
Set 5	**S25-7**	15916	25204.5	9059	19593.5	7991.6	10123.29	9850.8
	S11	13853.5	8134	6819.24	10641	10968	10460.5	10864.91
	S/S11	1.148879	3.09866	1.328447	1.841321	0.728629	0.967763	0.906662
Set 6	**S25-7**	17085	29258	10377	4846.5	10027.76	8561.56	4523
	S11	7032	13258.5	11011.5	13088	13358.41	10086	3956
	S/S11	2.429608	2.206735	0.942378	0.370301	0.75067	0.848856	1.143327
	Avg S25-7/S11	1.773	2.296	1.328	1.141	0.768	0.867	1.000
	St Dev	0.641	0.761	0.386	0.738	0.051	0.093	0.126

Table B.7: Densitometry analysis for northern blot analysis of S25-7 transcript level in PMA stimulated liver. The corrected intensity for the S25-7 band as well as the corresponding S11 band is listed in the table. The ratio of S25-7/S11 for each sample and the average ratio for each time point along with the standard deviation of each average are shown.

		Control	8h	24h	48h	96h	120h	168h
Set 1	**S25-7**	5505	7800.5	5477	4763	6134	3841	5151
	S11	23454	30630	23047.5	29105	30206	21405	14457
	S25-7/S11	0.234715	0.254669	0.23764	0.163649	0.203072	0.179444	0.356298
Set 2	**S25-7**	3418	1492.19	4249.66	5999.5	5429	5397	3538
	S11	14249	13891	15114	17319.5	15638	16666	11851
	S25-7/S11	0.239876	0.107421	0.281174	0.346401	0.347167	0.323833	0.29854
Set 3	**S25-7**	3801	7097	5272	1035	191	0	0
	S11	9651	20129	27787.5	21756	14563	12669	7555
	S25-7/S11	0.393845	0.352576	0.189726	0.047573	0.013115	0	0
Set 4	**S25-7**	3227	675	4148	4128	1205	0	3214
	S11	14405	13298	34779	34029	29907	15542	19454
	S25-7/S11	0.224019	0.05076	0.119267	0.121308	0.040292	0	0.16521
Set 5	**S25-7**	556	5632	4025	3566	1239	235	1280
	S11	10957	20387	10738	14964	16865	18117	19573
	S25-7/S11	0.050744	0.276254	0.374837	0.238305	0.073466	0.012971	0.065396
Set 6	**S25-7**	5810	5737	3146	230	0	245	0
	S11	25366	24763	34431	18398	10544	13614	12826
	S25-7/S11	0.229047	0.231676	0.091371	0.012501	0	0.017996	0
Avg S25-7/S11		0.229	0.212	0.216	0.155	0.113	0.089	0.148
St Dev		0.109	0.112	0.105	0.124	0.136	0.134	0.153

Table B.8: Densitometry analysis for northern blot analysis of INVX transcript level in PMA stimulated gill. The corrected intensity for the INVX band as well as the corresponding S11 band for all samples analyzed is listed in the table. The ratio of INVX/S11 for each sample and the average ratio for each time point along with the standard deviation of each average are shown.

		Control	8h	24h	48h	96h	120h	168h
Set 1	**INVX**	1204619	1638831	529528.1	296334	1215372	219245.2	557717
	S11	11855273	12487489	11645011	7034147	10660934	1893373	9330635
	INVX/S11	0.10161	0.131238	0.045473	0.042128	0.114002	0.115796	0.059773
Set 2	**INVX**	771368.1	1285036	3042473	664216.5	452888	654742	569722.8
	S11	6999406	9512237	14511253	5235107	7220916	6748375	5630448
	INVX/S11	0.110205	0.135093	0.209663	0.126877	0.062719	0.097022	0.101186
Set 3	**INVX**	717184.1	1275896	110517	444225.9	258347.7	329229	375425.1
	S11	7065818	5361763	7255308	5964688	6501396	6732971	8761975
	INVX/S11	0.101501	0.237962	0.015233	0.074476	0.039737	0.048898	0.042847
Set 4	**INVX**	677593.9	912586	197111	575907.3	706737.3	701844	724997.1
	S11	5401270	11460074	2381253	2861142	9504661	5338081	7780797
	INVX/S11	0.125451	0.079632	0.082776	0.201286	0.074357	0.131479	0.093178
Set 5	**INVX**	740814.5	1878443	568190.1	908131	929282	1210419	767834.6
	S11	8269132	10910129	4892447	11416121	8697078	8989596	9854748
	INVX/S11	0.089588	0.172174	0.116136	0.079548	0.10685	0.134647	0.077915
	Avg INVX/S11	0.106	0.151	0.094	0.105	0.080	0.106	0.075
	St Dev	0.013	0.059	0.075	0.062	0.031	0.035	0.024

Table B.9: Densitometry analysis for northern blot analysis of INVX transcript level in PMA stimulated spleen. The corrected intensity for the INVX band as well as the corresponding S11 band for all samples analyzed is listed in the table. The ratio of INVX/S11 for each sample and the average ratio for each time point along with the standard deviation of each average are shown.

		Control	8h	24h	48h	96h	120h	168h
Set 1	**INVX**	273465.6	52795.43	439351.1	211206.7	451727.1	385434	373378.2
	S11	3024717	1585574	2148420	1278191	2539613	2287924	671724.5
	INVX/S11	0.09041	0.033297	0.2045	0.165239	0.177872	0.168465	0.55585
Set 2	**INVX**	493332.4	998732.1	592692.5	484424.2	198409	92862	1336255
	S11	2694379	1791979	631457	4045215	1167348	848258	2431870
	INVX/S11	0.183097	0.557335	0.938611	0.119752	0.169966	0.109474	0.549476
Set 4	**INVX**	1021822	496612	467719.2	333827.2	349669	338744	407280.4
	S11	8432063	3433389	1820522	1566684	2878284	4310218	2692440
	INVX/S11	0.121183	0.144642	0.256915	0.213079	0.121485	0.078591	0.151268
Set 5	**INVX**	292653.3	464694.7	811953	685070.3	1501092	2322644	1185060
	S11	4678186	2808366	4123041	1659268	9008377	10076709	5406323
	INVX/S11	0.062557	0.165468	0.196931	0.412875	0.166633	0.230496	0.219199
Set 6	**INVX**	1629497	1734091	576889.6	801965	589157.7	652738.7	441268
	S11	9178445	8017214	1912394	12149083	2105986	2467958	5146212
	INVX/S11	0.177535	0.216296	0.301658	0.06601	0.279754	0.264485	0.085746
Avg INVX/S11		0.127	0.223	0.380	0.195	0.183	0.170	0.312
St Dev		0.053	0.198	0.315	0.133	0.058	0.078	0.224

Table B.10: Densitometry analysis for RT-PCR analysis of INVX transcript level in PMA stimulated gill. The corrected intensity for the INVX band as well as the corresponding Ef-1α band is listed in the table. The ratio of INVX/Ef-1α for each sample and the average ratio for each time point along with the standard deviation of each average are shown.

		Control	8h	24h	48h	96h	120h	168h
Set 1	**INVX**	13116842	16183073	6449169	11906954	13063446	13249923	12002006
	Ef1α	15192460	20324441	11132489	20012399	14014548	18087168	15042363
	INVX/Ef1α	0.863378	0.796237	0.579311	0.594979	0.932135	0.732559	0.79788
Set 2	**INVX**	12098262	6888496	5608070	5073344	3610632	6232246	5970277
	Ef1α	14796640	18253164	17448579	10081381	11728441	16093551	11526772
	INVX/Ef1α	0.817636	0.377386	0.321406	0.503239	0.307853	0.387251	0.517949
Set 3	**INVX**	21727546	13491312	11878298	11725531	7557823	11899050	11997952
	Ef1α	15291788	7838304	12107799	9165555	6572797	10392320	10481147
	INVX/Ef1α	1.420864	1.721203	0.981045	1.279304	1.149864	1.144985	1.144717
	Avg INVX/Ef1α	1.034	0.965	0.627	0.793	0.797	0.755	0.820
	St Dev	0.336	0.688	0.332	0.424	0.437	0.379	0.314

Table B.11: Densitometry analysis for RT-PCR analysis of INVX transcript level in PMA stimulated spleen. The corrected intensity for the INVX band as well as the corresponding Ef-1α band is listed in the table. The ratio of INVX/Ef-1α for each sample and the average ratio for each time point along with the standard deviation of each average are shown.

		Control	8h	24h	48h	96h	120h	168h
Set 1	**INVX**	8291045	11384165	6680067	9251647	7635968	6708432	5607507
	Ef1α	11910936	12973347	12552360	13208541	11301054	9882337	5470997
	INVX/Ef1α	0.696087	0.877504	0.532176	0.700429	0.675686	0.678831	1.024952
Set 2	**INVX**	21259805	14326302	12892980	7993317	9452385	11048100	14547544
	Ef1α	12173121	13258963	17927428	9248247	16724852	23260604	15978297
	INVX/Ef1α	1.746455	1.080499	0.719176	0.864306	0.56517	0.47497	0.910456
Set 3	**INVX**	12788665	8347107	6118785	7560332	7050828	4442668	4410610
	Ef1α	10400920	5275237	4181303	7348156	2516299	3062843	1972916
	INVX/Ef1α	1.229571	1.582319	1.463368	1.028875	2.802063	1.450504	2.23558
	Avg INVX/Ef1α	1.224	1.180	0.905	0.865	1.348	0.868	1.390
	St Dev	0.525	0.363	0.493	0.164	1.261	0.515	0.734

Table B.12: Densitometry analysis for RT-PCR analysis of INVX transcript level in PMA stimulated head kidney. The corrected intensity for the INVX band as well as the corresponding Ef-1α band is listed in the table. The ratio of INVX/Ef-1α for each sample and the average ratio for each time point along with the standard deviation of each average are shown.

		Control	8h	24h	48h	96h	120h	168h
Set 1	**INVX**	6381630	6529410	3218100	2725306	3836026	2846703	6094214
	Ef1α	15380286	22109683	9904066	11469209	19434194	13198850	15866414
	INVX/Ef1α	0.414923	0.295319	0.324927	0.237619	0.197385	0.215678	0.384095
Set 2	**INVX**	11131553	12606648	13244145	8500355	10209114	11467859	6659781
	Ef1α	19642216	20642669	22245028	21813610	16144385	21741552	17472075
	INVX/Ef1α	0.566716	0.610708	0.595375	0.389681	0.632363	0.527463	0.381167
Set 3	**INVX**	4480476	6427798	2875314	4384466	3991896	3616002	4765196
	Ef1α	8438391	8267087	6261917	7055607	7753010	7937105	9888673
	INVX/Ef1α	0.530963	0.777517	0.459175	0.621416	0.514883	0.455582	0.481884
Avg INVX/Ef1α		0.504	0.561	0.460	0.416	0.448	0.400	0.416
St Dev		0.079	0.245	0.135	0.193	0.225	0.163	0.057

Table B.13: Densitometry analysis for RT-PCR analysis of INVX transcript level in PMA stimulated liver. The corrected intensity for the INVX band as well as the corresponding Ef-1α band is listed in the table. The ratio of INVX/Ef-1α for each sample and the average ratio for each time point along with the standard deviation of each average are shown.

		Control	8h	24h	48h	96h	120h	168h
Set 1	**INVX**	0	1371603	0	0	0	0	0
	Ef1α	9859990	12155960	9534139	11071815	8311759	7614829	6688179
	INVX/Ef1α	0	0.112834	0	0	0	0	0
Set 2	**INVX**	3045983	3171581	2329545	0	3680165	3347928	4400390
	Ef1α	14892518	15426960	9552115	12705103	13720983	11820171	9820636
	INVX/Ef1α	0.204531	0.205587	0.243877	0	0.268214	0.283239	0.448076
Set 3	**INVX**	2011314	2084362	0	0	0	0	1759364
	Ef1α	10302934	10149239	5719179	11967671	7355119	11566288	13512202
	INVX/Ef1α	0.195218	0.205371	0	0	0	0	0.130206
Avg INVX/Ef1α		0.133	0.175	0.081	0.000	0.089	0.094	0.193
St Dev		0.115	0.053	0.141	0.000	0.155	0.164	0.230

Table B.14: Densitometry analysis for RT-PCR analysis of INVX transcript level in PMA stimulated PBL. The corrected intensity for the S25-7, INVX band as well as the corresponding Ef-1α band is listed in the table. The ratio of INVX/Ef-1α and S25-7/Ef-1α for each sample and the average ratio for each time point along with the standard deviation of each average are shown.

		Control	8h	24h	48h	96h	120h	168h
Set 1	**INVX**	12278078	9351550	9238318	11273417	17941586	10957467	14848362
	S25-7	11340531	10330174	11589962	10937334	12235440	7674857	11250602
	Ef1α	10965276	5127190	8571023	13692649	7629619	7654858	10949359
	INVX/Ef1α	1.119724	1.823913	1.077855	0.823319	2.35157	1.43144	1.356094
	S25-7/Ef1α	1.034222	2.014783	1.352226	0.798774	1.603676	1.002613	1.027512
Set 3	**INVX**	26300741	19501419	16318759	3935877	19175590	14611985	19634501
	S25-7	20741185	16466706	13381386	5784559	12758218	10951208	14647332
	Ef1α	19469591	14471294	13351444	7801827	14802429	14766547	10296050
	INVX/Ef1α	1.350863	1.347593	1.222247	0.504482	1.295435	0.989533	1.906994
	S25-7/Ef1α	1.065312	1.137888	1.002243	0.741436	0.8619	0.741623	1.422617
Set 4	**INVX**	16583450	12879603	9348481	7159478	12510489	13794570	20397065
	S25-7	13975777	10892470	6116648	4652328	9107396	9646095	14666359
	Ef1α	21553251	8687316	6432383	6889375	8668917	11011757	18428416
	INVX/Ef1α	0.769418	1.482576	1.453346	1.039206	1.443143	1.252713	1.106827
	S25-7/Ef1α	0.64843	1.253836	0.950915	0.67529	1.050581	0.875981	0.795856
Set 6	**INVX**	17062293	9093226	14032445	19595850	14976805	13561567	18019553
	S25-7	17400769	13375706	16470058	17444860	11711543	13342670	18773357
	Ef1α	14057935	12902851	13178686	15856262	10904656	10760257	14039864
	INVX/Ef1α	1.213713	0.704745	1.064783	1.235843	1.373432	1.260339	1.283456
	S25-7/Ef1a	1.23779	1.036647	1.24975	1.100187	1.073995	1.239995	1.337147
	Avg INVX/Ef1α	1.113	1.340	1.205	0.901	1.616	1.234	1.413
	St Dev	0.248	0.468	0.181	0.313	0.494	0.182	0.345
	Avg S25-7/Ef1α	0.996	1.361	1.139	0.829	1.148	0.965	1.146
	St Dev	0.249	0.445	0.193	0.188	0.319	0.212	0.288

Table B.15: Densitometry analysis for Western blot analysis of S25-7 protein level in PMA stimulated gill. Western blot analysis was performed on four sets of gill tissue. The S25-7 protein migrates as a doublet in western blot analysis, the S25-7_1 and S25-7_2 represent the corrected intensity for the upper and lower bands of the doublet. The corrected intensity of the 50kDa band in the ponceau stain is also shown and a ratio of the sum of the S25-7 bands to the 50kDa band is shown (Ratio B:P). Finally, the average S25-7/50kDa for each time point, along with the standard deviation for each, is shown at the bottom of the table.

		Control	8h	24h	48h	96h	120h	168h
Set 1	**S25-7_1**	6386702	4488196	4799727	13291612	11998297	7440181	11697595
	S25-7_2	1191134	798508.7	749617.9	2837217	2975654	2413988	4985681
	Sum	7.58E+06	5.29E+06	5.55E+06	1.61E+07	1.50E+07	9.85E+06	1.67E+07
	Ponceau	2467418	2164116	2714578	1598280	2314402	2789012	2093072
	Ratio B:P	3.07	2.44	2.04	10.09	6.47	3.53	7.97
Set 2	**S25-7_1**	9260060	14009986	15399030	16251988	14844345	18708859	21887339
	S25-7_2	1988499	4836461	5257705	4832752	3865585	6892995	
	Sum	1.12E+07	1.88E+07	2.07E+07	2.11E+07	1.87E+07	2.56E+07	2.19E+07
	Ponceau	2690012	1498625	1474151	1558043	1785011	1313421	1500364
	Ratio B:P	4.18	12.58	14.01	13.53	10.48	19.49	14.59
Set 3	**S25-7_1**	13260819	18850200	20350069	17129269	10387458	17434571	18412618
	S25-7_2	5259948	9502389	5893817	5526874	2389580	7763188	4094973
	Sum	1.85E+07	2.84E+07	2.62E+07	2.27E+07	1.28E+07	2.52E+07	2.25E+07
	Ponceau	3029301	1804044	1249328	2096624	2488209	2170708	949062.9
	Ratio B:P	6.11387	15.71613	21.00641	10.80601	5.13503	11.60808	23.71560
Set 4	**S25-7_1**	23871853	21995830	23781302	25879763	23655739	21653328	20700222
	S25-7_2	13763031	15135069	20491505	18051913	13533540	11667332	13482271
	Sum	3.76E+07	3.71E+07	4.43E+07	4.39E+07	3.72E+07	3.33E+07	3.42E+07
	Ponceau	1877603	2103291	1868034	1792940	1887770	2129252	2126190
	Ratio B:P	20.0441	17.6537	23.7002	24.5026	19.7001	15.6490	16.0769
	Avg B:P	8.35	12.10	15.19	14.73	10.45	12.57	15.59
	St Dev	7.90	6.77	9.67	6.68	6.57	6.83	6.46

Table B.16: Densitometry analysis for Western blot analysis of S25-7 protein level in PMA stimulated spleen. Western blot analysis was performed on four sets of spleen tissue. The S25-7 protein migrates as a doublet in western blot analysis, the S25-7_1 and S25-7_2 represent the corrected intensity for the upper and lower bands of the doublet. The corrected intensity of the 50kDa band in the ponceau stain is also shown and a ratio of the sum of the S25-7 bands to the 50kDa band is shown (Ratio B:P). Finally, the average S25-7/50kDa for each time point, along with the standard deviation for each, is shown at the bottom of the table.

		Control	8	24	48	96	120	168
Set 1	**S25-7_1**	22112122	24048001	2479184	13674706	6851555	493685.9	3587799
	S25-7_2	0	0	2014664	2437832	1525796	0	0
	Sum	22112122	24048001	4493848	16112537	8377351	493685.9	3587799
	Ponceau	4650990	2294717	1936047	1770045	2394214	2503051	1844504
	Ratio B:P	4.754283	10.47973	2.321146	9.102896	3.498999	0.197234	1.945129
Set 2	**S25-7_1**	1714290	25278513	1120053	2921085	7817702	814809.1	546579.9
	S25-7_2	2098012	0	0	0	2426091	0	1020179
	Sum	3812302	25278513	1120053	2921085	10243793	814809.1	1566759
	Ponceau	1418869	1821340	1216727	814284.9	1471538	1555698	1917999
	Ratio B:P	2.686859	13.87907	0.920546	3.587302	6.961283	0.523758	0.816872
Set 3	**S25-7_1**	2872840	29908581	9686591	16107566	6183260	6404500	15674287
	S25-7_2	8732133	0	0	11010702	10328789	3157588	0
	Sum	11604973	29908581	9686591	27118268	16512049	9562088	15674287
	Ponceau	1890346	1239473	1087962	993271.6	1280840	1159146	1814852
	Ratio B:P	6.139075	24.13009	8.90343	27.30197	12.89158	8.249255	8.636675
Set 4	**S25-7_1**	8200916	2856899	479288.1	2572266	2125340	431540.6	330560.7
	S25-7_2	0	0	820313.4	0	0	1011062	0
	Sum	8200916	2856899	1299601	2572266	2125340	1442602	330560.7
	Ponceau	3428744	3498548	3746557	2193836	1338357	2173468	2216912
	Ratio B:P	2.391814	0.816596	0.346879	1.172497	1.588022	0.663733	0.149109
	Avg B:P	3.993	12.326	3.123	10.291	6.235	2.408	2.887
	St Dev	1.775	9.620	3.942	11.816	4.964	3.899	3.904

Table B.17: Densitometry analysis for Western blot analysis of INVX protein level in PMA stimulated gill. Western blot analysis was performed on four sets of gill tissue. The INVX protein migrates as a doublet or triplet in western blot analysis, the INVX_1, INVX_2 and INVX_3 represent the corrected intensity for the upper and lower bands of the doublet. The corrected intensity of the 50kDa band in the ponceau stain is also shown and a ratio of the sum of the INVX bands to the 50kDa band is shown (Ratio B:P). Finally, the average INVX/50kDa for each time point, along with the standard deviation for each, is shown at the bottom of the table.

		Control	8h	24h	48h	96h	120h	168h
Set 1	**INVX_1**	9471306	4996817	2338256	9159438	7085246	6921288	27284675
	INVX_2	8434117	8420798	2585998	12611300	9191597	10922038	0
	INVX_3	0	0	5847380	6647854	0	0	0
	Sum	1.79E+07	1.34E+07	1.08E+07	2.84E+07	1.63E+07	1.78E+07	2.73E+07
	Ponceau	1961918	2241406	2194428	1377526	1181006	1437877	1760403
	Ratio B:P	9.13	5.99	4.91	20.63	13.78	12.41	15.50
Set 2	**INVX_1**	4486261	15122744	10091327	8737615	6940461	8655682	3208322
	INVX_2	2443502	15890664	10451293	6170868	9434778	10344054	2358669
	INVX_3	0	0	0	0	0	0	4358558
	Sum	6.93E+06	3.10E+07	2.05E+07	1.49E+07	1.64E+07	1.90E+07	9.93E+06
	Ponceau	3400280	1621180	1521451	1614725	2259484	1677400	1653446
	Ratio B:P	2.04	19.13	13.50	9.23	7.25	11.33	6.00
Set 3	**INVX_1**	6717621	7464497	10159831	5075980	2148043	4558961	8291831
	INVX_2	0	15245691	20103534	6560194	1591362	14541643	7066016
	INVX_3	0	0	0	3562339	0	0	0
	Sum	6.72E+06	2.27E+07	3.03E+07	1.52E+07	3.74E+06	1.91E+07	1.54E+07
	Ponceau	2451159	2044603	1753080	2208933	2439674	1859991	988161.5
	Ratio B:P	2.74	11.11	17.26	6.88	1.53	10.27	15.54
Set 4	**INVX_1**	1287535	3496949	5343226	9548070	4178750	4519410	7048133
	INVX_2	2189280	3370409	6954363	2145323	5728738	6173405	4429439
	Sum	3.48E+06	6.87E+06	1.23E+07	1.17E+07	9.91E+06	1.07E+07	1.15E+07
	Ponceau	1829425	1466759	1124086	884165.4	963792.2	703774	896882.2
	Ratio B:P	1.90	4.68	10.94	13.23	10.28	15.19	12.80
	Avg B:P	3.95	10.23	11.65	12.49	8.21	12.30	12.46
	St Dev	3.469627	6.551646	5.192471	6.024363	5.191188	2.117833	4.492258

Table B.18: Densitometry analysis for Western blot analysis of INVX protein level in PMA stimulated spleen. Western blot analysis was performed on four sets of spleen tissue. The INVX protein migrates as a doublet in western blot analysis, the INVX_1 and INVX_2 represent the corrected intensity for the upper and lower bands of the doublet. The corrected intensity of the 50kDa band in the ponceau stain is also shown and a ratio of the sum of the INVX bands to the 50kDa band is shown (Ratio B:P). Finally, the average INVX/50kDa for each time point, along with the standard deviation for each, is shown at the bottom of the table.

		Control	8h	24h	48h	96h	120h	168h
Set 1	**INVX_1**	13536954	4087483	0	0	0	0	0
	INVX_2	22898050	8897641	0	0	0	0	0
	Sum	36435004	12985124	0	0	0	0	0
	Ponceau	2409076	1304556	1404269	1141416	1737189	1916466	2038584
	Ratio B:P	15.12406	9.95367	0	0	0	0	0
Set 2	**INVX_1**	299699.7	27555258	356043.1	5132668	3164355	2338534	2140404
	INVX_2	1068210		2121551				
	Sum	1367910	27555258	2477594	5132668	3164355	2338534	2140404
	Ponceau	1205481	1942968	1097733	1972950	1915756	1395714	1815843
	Ratio B:P	1.134741	14.18204	2.25701	2.60152	1.651752	1.67551	1.178738
Set 3	**INVX_1**	445893.7	17679643	3300255	17678632	8437821	265369.5	574745.6
	INVX_2	2499743					3364231	3256492
	Sum	2945637	17679643	3300255	17678632	8437821	3629601	3831237
	Ponceau	2772355	1239245	1578284	1493492	1693972	2312441	2666162
	Ratio B:P	1.062503	14.26646	2.09104	11.83711	4.981086	1.569597	1.436986
Set 4	**INVX_1**	1525862	182149.3	0	180572.8	233074	0	258051.2
	INVX_2	2717058	747182.4	0	0	568776.8	0	0
	Sum	4242920	929331.7	0	180572.8	801850.7	0	258051.2
	Ponceau	2553576	2120536	2476337	2576459	1960165	2236291	2385560
	Ratio B:P	1.66156	0.438253	0	0.070086	0.409073	0	0.108172
	Avg B:P	4.746	9.710	1.087	3.627	1.760	0.811	0.681
	St Dev	8.098	2.466	1.258	6.221	2.537	0.938	0.766

Table B.19: Densitometry analysis for RT-PCR analysis of INVX transcript level in PMA stimulated RTS11. The corrected intensity for the S25-7, INVX band as well as the corresponding Ef-1α band is listed in the table. The ratio of INVX/Ef-1α and S25-7/Ef-1α for each sample and the average ratio for each time point along with the standard deviation of each average are shown.

		Control	8h	24h	48h	96h	120h	168h
Set 1	**INVX**	19025806	12629827	10643073	4544289	8430951	11365087	11418943
	S25-7	17142471	15714796	15170387	9301579	13548318	19139384	14120886
	Ef1α	13812667	10780858	10318873	8493475	10159106	10790358	11635673
	INVX/Ef1α	1.377417	1.171505	1.031418	0.535033	0.829891	1.053263	0.981374
	S25-7/Ef1α	1.241069	1.457657	1.470159	1.095144	1.333613	1.773749	1.213586
Set 2	**INVX**	17587749	11016102	5463220	4364767	2318306	6823268	6015167
	S25-7	26008558	21364800	19572850	13264714	10754900	23338325	16997931
	Ef1α	13480148	13001302	9123052	11500540	6525857	11214839	8943512
	INVX/Ef1α	1.304715	0.847308	0.598837	0.379527	0.355249	0.608414	0.672573
	S25-7/Ef1α	1.929397	1.643282	2.145428	1.153399	1.648044	2.081022	1.900588
Set 3	**INVX**	10737345	10797999	11582737	8702796	5839413	7718583	10758916
	S25-7	11070283	10865791	11698725	9537938	6781220	7661509	8779635
	Ef1α	9209861	10529102	11234584	13396560	8857660	8899872	7363618
	INVX/Ef1α	1.165853	1.025538	1.030989	0.649629	0.65925	0.867269	1.461091
	S25-7/Ef1α	1.202003	1.031977	1.041314	0.711969	0.765577	0.860856	1.192299
Avg INVX/Ef1 α		1.282662	1.014784	0.887081	0.521396	0.614797	0.842982	1.038346
	St Dev	0.107492	0.162366	0.249627	0.135566	0.240423	0.223417	0.397334
Avg S25-7/Ef1 α		1.457	1.378	1.552	0.987	1.249	1.572	1.435
	St Dev	0.409	0.313	0.557	0.240	0.447	0.635	0.403

Table B.20: Densitometry analysis for Western blot analysis of INVX protein level in PMA stimulated RTS11. Western blot analysis was performed on three sets of RTS11. The INVX protein migrates as a doublet in western blot analysis, the INVX_1 and INVX_2 represent the corrected intensity for the upper and lower bands of the doublet. The corrected intensity of the 50kDa band in the ponceau stain is also shown and a ratio of the sum of the INVX bands to the 50kDa band is shown (Ratio B:P). Finally, the average INVX/50kDa for each time point, along with the standard deviation for each, is shown at the bottom of the table.

		Control	8h	24h	48h	96h	120h	168h
Set 1	**INVX_1**	2379098	2572181	2040546	1871130	1250120	1706647	2064766
	INVX_2	546077	484072.5	291863.7	72261.5	113586.2	195750.7	290506.7
	Sum	2.93E+06	3.06E+06	2.33E+06	1.94E+06	1.36E+06	1.90E+06	2.36E+06
	Ponceau	926967.4	786292.4	815338.2	1130766	1350114	1756150	2520134
	Ratio B:P	3.16	3.89	2.86	1.72	1.01	1.08	0.93
Set 2	**INVX_1**	825548.1	1503690	714245.1	633566.2	488568.6	316896	678139.9
	INVX_2	4033154	4277444	3090600	2789332	2483171	1353963	2169293
	Sum	4.86E+06	5.78E+06	3.80E+06	3.42E+06	2.97E+06	1.67E+06	2.85E+06
	Ponceau	1017589	963264.5	920492.5	792174	684125.8	245834.2	1013756
	Ratio B:P	4.77	6.00	4.13	4.32	4.34	6.80	2.81
Set 3	**INVX_1**	575826.3	901168.7	639342.5	921060.3	761760	846205.7	1279946
	INVX_2	1861621	1491867	998765.5	2529228	3373179	4497368	5008831
	Sum	2.44E+06	2.39E+06	1.64E+06	3.45E+06	4.13E+06	5.34E+06	6.29E+06
	Ponceau	1164852	1758672	1246990	1784311	1139539	1005240	1617337
	Ratio B:P	2.09	1.36	1.31	1.93	3.63	5.32	3.89
	Avg B:P	3.34	3.75	2.77	2.66	2.99	4.40	2.54
	St Dev	1.35068	2.323489	1.412139	1.444338	1.755108	2.965073	1.494595

Table B.21: Densitometry analysis for Western blot analysis of S25-7 protein level in PMA stimulated RTS11. Western blot analysis was performed on two sets of RTS11. The S25-7 protein migrates as a doublet in western blot analysis, the S25-7_1 and S25-7_2 represent the corrected intensity for the upper and lower bands of the doublet. The corrected intensity of the 50kDa band in the ponceau stain is also shown and a ratio of the sum of the INVX bands to the 50kDa band is shown (Ratio B:P). Finally, the average S25-7/50kDa for each time point, along with the standard deviation for each, is shown at the bottom of the table.

		Control	8h	24h	48h	96h	120h	168h
Set 2	**S25-7_1**	14941285	9537447	12904742	10768662	11147291	9286578	5654822
	S25-7_2	15020643	8335006	9794905	5658449	7282035	4618839	6685085
	Sum	3.00E+07	1.79E+07	2.27E+07	1.64E+07	1.84E+07	1.39E+07	1.23E+07
	Ponceau	865618.3	643905	1171181	911384.7	826288.7	818345.9	992787.9
	Ratio B:P	34.61	27.76	19.38	18.02	22.30	16.99	12.43
Set 3	**S25-7_1**	9399268	9878345	5401350	3649803	4523715	1640100	2776325
	S25-7_2	9843977	7840849	5043136	1415580	1524985	2366564	3967253
	Sum	1.92E+07	1.77E+07	1.04E+07	5.07E+06	6.05E+06	4.01E+06	6.74E+06
	Ponceau	882759.9	699817.8	1076706	1572068	828083.6	1287304	680817.8
	Ratio B:P	21.80	25.32	9.70	3.22	7.30	3.11	9.91
	Avg B:P	28.21	26.54	14.54	10.62	14.80	10.05	11.17
	St Dev	9.06	1.72	6.85	10.47	10.61	9.81	1.79

References

Adams,S. and Humphreys,R.E. (1995). Invariant chain peptides enhancing or inhibiting the presentation of antigenic peptides by major histocompatibility complex class II molecules. Eur. J. Immunol. *25*, 1693-1702.

Ahluwalia,N., Bergeron,J.J., Wada,I., Degen,E., and Williams,D.B. (1992). The p88 molecular chaperone is identical to the endoplasmic reticulum membrane protein, calnexin. J. Biol. Chem. *267*, 10914-10918.

Aitken,A. (1996). 14-3-3 and its possible role in co-ordinating multiple signalling pathways. Trends Cell Biol. *6*, 341-347.

Albanesi,C., Cavani,A., and Girolomoni,G. (1998). Interferon-gamma-stimulated human keratinocytes express the genes necessary for the production of peptide-loaded MHC class II molecules. J. Invest Dermatol. *110*, 138-142.

Alberts, B., Johnson, A., Lewis, J., Raff, M., Roberts, K. and Walter, P. (2002). Molecular biology of the cell, 4th Ed. Garland Science, New York. Pp 664-665.

Anderson,H.A. and Roche,P.A. (1998). Phosphorylation regulates the delivery of MHC class II invariant chain complexes to antigen processing compartments. J. Immunol. *160*, 4850-4858.

Anderson,K.S. and Cresswell,P. (1994). A role for calnexin (IP90) in the assembly of class II MHC molecules. EMBO J. *13*, 675-682.

Anderson,M.S. and Miller,J. (1992). Invariant chain can function as a chaperone protein for class II major histocompatibility complex molecules. Proc. Natl. Acad. Sci. U. S. A *89*, 2282-2286.

Arneson,L.S. and Miller,J. (1995). Efficient endosomal localization of major histocompatibility complex class II-invariant chain complexes requires multimerization of the invariant chain targeting sequence. J. Cell Biol. *129*, 1217-1228.

Arunachalam,B., Lamb,C.A., and Cresswell,P. (1994). Transport properties of free and MHC class II-associated oligomers containing different isoforms of human invariant chain. Int. Immunol. *6*, 439-451.

Baneyx,F. (1999). Recombinant protein expression in Escherichia coli. Curr. Opin. Biotechnol. *10*, 411-421.

Barr,C.L. and Saunders,G.F. (1991). Interferon-gamma-inducible regulation of the human invariant chain gene. J. Biol. Chem. *266* , 3475-3481.

Barton,G.M. and Rudensky,A.Y. (1998). An altered invariant chain protein with an antigenic peptide in place of CLIP forms SDS-stable complexes with class II alphabeta dimers and facilitates highly efficient peptide loading. Int. Immunol. *10*, 1159-1165.

Bevec,T., Stoka,V., Pungercic,G., Dolenc,I., and Turk,V. (1996). Major histocompatibility complex class II-associated p41 invariant chain fragment is a strong inhibitor of lysosomal cathepsin L. J. Exp. Med. *183*, 1331-1338.

Bijlmakers,M.J., Benaroch,P., and Ploegh,H.L. (1994). Mapping functional regions in the lumenal domain of the class II-associated invariant chain. J. Exp. Med. *180*, 623-629.

Boss,J.M. and Jensen,P.E. (2003). Transcriptional regulation of the MHC class II antigen presentation pathway. Curr. Opin. Immunol. *15*, 105-111.

Bourguignon,L.Y., Zhu,H., Shao,L., and Chen,Y.W. (2001). CD44 interaction with c-Src kinase promotes cortactin-mediated cytoskeleton function and hyaluronic acid-dependent ovarian tumor cell migration. J. Biol. Chem. *276*, 7327-7336.

Brachet,V., Pehau-Arnaudet,G., Desaymard,C., Raposo,G., and Amigorena,S. (1999). Early endosomes are required for major histocompatiblity complex class II transport to peptide-loading compartments. Mol. Biol. Cell *10*, 2891-2904.

Bremnes,B., Madsen,T., Gedde-Dahl,M., and Bakke,O. (1994). An LI and ML motif in the cytoplasmic tail of the MHC-associated invariant chain mediate rapid internalization. J. Cell Sci. *107 (Pt 7)*, 2021-2032.

Brendolan,A., Rosado,M.M., Carsetti,R., Selleri,L., and Dear,T.N. (2007). Development and function of the mammalian spleen. Bioessays *29*, 166-177.

Busch,R., Doebele,R.C., Patil,N.S., Pashine,A., and Mellins,E.D. (2000). Accessory molecules for MHC class II peptide loading. Curr. Opin. Immunol. *12*, 99-106.

Busch,R., Rinderknecht,C.H., Roh,S., Lee,A.W., Harding,J.J., Burster,T., Hornell,T.M., and Mellins,E.D. (2005). Achieving stability through editing and chaperoning: regulation of MHC class II peptide binding and expression. Immunol. Rev. *207*, 242-260.

Campos-Perez,J.J., Ward,M., Grabowski,P.S., Ellis,A.E., and Secombes,C.J. (2000). The gills are an important site of iNOS expression in rainbow trout Oncorhynchus mykiss after challenge with the gram-positive pathogen Renibacterium salmoninarum. Immunology *99*, 153-161.

Castellino,F. and Germain,R.N. (1995). Extensive trafficking of MHC class II-invariant chain complexes in the endocytic pathway and appearance of peptide-loaded class II in multiple compartments. Immunity. *2* , 73-88.

Claesson-Welsh,L., Barker,P.E., Larhammar,D., Rask,L., Ruddle,F.H., and Peterson,P.A. (1984). The gene encoding the human class II antigen-associated gamma chain is located on chromosome 5. Immunogenetics *20* , 89-93.

Collins,T., Korman,A.J., Wake,C.T., Boss,J.M., Kappes,D.J., Fiers,W., Ault,K.A., Gimbrone,M.A., Jr., Strominger,J.L., and Pober,J.S. (1984). Immune interferon activates multiple class II major histocompatibility complex genes and the associated invariant chain gene in human endothelial cells and dermal fibroblasts. Proc. Natl. Acad. Sci. U. S. A *81*, 4917-4921.

Crivellato,E., Vacca,A., and Ribatti,D. (2004). Setting the stage: an anatomist's view of the immune system. Trends Immunol. *25* , 210-217.

Denzin,L.K. and Cresswell,P. (1995). HLA-DM induces CLIP dissociation from MHC class II alpha beta dimers and facilitates peptide loading. Cell *82*, 155-165.

Dewitte-Orr,S.J., Hsu,H.C., and Bols,N.C. (2007). Induction of homotypic aggregation in the rainbow trout macrophage-like cell line, RTS11. Fish. Shellfish. Immunol. *22*, 487-497.

Fange,R. (1986). Lymphoid organs in sturgeons (Acipenseridae). Vet. Immunol. Immunopathol. *12*, 153-161.

Fiebiger,E., Maehr,R., Villadangos,J., Weber,E., Erickson,A., Bikoff,E., Ploegh,H.L., and Lennon-Dumenil,A.M. (2002). Invariant chain controls the activity of extracellular cathepsin L. J. Exp. Med. *196*, 1263-1269.

Fineschi,B., Arneson,L.S., Naujokas,M.F., and Miller,J. (1995). Proteolysis of major histocompatibility complex class II-associated invariant chain is regulated by the alternatively spliced gene product, p41. Proc. Natl. Acad. Sci. U. S. A *92*, 10257-10261.

Fischer,U., Utke,K., Ototake,M., Dijkstra,J.M., and Kollner,B. (2003). Adaptive cell-mediated cytotoxicity against allogeneic targets by CD8-positive lymphocytes of rainbow trout (Oncorhynchus mykiss). Dev. Comp Immunol. *27*, 323-337.

Freisewinkel,I.M., Schenck,K., and Koch,N. (1993). The segment of invariant chain that is critical for association with major histocompatibility complex class II molecules contains the sequence of a peptide eluted from class II polypeptides. Proc. Natl. Acad. Sci. U. S. A *90*, 9703-9706.

Fujii,S., Senju,S., Chen,Y.Z., Ando,M., Matsushita,S., and Nishimura,Y. (1998). The CLIP-substituted invariant chain efficiently targets an antigenic peptide to HLA class II pathway in L cells. Hum. Immunol. *59*, 607-614.

Fujiki,K., Smith,C.M., Liu,L., Sundick,R.S., and Dixon,B. (2003). Alternate forms of MHC class II-associated invariant chain are not produced by alternative splicing in rainbow trout (Oncorhynchus mykiss) but are encoded by separate genes. Dev. Comp Immunol. *27*, 377-391.

Gelperin,D., Weigle,J., Nelson,K., Roseboom,P., Irie,K., Matsumoto,K., and Lemmon,S. (1995). 14-3-3 proteins: potential roles in vesicular transport and Ras signaling in Saccharomyces cerevisiae. Proc. Natl. Acad. Sci. U. S. A *92*, 11539-11543.

Ghosh,P., Amaya,M., Mellins,E., and Wiley,D.C. (1995). The structure of an intermediate in class II MHC maturation: CLIP bound to HLA-DR3. Nature *378*, 457-462.

Guncar,G., Pungercic,G., Klemencic,I., Turk,V., and Turk,D. (1999). Crystal structure of MHC class II-associated p41 Ii fragment bound to cathepsin L reveals the structural basis for differentiation between cathepsins L and S. EMBO J. *18*, 793-803.

Hansen,J.D., Strassburger,P., Thorgaard,G.H., Young,W.P., and Du,P.L. (1999). Expression, linkage, and polymorphism of MHC-related genes in rainbow trout, Oncorhynchus mykiss. J. Immunol. *163*, 774-786.

Hansen,J.D. and La,P.S. (2002). Induction of the rainbow trout MHC class I pathway during acute IHNV infection. Immunogenetics *54*, 654-661.

Henne,C., Schwenk,F., Koch,N., and Moller,P. (1995). Surface expression of the invariant chain (CD74) is independent of concomitant expression of major histocompatibility complex class II antigens. Immunology *84*, 177-182.

Hoppe,T., Rape,M., and Jentsch,S. (2001). Membrane-bound transcription factors: regulated release by RIP or RUP. Curr. Opin. Cell Biol. *13*, 344-348.

Hsing,L.C. and Rudensky,A.Y. (2005). The lysosomal cysteine proteases in MHC class II antigen presentation. Immunol. Rev. *207*, 229-241.

Janeway C.A., Travers P., Walport M. and Schlomchik M. (2001) Immunobiology: The immune system in health and disease 5TH edition. Garland Publishing New York.

Jones P.P., Murphy D.B., Hewgill D., and McDevitt H.O. Detection of a common polypeptide chain in I-A and I-E sub-region immunoprecipitates. Immunochemistry 16, 51-60. 1978.
Ref Type: Generic

Kaattari,S.L. and Irwin,M.J. (1985). Salmonid spleen and anterior kidney harbor populations of lymphocytes with different B cell repertoires. Dev. Comp Immunol. *9*, 433-444.

Kaushansky,K. (2006). Lineage-specific hematopoietic growth factors. N. Engl. J. Med. *354*, 2034-2045.

Khalil,H., Brunet,A., Saba,I., Terra,R., Sekaly,R.P., and Thibodeau,J. (2003). The MHC class II beta chain cytoplasmic tail overcomes the invariant chain p35-encoded endoplasmic reticulum retention signal. Int. Immunol. *15*, 1249-1263.

Kollner,B., Blohm,U., Kotterba,G., and Fischer,U. (2001). A monoclonal antibody recognising a surface marker on rainbow trout (Oncorhynchus mykiss) monocytes. Fish. Shellfish. Immunol. *11*, 127-142.

Kropshofer,H., Vogt,A.B., Stern,L.J., and Hammerling,G.J. (1995). Self-release of CLIP in peptide loading of HLA-DR molecules. Science *270*, 1357-1359.

Kuwana,T., Peterson,P.A., and Karlsson,L. (1998). Exit of major histocompatibility complex class II-invariant chain p35 complexes from the endoplasmic reticulum is modulated by phosphorylation. Proc. Natl. Acad. Sci. U. S. A *95*, 1056-1061.

Laing,K.J., Zou,J.J., Purcell,M.K., Phillips,R., Secombes,C.J., and Hansen,J.D. (2006). Evolution of the CD4 family: teleost fish possess two divergent forms of CD4 in addition to lymphocyte activation gene-3. J. Immunol. *177*, 3939-3951.

Lamb,C.A. and Cresswell,P. (1992). Assembly and transport properties of invariant chain trimers and HLA-DR-invariant chain complexes. J. Immunol. *148*, 3478-3482.

Lambrecht,B.N., Prins,J.B., and Hoogsteden,H.C. (2001). Lung dendritic cells and host immunity to infection. Eur. Respir. J. *18* , 692-704.

Lautwein,A., Kraus,M., Reich,M., Burster,T., Brandenburg,J., Overkleeft,H.S., Schwarz,G., Kammer,W., Weber,E., Kalbacher,H., Nordheim,A., and Driessen,C. (2004). Human B lymphoblastoid cells contain distinct patterns of cathepsin activity in endocytic compartments and regulate MHC class II transport in a cathepsin S-independent manner. J. Leukoc. Biol. *75*, 844-855.

Lenarcic,B. and Bevec,T. (1998). Thyropins--new structurally related proteinase inhibitors. Biol. Chem. *379*, 105-111.

Leng,L., Metz,C.N., Fang,Y., Xu,J., Donnelly,S., Baugh,J., Delohery,T., Chen,Y., Mitchell,R.A., and Bucala,R. (2003). MIF signal transduction initiated by binding to CD74. J. Exp. Med. *197*, 1467-1476.

Lennon-Dumenil,A.M., Roberts,R.A., Valentijn,K., Driessen,C., Overkleeft,H.S., Erickson,A., Peters,P.J., Bikoff,E., Ploegh,H.L., and Wolf,B.P. (2001). The p41 isoform of invariant chain is a chaperone for cathepsin L. EMBO J. *20*, 4055-4064.

Lennon-Dumenil,A.M., Bakker,A.H., Wolf-Bryant,P., Ploegh,H.L., and Lagaudriere-Gesbert,C. (2002). A closer look at proteolysis and MHC-class-II-restricted antigen presentation. Curr. Opin. Immunol. *14*, 15-21.

Letourneur,F. and Klausner,R.D. (1992). A novel di-leucine motif and a tyrosine-based motif independently mediate lysosomal targeting and endocytosis of CD3 chains. Cell *69*, 1143-1157.

Li,P., Gregg,J.L., Wang,N., Zhou,D., O'Donnell,P., Blum,J.S., and Crotzer,V.L. (2005). Compartmentalization of class II antigen presentation: contribution of cytoplasmic and endosomal processing. Immunol. Rev. *207*, 206-217.

Long,A.B. and Boss,J.M. (2005). Evolutionary conservation and characterization of the bare lymphocyte syndrome transcription factor RFX-B and its paralogue ANKRA2. Immunogenetics *56*, 788-797.

Long,E.O., Mach,B., and Accolla,R.S. (1984). Ia-negative B-cell variants reveal a coordinate regulation in the transcription of the HLA class II gene family. Immunogenetics *19*, 349-353.

Lotteau,V., Teyton,L., Peleraux,A., Nilsson,T., Karlsson,L., Schmid,S.L., Quaranta,V., and Peterson,P.A. (1990). Intracellular transport of class II MHC molecules directed by invariant chain. Nature *348*, 600-605.

Martin,T.R. and Frevert,C.W. (2005). Innate immunity in the lungs. Proc. Am. Thorac. Soc. *2*, 403-411.

Matsuyama,T., Fujiwara,A., Nakayasu,C., Kamaishi,T., Oseko,N., Hirono,I., and Aoki,T. (2007). Gene expression of leucocytes in vaccinated Japanese flounder (Paralichthys olivaceus) during the course of experimental infection with Edwardsiella tarda. Fish. Shellfish. Immunol. *22*, 598-607.

Matza,D., Wolstein,O., Dikstein,R., and Shachar,I. (2001). Invariant chain induces B cell maturation by activating a TAF(II)105-NF-kappaB-dependent transcription program. J. Biol. Chem. *276*, 27203-27206.

Matza,D., Lantner,F., Bogoch,Y., Flaishon,L., Hershkoviz,R., and Shachar,I. (2002). Invariant chain induces B cell maturation in a process that is independent of its chaperonic activity. Proc. Natl. Acad. Sci. U. S. A *99*, 3018-3023.

Matza,D., Kerem,A., Medvedovsky,H., Lantner,F., and Shachar,I. (2002). Invariant chain-induced B cell differentiation requires intramembrane proteolytic release of the cytosolic domain. Immunity. *17*, 549-560.

Matza,D., Kerem,A., and Shachar,I. (2003). Invariant chain, a chain of command. Trends Immunol. *24*, 264-268.

Mebius,R.E. and Kraal,G. (2005). Structure and function of the spleen. Nat. Rev. Immunol. *5*, 606-616.

Moore,L.J., Somamoto,T., Lie,K.K., Dijkstra,J.M., and Hordvik,I. (2005). Characterisation of salmon and trout CD8alpha and CD8beta. Mol. Immunol. *42*, 1225-1234.

Mosyak,L., Zaller,D.M., and Wiley,D.C. (1998). The structure of HLA-DM, the peptide exchange catalyst that loads antigen onto class II MHC molecules during antigen presentation. Immunity. *9*, 377-383.

Nakagawa,T.Y., Brissette,W.H., Lira,P.D., Griffiths,R.J., Petrushova,N., Stock,J., McNeish,J.D., Eastman,S.E., Howard,E.D., Clarke,S.R., Rosloniec,E.F., Elliott,E.A., and Rudensky,A.Y. (1999). Impaired invariant chain degradation and antigen presentation and diminished collagen-induced arthritis in cathepsin S null mice. Immunity. *10*, 207-217.

Nath,S., Kales,S., Fujiki,K., and Dixon,B. (2006). Major histocompatibility class II genes in rainbow trout (Oncorhynchus mykiss) exhibit temperature dependent downregulation. Immunogenetics *58*, 443-453.

Naujokas,M.F., Morin,M., Anderson,M.S., Peterson,M., and Miller,J. (1993). The chondroitin sulfate form of invariant chain can enhance stimulation of T cell responses through interaction with CD44. Cell *74*, 257-268.

Neefjes,J. (1999). CIIV, MIIC and other compartments for MHC class II loading. Eur. J. Immunol. *29*, 1421-1425.

Nishizuka,Y. (1984). The role of protein kinase C in cell surface signal transduction and tumour promotion. Nature *308*, 693-698.

O'Sullivan,D.M., Noonan,D., and Quaranta,V. (1987). Four Ia invariant chain forms derive from a single gene by alternate splicing and alternate initiation of transcription/translation. J. Exp. Med. *166*, 444-460.

Odorizzi,C.G., Trowbridge,I.S., Xue,L., Hopkins,C.R., Davis,C.D., and Collawn,J.F. (1994). Sorting signals in the MHC class II invariant chain cytoplasmic tail and transmembrane region determine trafficking to an endocytic processing compartment. J. Cell Biol. *126*, 317-330.

Ogrinc,T., Dolenc,I., Ritonja,A., and Turk,V. (1993). Purification of the complex of cathepsin L and the MHC class II-associated invariant chain fragment from human kidney. FEBS Lett. *336*, 555-559.

Ohta,Y., Landis,E., Boulay,T., Phillips,R.B., Collet,B., Secombes,C.J., Flajnik,M.F., and Hansen,J.D. (2004). Homologs of CD83 from elasmobranch and teleost fish. J. Immunol. *173*, 4553-4560.

Pamer,E. and Cresswell,P. (1998). Mechanisms of MHC class I--restricted antigen processing. Annu. Rev. Immunol. *16*, 323-358.

Pardoll,D.M. and Topalian,S.L. (1998). The role of CD4+ T cell responses in antitumor immunity. Curr. Opin. Immunol. *10*, 588-594.

Paulnock-King,D., Sizer,K.C., Freund,Y.R., Jones,P.P., and Parnes,J.R. (1985). Coordinate induction of Ia alpha, beta, and Ii mRNA in a macrophage cell line. J. Immunol. *135*, 632-636.

Peters,C., Braun,M., Weber,B., Wendland,M., Schmidt,B., Pohlmann,R., Waheed,A., and von,F.K. (1990). Targeting of a lysosomal membrane protein: a tyrosine-containing endocytosis signal in the cytoplasmic tail of lysosomal acid phosphatase is necessary and sufficient for targeting to lysosomes. EMBO J. *9*, 3497-3506.

Peters,P.J., Neefjes,J.J., Oorschot,V., Ploegh,H.L., and Geuze,H.J. (1991). Segregation of MHC class II molecules from MHC class I molecules in the Golgi complex for transport to lysosomal compartments. Nature *349*, 669-676.

Pieters,J., Bakke,O., and Dobberstein,B. (1993). The MHC class II-associated invariant chain contains two endosomal targeting signals within its cytoplasmic tail. J. Cell Sci. *106 (Pt 3)*, 831-846.

Pinet,V., Vergelli,M., Martin,R., Bakke,O., and Long,E.O. (1995). Antigen presentation mediated by recycling of surface HLA-DR molecules. Nature *375*, 603-606.

Pond,L. and Watts,C. (1997). Characterization of transport of newly assembled, T cell-stimulatory MHC class II-peptide complexes from MHC class II compartments to the cell surface. J. Immunol. *159*, 543-553.

Pond,L. and Watts,C. (1999). Functional early endosomes are required for maturation of major histocompatibility complex class II molecules in human B lymphoblastoid cells. J. Biol. Chem. *274*, 18049-18054.

Ponta,H., Sherman,L., and Herrlich,P.A. (2003). CD44: from adhesion molecules to signalling regulators. Nat. Rev. Mol. Cell Biol. *4*, 33-45.

Press, C. McL and Evensen, O. The morphology of the Immune System in Teleost Fishes. Fish.Shellfish.Immunol. 9, 309-318. 1999.
Ref Type: Generic

Purcell,M.K., Nichols,K.M., Winton,J.R., Kurath,G., Thorgaard,G.H., Wheeler,P., Hansen,J.D., Herwig,R.P., and Park,L.K. (2006). Comprehensive gene expression profiling following DNA vaccination of rainbow trout against infectious hematopoietic necrosis virus. Mol. Immunol. *43*, 2089-2106.

Roche,P.A. and Cresswell,P. (1990). Invariant chain association with HLA-DR molecules inhibits immunogenic peptide binding. Nature *345*, 615-618.

Roche,P.A., Marks,M.S., and Cresswell,P. (1991). Formation of a nine-subunit complex by HLA class II glycoproteins and the invariant chain. Nature *354*, 392-394.

Roche,P.A., Teletski,C.L., Stang,E., Bakke,O., and Long,E.O. (1993). Cell surface HLA-DR-invariant chain complexes are targeted to endosomes by rapid internalization. Proc. Natl. Acad. Sci. U. S. A *90*, 8581-8585.

Romagnoli,P., Layet,C., Yewdell,J., Bakke,O., and Germain,R.N. (1993). Relationship between invariant chain expression and major histocompatibility complex class II transport into early and late endocytic compartments. J. Exp. Med. *177*, 583-596.

Ruane,N.M., Wendelaar Bonga,S.E., and Balm,P.H. (1999). Differences between rainbow trout and brown trout in the regulation of the pituitary-interrenal axis and physiological performance during confinement. Gen. Comp Endocrinol. *115*, 210-219.

Sadegh-Nasseri,S., Stern,L.J., Wiley,D.C., and Germain,R.N. (1994). MHC class II function preserved by low-affinity peptide interactions preceding stable binding. Nature *370*, 647-650.

Sakai, M., Savan, R., Kuragasaki, H., and Aman, A. Diversification in MHC class II invariant chain-like proteins among fishes. J.Appl.Ichthyol. 252-257. 2004.
Ref Type: Generic

Sanchez,C., Alvarez,A., Castillo,A., Zapata,A., Villena,A., and Dominguez,J. (1995). Two different subpopulations of Ig-bearing cells in lymphoid organs of rainbow trout. Dev. Comp Immunol. *19*, 79-86.

Sanderson,S., Frauwirth,K., and Shastri,N. (1995). Expression of endogenous peptide-major histocompatibility complex class II complexes derived from invariant chain-antigen fusion proteins. Proc. Natl. Acad. Sci. U. S. A *92*, 7217-7221.

Sato,A., Figueroa,F., Murray,B.W., Malaga-Trillo,E., Zaleska-Rutczynska,Z., Sultmann,H., Toyosawa,S., Wedekind,C., Steck,N., and Klein,J. (2000). Nonlinkage of major histocompatibility complex class I and class II loci in bony fishes. Immunogenetics *51*, 108-116.

Schutze,M.P., Peterson,P.A., and Jackson,M.R. (1994). An N-terminal double-arginine motif maintains type II membrane proteins in the endoplasmic reticulum. EMBO J. *13*, 1696-1705.

Shachar,I. and Flavell,R.A. (1996). Requirement for invariant chain in B cell maturation and function. Science *274*, 106-108.

Shand, R. and Dixon, B. Teleost Major Histocompatibility Genes: Diverse but not Complex. Mod.Asp.Immunobiol. 2[2], 66-72. 2001.
Ref Type: Generic

Shi,X., Leng,L., Wang,T., Wang,W., Du,X., Li,J., McDonald,C., Chen,Z., Murphy,J.W., Lolis,E., Noble,P., Knudson,W., and Bucala,R. (2006). CD44 is the signaling component of the macrophage migration inhibitory factor-CD74 receptor complex. Immunity. *25*, 595-606.

Siebenkotten,I.M., Carstens,C., and Koch,N. (1998). Identification of a sequence that mediates promiscuous binding of invariant chain to MHC class II allotypes. J. Immunol. *160*, 3355-3362.

Siemasko,K., Eisfelder,B.J., Williamson,E., Kabak,S., and Clark,M.R. (1998). Cutting edge: signals from the B lymphocyte antigen receptor regulate MHC class II containing late endosomes. J. Immunol. *160*, 5203-5208.

Sloan,V.S., Cameron,P., Porter,G., Gammon,M., Amaya,M., Mellins,E., and Zaller,D.M. (1995). Mediation by HLA-DM of dissociation of peptides from HLA-DR. Nature *375*, 802-806.

Strubin,M., Berte,C., and Mach,B. (1986). Alternative splicing and alternative initiation of translation explain the four forms of the Ia antigen-associated invariant chain. EMBO J. *5*, 3483-3488.

Sultmann,H., Mayer,W.E., Figueroa,F., O'hUigin,C., and Klein,J. (1993). Zebrafish Mhc class II alpha chain-encoding genes: polymorphism, expression, and function. Immunogenetics *38*, 408-420.

Sultmann,H., Mayer,W.E., Figueroa,F., O'hUigin,C., and Klein,J. (1994). Organization of Mhc class II B genes in the zebrafish (Brachydanio rerio). Genomics *23*, 1-14.

Ting,J.P. and Zhu,X.S. (1999). Class II MHC genes: a model gene regulatory system with great biologic consequences. Microbes. Infect. *1*, 855-861.

Ting,J.P. and Trowsdale,J. (2002). Genetic control of MHC class II expression. Cell *109 Suppl*, S21-S33.

Tosi,M.F. (2005). Innate immune responses to infection. J. Allergy Clin. Immunol. *116*, 241-249.

Turk,D., Guncar,G., and Turk,V. (1999). The p41 fragment story. IUBMB. Life *48*, 7-12.

van,B.J., Schoenberger,S.P., Verreck,F., Amons,R., Offringa,R., and Koning,F. (1997). Efficient loading of HLA-DR with a T helper epitope by genetic exchange of CLIP. Proc. Natl. Acad. Sci. U. S. A *94*, 7499-7502.

Villadangos,J.A., Bryant,R.A., Deussing,J., Driessen,C., Lennon-Dumenil,A.M., Riese,R.J., Roth,W., Saftig,P., Shi,G.P., Chapman,H.A., Peters,C., and Ploegh,H.L. (1999). Proteases involved in MHC class II antigen presentation. Immunol. Rev. *172*, 109-120.

Viville,S., Neefjes,J., Lotteau,V., Dierich,A., Lemeur,M., Ploegh,H., Benoist,C., and Mathis,D. (1993). Mice lacking the MHC class II-associated invariant chain. Cell *72*, 635-648.

Vogt,A.B., Stern,L.J., Amshoff,C., Dobberstein,B., Hammerling,G.J., and Kropshofer,H. (1995). Interference of distinct invariant chain regions with superantigen contact area and antigenic peptide binding groove of HLA-DR. J. Immunol. *155*, 4757-4765.

Wang,R.F. (2001). The role of MHC class II-restricted tumor antigens and CD4+ T cells in antitumor immunity. Trends Immunol. *22* , 269-276.

Williams,M.A. and Fukuda,M. (1990). Accumulation of membrane glycoproteins in lysosomes requires a tyrosine residue at a particular position in the cytoplasmic tail. J. Cell Biol. *111*, 955-966.

Williams,T.M. (2001). Human leukocyte antigen gene polymorphism and the histocompatibility laboratory. J. Mol. Diagn. *3*, 98-104.

Wolf Bryant P, Lennon-Dumenil A.M, Fiebiger E, Lagaudriere-Gesbert C., and Ploegh H.L. Proteolysis and antigen presentation by MHC class II molecules. Advances in Immunology 80, 71-113. 2002. Ref Type: Generic

Woodland,D.L. and Scott,I. (2005). T cell memory in the lung airways. Proc. Am. Thorac. Soc. *2*, 126-131.

Yoder,J.A., Haire,R.N., and Litman,G.W. (1999). Cloning of two zebrafish cDNAs that share domains with the MHC class II-associated invariant chain. Immunogenetics *50*, 84-88.

Zou,J., Holland,J., Pleguezuelos,O., Cunningham,C., and Secombes,C.J. (2000). Factors influencing the expression of interleukin-1 beta in cultured rainbow trout (Oncorhynchus mykiss) leucocytes. Dev. Comp Immunol. *24*, 575-582.

Zou,J., Peddie,S., Scapigliati,G., Zhang,Y., Bols,N.C., Ellis,A.E., and Secombes,C.J. (2003). Functional characterisation of the recombinant tumor necrosis factors in rainbow trout, Oncorhynchus mykiss. Dev. Comp Immunol. *27*, 813-822.

Zou,J., Carrington,A., Collet,B., Dijkstra,J.M., Yoshiura,Y., Bols,N., and Secombes,C. (2005). Identification and bioactivities of IFN-gamma in rainbow trout Oncorhynchus mykiss: the first Th1-type cytokine characterized functionally in fish. J. Immunol. *175*, 2484-2494.